Virtual Trials for Breast Imaging

Tomic, Hanna

2026

Document Version:
Publisher's PDF, also known as Version of record

Virtual Trials for Breast Imaging

Dynamic simulation of breast cancer screening

HANNA TOMIC
DEPARTMENT OF TRANSLATIONAL MEDICINE | FACULTY OF MEDICINE | LUND UNIVERSITY

Virtual Trials for Breast Imaging

Virtual Trials for Breast Imaging

Dynamic simulation of breast cancer screening

Hanna Tomic

LUND
UNIVERSITY

DOCTORAL DISSERTATION

Doctoral dissertation for the degree of Doctor of Philosophy (PhD) at the Faculty of Medicine at Lund University to be publicly defended on 10th of April at 09.00 at the Department of Radiology and Physiology, Room 2005/2007, Skåne University Hospital, Malmö

Faculty opponent
Professor Ehsan Samei
Duke University, United States

Organization: Lund University

Document name: Doctoral Dissertation **Date of issue** 2026-03-03

Author: Hanna Tomic **Sponsoring organization:**

Title and subtitle: Virtual Trials for Breast Imaging: Dynamic simulation of breast cancer screening

Abstract:

Background and aim
Breast cancer is the most common cancer among women worldwide and a major cause of cancer-related mortality. Rapid advances in breast imaging, driven by quantitative image analysis and artificial intelligence, increase the need for reliable methods to evaluate new imaging technologies. Traditional validation approaches such as clinical trials are costly, time consuming, and limited in their ability to capture population variability. Virtual imaging trials (VITs) have therefore emerged as a complementary in silico framework. The aim of this thesis is to advance VITs for breast imaging by improving the realism of computational phantoms and virtual populations, and by enabling longitudinal modeling based on real-world data.

Methods
Paper I presents a method for simulating tumor growth using growth rates derived from real-world data. Paper II introduces a technique for simulating soft tissue breast lesions, utilizing Perlin noise, evaluated by radiologists according to BI-RADS malignancy score. Paper III describes STELLA-R, a framework for longitudinal VITs that incorporates multivariate models of breast density, age, and breast volume to simulate anatomical changes over time. Paper IV reports lesion detection performance across women's subgroups in a hybrid imaging study.

Results
Paper I showed close agreement between simulated and real-world tumor growth rates. Paper II demonstrated that the lesion models captured morphological subtypes with acceptable levels of realism. Paper III revealed strong correlations between simulated and real-world data and illustrated the use of STELLA-R for visualizing longitudinal breast density changes. Paper IV found higher odds of lesion detection in non-Hispanic Black women, an effect largely mediated by breast density, with higher BI-RADS density categories associated with lower detection odds.

Conclusions
This thesis culminated in the development of STELLA-R, a framework enabling longitudinal virtual imaging trials, and demonstrated its successful application in hybrid studies with robust and clinically relevant results.

Key words: breast cancer, breast imaging, mammography, virtual imaging trials, virtual clinical trials, in silico trials

Classification system and/or index terms (if any) Supplementary bibliographical information

Language: English **Number of pages**: 120

ISSN and key title: 1652-8220

ISBN: 978-91-8021-846-7

Recipient's notes Price Security classification

Signature Date 2026-03-03

Virtual Trials for Breast Imaging

Dynamic simulation of breast cancer screening

Hanna Tomic

LUND
UNIVERSITY

Cover image by Hanna Tomic

Disclaimer on the use of AI

Artificial intelligence (AI) models (OpenAI's ChatGPT-5, v 5.1 and 5.2) were used during the preparation of this thesis. Their use was limited to spellchecking, improving grammar, and enhancing readability. AI was not used to generate original scientific content or to write complete sections of text. All scientific interpretations, data analysis, and conclusions are my own and I take full responsibility for the content.

Published by:

Diagnostic Radiology, Department of Translational Medicine

Faculty of Medicine

Lund University

Malmö 2026

ISBN 978-91-8021-846-7

Series title: 2026:48

ISSN 1652-8220

Printed in Sweden by Media-Tryck, Lund University,
Lund, 2026

Media-Tryck is a Nordic Swan Ecolabel certified provider of printed material. Read more about our environmental work at www.mediatryck.lu.se

MADE IN SWEDEN

To my parents

"A good traveler has no fixed plans, and is not intent on arriving" – Lao Tzu

Table of contents

List of papers

Papers included in the thesis

Paper I

Development and evaluation of a method for tumor growth simulation in virtual clinical trials of breast cancer screening
Hanna Tomic, Anna Bjerkén, Gustav Hellgren, Kristin Johnson, Daniel Förnvik, Sophia Zackrisson, Anders Tingberg, Magnus Dustler, Predrag R. Bakic
Journal of Medical Imaging. 2022. Vol. 9, Issue 3: 033502

Paper II

Simulation of breast lesions based upon fractal Perlin noise
Hanna Tomic, Arthur C. Costa, Anna Bjerkén, Marcelo A.C. Vieira, Sophia Zackrisson, Anders Tingberg, Pontus Timberg, Magnus Dustler, Predrag R. Bakic
Physica Medica. 2023. Vol. 114: 102681

Paper III

A framework for simulation of temporal evolution and longitudinal studies of breast anatomy in radiology
Hanna Tomic, Jakob Olinder, John-Henry Markbo, Pontus Timberg, Sophia Zackrisson, Anders Tingberg, Magnus Dustler, Predrag R. Bakic
Medical Physics. 2025. Vol. 52, Issue 12: e70207

Paper IV

Lesion detectability and masking disparity assessment in breast tomosynthesis across diverse populations using in-silico imaging trials
Bruno Barufaldi, Rodrigo B. Vimieiro, Vincent Dong, ***Hanna Tomic***, Quy Cao, Marcelo C. Vieira, Predrag R. Bakic, Peter R. Eby, Sophia Zackrisson, Anne Marie McCarthy, Andrew Maidment
Submitted, under revision

Related papers not included in the thesis

Published papers

Characterization of optically stimulated luminescence dosimetry using NaCl pellets in breast x-ray imaging
Anna Bjerkén, Maria Karampiperi, ***Hanna Tomic***, Magnus Dustler, Christopher Rääf, Anders Tingberg, Christian Bernhardsson, Predrag Bakic
Radiation Protection Dosimetry. 2025. Vol. 201, Issue 13-14: 960-965

Estimation of the absorbed dose in simultaneous digital breast tomosynthesis and mechanical imaging
Anna Bjerkén, ***Hanna Tomic***, Sophia Zackrisson, Magnus Dustler, Predrag Bakic, Anders Tingberg
Journal of Medical Imaging. 2024. Vol. 12, Issue S1: S13003

Assessing Digital Breast Tomosynthesis Impact on Early Cancer Detection: Insights from Consecutive Screening
Annika Jögi, Kristin Johnson, Sofia Wittgren, Victor Sundgren, ***Hanna Tomic***, Jakob Olinder, Anna Åkesson, Ingvar Andersson, Sophia Zackrisson, Predrag R. Bakic
Radiology. 2024. Vol. 312, Issue 1: e233417

Finite element model of mechanical imaging of the breast
Rebecca Axelsson, ***Hanna Tomic***, Sophia Zackrisson, Anders Tingberg, Hanna Isaksson, Predrag R. Bakic, Magnus Dustler
Journal of Medical Imaging. 2022. Vol. 9, Issue 3: 033502

Virtual Clinical Trials in Medical Imaging System Evaluation and Optimisation
Bruno Barufaldi, Andrew Maidment, Magnus Dustler, Rebecca Axelsson, ***Hanna Tomic***, Sophia Zackrisson, Anders Tingberg, Predrag R. Bakic
Radiation Protection Dosimetry. 2021. Vol 195, Issue 3-4: ncab080.

Abstracts published as proceedings

Simulation of heterogeneity within breast lesions based upon Perlin noise
Hanna Tomic, Arthur C. Costa, Marcelo A. C. Vieira, Magnus Dustler, Sophia Zackrisson, Anders Tingberg, Predrag Bakic
17th International Workshop on Breast Imaging (IWBI). 2024. Giger M L, Whitney H M, Drukker K, Li H, (red.). Proceedings of SPIE: The International Society for Optical Engineering; vol. 13174: 1317418

Using simulated breast lesions based on Perlin noise for evaluation of lesion segmentation
Hanna Tomic, Zhikai Yang, Anders Tingberg, Sophia Zackrisson, Rodrigo Moreno, Örjan Smedby, Magnus Dustler, Predrag Bakic
SPIE Medical Imaging: Physics of Medical Imaging. 2024. Fahrig R, Sabol J M, Li K (red.). Proceedings of SPIE: The International Society for Optical Engineering; vol. 12925: 129251P

Simulation of volumetric breast densities for virtual clinical trials
Hanna Tomic, Daniel Förnvik, Sophia Zackrisson, Anders Tingberg, Magnus Dustler, Predrag Bakic
SPIE Medical Imaging: Physics of Medical Imaging. 2022. Zhao W, Yu L (red.). Proceedings of SPIE: The International Society for Optical Engineering; vol. 12031: 12031

Tumor growth rate estimations in a breast cancer screening population
Hanna Tomic, Akane Ohashi, Victor Dahlblom, Anna Bjerkén, Daniel Förnvik, Magnus Dustler, Sophia Zackrisson, Anders Tingberg, Predrag Bakic
16th International Workshop on Breast Imaging (IWBI). 2022. Bosmans H, Marshall N, Van Ongeval C, (red.). Proceedings of SPIE: The International Society for Optical Engineering; vol. 12286: 1228613

Evaluation of 3D printed contrast detail phantoms for mammography quality assurance
Måns Boll, Trevor Vent, ***Hanna Tomic***, Christian Bernhardsson, Magnus Dustler, Anders Tingberg, Predrag R. Bakic
16th International Workshop on Breast Imaging (IWBI). 2022. Bosmans H, Marshall N, Van Ongeval C, (red.). Proceedings of SPIE: The International Society for Optical Engineering; vol. 12286: 122860J

Abstracts not yet published as proceedings

Towards Improved Control of Breast Density in Simulated Mammograms via Perlin Noise Parameterization
Hanna Tomic, Magnus Dustler, Predrag R. Bakic
SPIE Medical Imaging: Physics of Medical Imaging. 2026. (Accepted)

Author contributions

Paper I: Contributed to the conceptualization of the study design and methodology. I carried out the modeling, simulations and data analyses, including the creation of figures and graphs. I also led the writing and revision of the manuscript and led the administrative aspects of the submission process.

Paper II: Contributed to the study design and performed the simulations and data analyses, including generation of figures and graphs. I led the writing and revision of the manuscript, as well as the administrative aspects of the submission process.

Paper III: Contributed to the formulation of the STELLA-R framework, specifically the use of multivariate models and the lesion insertion algorithm. I performed the simulations and conducted the data analysis. I led the writing and revision of the manuscript, as well as the administrative aspects of the submission process.

Paper IV: Contributed to the conceptualization of the study design related to the simulated lesions. I subsequently generated the computer simulated tumors and participated in multiple rounds of manuscript proofreading and revision.

Abstract

Background and aim

Breast cancer is the most common cancer among women worldwide and a major cause of cancer related mortality. Rapid advances in breast imaging, driven by quantitative image analysis and artificial intelligence, increase the need for reliable methods to evaluate new imaging technologies.

Traditional validation approaches such as clinical trials are costly, time consuming, and limited in their ability to capture population variability. Virtual imaging trials (VITs) have therefore emerged as a complementary in silico framework. The aim of this thesis is to advance VITs for breast imaging by improving the realism of computational phantoms and virtual populations, and by enabling longitudinal modeling based on real-world data.

Methods

Paper I presents a method for simulating tumor growth using growth rates derived from real-world data. Paper II introduces a technique for simulating soft tissue breast lesions, utilizing Perlin noise, evaluated by radiologists according to BI-RADS malignancy score. Paper III describes STELLA-R, a framework for longitudinal VITs that incorporates multivariate models of breast density, age, and breast volume to simulate anatomical changes over time. Paper IV reports lesion detection performance across women's subgroups in a hybrid imaging study.

Results

Paper I showed close agreement between simulated and real-world tumor growth rates. Paper II demonstrated that the lesion models captured morphological subtypes with acceptable levels of realism. Paper III revealed strong correlations between simulated and real-world data and illustrated the use of STELLA-R for visualizing longitudinal breast density changes. Paper IV found higher odds of lesion detection in non-Hispanic Black women, an effect largely mediated by breast density, with higher BI-RADS density categories associated with lower detection odds.

Conclusions

This thesis culminated in the development of STELLA-R, a framework enabling longitudinal virtual imaging trials, and demonstrated its successful application in hybrid studies with robust and clinically relevant results.

Populärvetenskaplig sammanfattning

Bröstcancer är den vanligaste cancerformen bland kvinnor i världen och orsakar över 600 000 dödsfall varje år (WHO). Tidig upptäckt med hjälp av bröstavbildning, som mammografi, är avgörande för att rädda liv. Samtidigt utvecklas bildtekniken snabbt, med artificiell intelligens och avancerad bildanalys som allt oftare används för att hitta cancer tidigt och träffsäkert. För att dessa nya tekniker ska kunna införas på ett säkert sätt i vården krävs tillförlitliga metoder för att testa och utvärdera dem.

Traditionellt har nya bildtekniker utvärderats genom omfattande kliniska studier på människor. Dessa studier är dock både dyra och tidskrävande och kan vara svåra att genomföra på ett sätt som speglar hela befolkningens variation. Därför har så kallade virtuella bilddiagnostiska studier vuxit fram som ett viktigt komplement. I dessa används datorbaserade modeller för att simulera mänsklig anatomi, sjukdom, bildtagning och bildgranskning, utan att verkliga individer behöver undersökas och därmed exempelvis slippa utsättas för röntgenstrålning.

I den här avhandlingen utvecklas nya metoder för virtuella bilddiagnostiska studier inom röntgenbaserad bröstavbildning, där målet är att simulera anatomiska förändringar i bröstet för att bättre förstå hur bröstcancer utvecklas och framträder i röntgenbilder. Arbetet omfattar bland annat modellering av hur tumörer växer över tid baserat på verkliga patientdata (delarbete 1), samt utveckling av datorsimulerade tumörer med hjälp av en matematisk metod kallad Perlin noise (delarbete 2). Avhandlingen presenterar även STELLA-R (delarbete 3), ett nytt ramverk som gör det möjligt att simulera bröst och följa förändringar i vävnad och tumörer över tid i en virtuell miljö. Slutligen visar avhandlingen hur datormodellerna kan kombineras med verkliga mammografibilder i så kallade hybridstudier, för att undersöka hur väl bröstcancer upptäcks hos olika grupper av kvinnor (delarbete 4).

Resultaten visar att modellerna överensstämmer med verkliga patientdata och kan användas för att studera hur bröstförändringar utvecklas över tid (delarbete 1 och 3). Utseendet på de simulerade tumörerna efterliknade det som ses i kliniska bilder (delarbete 2) och i hybridstudien (delarbete 4) sågs att chansen att upptäcka bröstcancer minskar för kvinnor med stor andel bröstkörtelvävnad.

Sammantaget visar avhandlingen att virtuella bildstudier kan efterlikna hur bröstcancer utvecklas och syns på röntgenbilder. Detta öppnar möjligheter att utvärdera framtidens bildtekniker snabbare och mer kostnadseffektivt, och kan bidra till bättre metoder för tidig upptäckt av bröstcancer.

Thesis at a glance

Study	Aim	Method	Results and Conclusions
I	Develop a method to simulate growing breast lesions.	Real-world TVDT[A] data (n=31) were used to simulate lesion growth with plausible growth rates. Simulated lesions and corresponding breast phantoms were generated using the OpenVCT framework. The approach was validated by comparing real-world, simulated, and estimated tumor growth data.	Non-significant difference between the data sets (real-world, simulated and estimated TVDT), p>0.5.
II	Develop computer simualted lesions with clinically plausible morphologies.	An in-house algorithm, based on Perlin noise, was used to generate lesions and produce DM[B] images of virtual phantoms. Radiologists assessed the lesions for realism and categorized the findings according to BI-RADS malignancy score.	The simulated lesions exhibited round, oval, and irregular shapes, with margins that were circumscribed, obscured, microlobulated, or indistinct, and demonstrated moderate to high realism.
III	Create a framework for simulating temporal changes in breast density and tumor evolution.	Real-world data (n=25 188) on annual changes in breast density and volume were used to model multivariate relationships and temporal changes in breast density and tumor evolution.	First deployment of the STELLA-R pipeline. No significant difference between modeled and real-world correlations. Case examples illustrate longitudinal changes in breast density in virtual women.
IV	Investigate the cancer detection performance between different groups of women and different breast density categories through a hybrid framework.	Simulated tumors were inserted in real clinical images (cases=451, controls=451). Participants were stratified by ethnicity and BI-RADS breast density category. The detection performance by virtual observers (CHO[C]) was evaluated through ROC[D] analysis, odds ratio from logistic regression, and mediation analysis.	Detectability was reduced with increased BI-RADS breast density category (AUC[E] 0.94 vs. 0.84 between category A and C/D, p<0.001). Cancer detection performance was mediated by breast density in 39–55% of the observed ethnicity-related differences.

[A]Tumor Volume Doubling Time (TVDT)
[B]Digital Mammography (DM)
[C]Channel Hotelling Observer (CHO)
[D]Receiver Operating Characteristic (ROC)
[E]Area Under the Curve (AUC)

Abbreviations

AAPI	Asian American and Pacific Islander
AI	Artificial Intelligence
AUC	Area Under the Curve
BMI	Body Mass Index
CC	Craniocaudal
CI	Confidence Interval
CEM	Contrast Enhanced Mammography
CGI	Computer Generated Imagery
CHO	Channelized Hotelling Observer
CT	Computed Tomography
DBT	Digital Breast Tomosynthesis
DCIS	Ductal Carcinoma In Situ
DM	Digital Mammography
FDA	Food and Drug Administration
GAN	Generative Adversarial Networks
IDC	Invasive Ductal Carcinoma
ILC	Invasive Lobular Carcinoma
MBTST	Malmö Breast Tomosynthesis Screening Trial
MLO	Mediolateral Oblique
MRI	Magnetic Resonance Imaging
NHB	Non-Hispanic Black
NHW	Non-Hispanic White
OR	Odds Ratio
ROC	Receiver Operating Characteristic
TVDT	Tumor Volume Doubling Time
VBD	Volumetric Breast Density
VIT	Virtual Imaging Trial

Introduction

Breast cancer remains a major global health burden and is the most common cancer among women worldwide.[1,2] Screening with mammography has long played a key role in reducing breast cancer mortality by enabling earlier tumor detection and improved prognosis, particularly when women attend screening regularly.[3-5]

Over the past decades, evidence supporting the effectiveness of mammographic screening has accumulated alongside major advances in treatment.[3,6-8] Today, digital mammography (DM) is increasingly complemented by more advanced imaging techniques such as digital breast tomosynthesis (DBT).[9] In parallel, discussions around risk-based and personalized screening are intensified, with growing interest in identifying women who may benefit from supplemental imaging modalities with higher sensitivity compared to DM or DBT, such as magnetic resonance imaging (MRI).[10,11] These developments introduce new challenges, including increased workload for radiologists and radiographers, and greater reliance on robust risk stratification tools.

At the same time, evaluation of breast images is moving toward more quantitative approaches. This includes objective assessment of risk markers such as breast density, as well as computer-aided and AI-assisted methods for lesion detection.[12-15] These advances highlight a persistent challenge when it comes to validating new diagnostic tools. Clinical studies are expensive, time consuming, ethically constrained, and often lack a clear ground truth, limiting the ability to systematically evaluate imaging performance.

Virtual imaging trials (VITs), also known as virtual clinical trials (VCTs) or in silico trials, have emerged as a way to bridge this gap by simulating human anatomy, image acquisition, and interpretation within a controlled environment.[16-20] The broader adoption of VITs in breast imaging is relatively recent and has accelerated during the 21st century in the context of regulatory testing and methodological development.[20]

Given this background, the aim of this thesis is to address key limitations of current VIT frameworks by improving anatomical realism, enabling population-based models grounded in real-world data and supporting longitudinal studies that capture changes over time. This is an essential step toward more clinically relevant virtual trials for the development and evaluation of breast imaging technologies.

Background

The development of modern virtual imaging trials offers a promising way to improve diagnostic imaging and breast cancer screening. Achieving this requires realistic computer models that capture breast anatomy and the development of abnormalities in the breast. This thesis explores how computer simulations can be used to model the breast and imaging of the breast. The work therefore starts with an overview of breast anatomy and the imaging methods used in clinical practice, laying the groundwork for the simulation models developed in the chapters that follow.

The female breast

Teachings about the anatomy of the female breast likely date back to prehistoric times, long before written records. Throughout history, humans have sought to explore, understand, and treat diseases of the breast. Early mentions include Hippocrates (460–377 BCE), often called the "father of medicine," who is said to have coined the term breast cancer and even considered risk factors and prognosis.[21,22] Later, Roman physicians such as Galen (129–216 CE) advanced treatments and even proposed radical mastectomy for advanced cases.[21-23] Over centuries, research and innovation have greatly improved our understanding of the female breast and the ways we can treat and improve outcomes for breast diseases.[22,24]

The healthy breast

Anatomy

Today, it is well established that the breast (Figure 1) is primarily composed of two tissue types: adipose (fat) and fibroglandular tissue.[25] The fibroglandular component includes milk-producing lobules embedded within supportive connective tissue. A branching network of ducts converges toward the nipple, along with blood vessels and lymphatic channels. The entire breast structure is supported by the chest wall and extends upward toward the axilla and the pectoralis muscle.

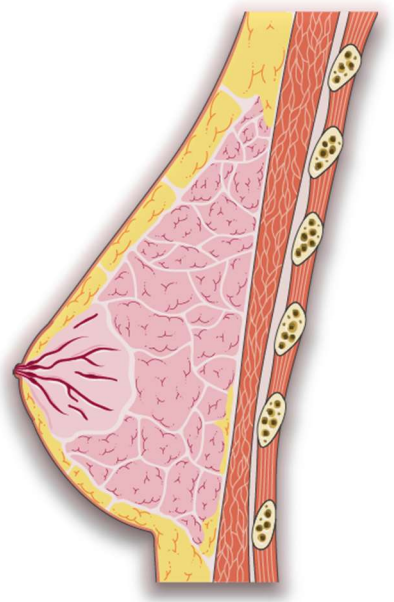

Figure 1. Schematic anatomy of the female breast
Sagittal view showing the internal structures of the breast. Adipose tissue is shown in yellow, glandular tissue in pink, and the pectoralis major muscle in red along the chest wall. Cooper's ligaments appear as supportive fibrous bands in white forming compartments between the glandular lobules, while milk ducts in red extend toward the areola and nipple. Image provided by Servier Medical Art (https://smart.servier.com), licensed under CC BY 4.0.

Breast density

Breast density is a radiological term that refers to the relative proportion of fibroglandular tissue as seen on a mammographic image. Breasts with a higher proportion of adipose (fatty) tissue appear darker and are described as less dense or radiolucent on mammograms, whereas breasts with more fibroglandular tissue appear brighter and are considered more dense or radiopaque.[26]

Breast density varies considerably among women and is influenced by factors such as genetic background, age, hormonal status, menopausal state, and the use of hormone therapy. In clinical practice, radiologists typically assign mammographic breast density qualitatively using the Breast Imaging Reporting and Data System (BI-RADS) density scale (5th edition; Figure 2).[27] A newer edition is also available since of late 2025 (BI-RADS v2025/6th edition).[28] While the density categories remain essentially unchanged, the new edition provides slightly more explicit guidance on how density can affect lesion detection. In recent decades, automated image analysis software have been developed to provide quantitative estimates of percent dense volume or percent dense area, thereby reducing the interobserver variability associated with visual assessments by radiologists.[29-33]

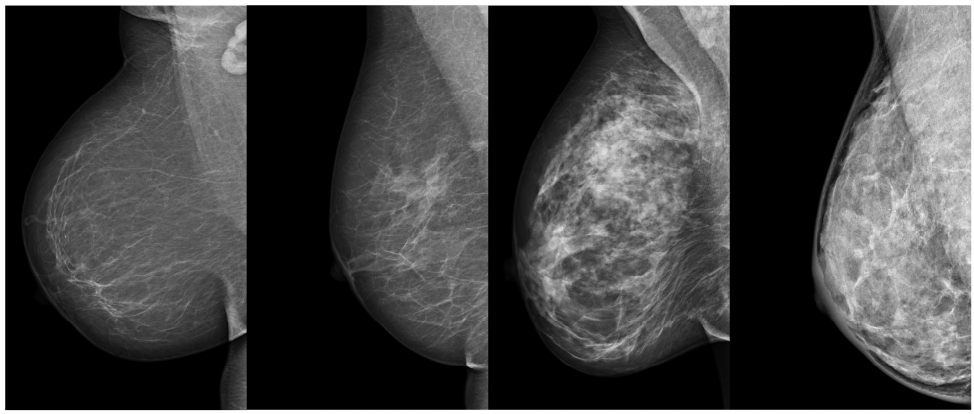

Figure 2. BI-RADS (5th Ed.) breast density categories
Representative mammographic examples of the four BI-RADS density categories (A–D), arranged from left to right in order of increasing fibroglandular tissue.

Breast density is an important imaging characteristic and an established risk marker for breast cancer. Malignancies arising in dense breasts are more likely to be masked by the surrounding fibroglandular tissue, which can reduce the sensitivity of mammography.[34-38] In addition to the masking effect, higher breast density is associated with an increased risk of developing breast cancer.[34-38] According to a recent review, women with BI-RADS D have almost a twofold increased breast cancer risk compared to those with BI-RADS B.[36] However, more recent evidence suggest that the association might be more modest, with about 30% higher odds when comparing BI-RADS D with BI-RADS A[39]

Consequently, breast density has become an important focus in risk stratification and screening optimization. For example, to guide individualized screening strategies based on breast density and improve diagnostic sensitivity.[10,40] Recently, countries such as the United States and Australia have introduced legislations and policies to ensure that women are personally informed of their individual breast density as part of their mammographic screening.[41,42]

It is important to note that breast density is only one of many established risk factors for breast cancer, alongside some of them being age, BMI, age at menarche and menopause, hormonal and genetic factors.[43-45] Among these, inherited mutations in the BRCA1 and BRCA2 genes substantially increase breast cancer risk, although such mutations are relatively rare in the general population.[46] Moreover, many breast cancers cannot be explained solely by known risk factors, as discussed further in the section on cancer development.

Breast development

The breast composition is an evolving process throughout a woman's life. Breast density changes in response to biological and hormonal factors such as the menstrual cycle, pregnancy, lactation, menopause, and the use of hormonal therapies.[47,48] With increasing age, the fibroglandular component typically involutes, gradually being replaced by adipose tissue. Since lesions are more easily detected in adipose breasts, mammograms typically become easier to interpret with increasing age. The evolution of breast density has commonly been described by exponential or stepwise mathematical functions.[47-49] These functions model or predict age dependent changes in density, thereby enabling a better understanding of how breast composition evolves over time.

The diseased breast

Breast cancer remains the leading cause of cancer related death among women worldwide.[1] It is a heterogeneous disease, with lesions that can differ substantially in their clinical presentation and biological behavior. Breast tumors are commonly classified using radiographic, histopathologic, and molecular characteristics, reflecting the complexity of their underlying biology.[50-52] These characteristics may also provide prognostic and predictive information regarding treatment response.[50,53] Despite this diversity, breast cancers share fundamental principles of cancer development in general.

Cancer development

Cancer is fundamentally a genetic disease, arising from abnormalities in gene expression, e.g. mutations that activate oncogenes or inactivate tumor suppressor genes, leading to uncontrolled cell division.[54] Recent research also highlights the importance of the tumor microenvironment and the immune system in cancer development and progression.[55,56]

A complex interplay between genetic mutations, tissue environment, and immune response determines whether cancer develops and how aggressive it becomes, including differences in tumor growth rates. As tumors evolve, they typically exhibit features such as abnormal cell proliferation, chronic inflammation, and rapid, disorganized formation of new blood vessels.[54] This early onset usually exhibits an exponential growth, as cells proliferate without any obstruction. Because this neovasculature is often inefficient, tumors may eventually be unable to obtain sufficient oxygen and nutrients, eventually resulting in cell necrosis and a growth stagnation.[57,58]

Subtypes of breast cancer

Breast cancer is commonly divided into subtypes based on histopathological and molecular features. Histopathology describes the tumor's microscopic appearance, including whether disease is in situ (confined by the basement membrane) or invasive (able to infiltrate surrounding tissue and metastasize).[59] The most common invasive subtypes are *invasive ductal carcinoma* (IDC/NST; ~80% of all breast cancer cases) and *invasive lobular carcinoma* (ILC; ~15%)[60], while ductal carcinoma in situ (DCIS) is the most frequent in situ lesion (~25%).[61] DCIS is also known to be a potential precursor to invasive disease.[59] These subtypes can differ in radiographic appearance and are therefore relevant when simulating tumor shape and margins, as discussed in the following chapters.

Molecular subtypes are often related to proliferation and tumor growth: Luminal A tumors tend to be slower growing, whereas Luminal B, HER2-positive, and triple-negative cancers typically show higher proliferation and more aggressive behavior. Triple-negative breast cancer is particularly challenging, and is also disproportionately diagnosed in younger women (often <40 years) and individuals who carry a the BRCA mutation.[62] Certain demographic groups, such as African American women in the USA, have also been shown to have higher rates of advanced cancers with poorer prognosis.[62]

Cancer growth models

Despite major advances in cancer biology, the precise biological processes that drive tumor initiation and progression are still not fully understood. Nevertheless, several mathematical models have been proposed to approximate and describe tumor growth behavior. The most common classes include exponential, exponential–linear, and sigmoidal models such as the Gompertz function (Figure 3).[63] While more complex models exist, these simpler formulations provide accurate approximations for tumor sizes within the macroscale of a clinical screening window (5-35 mm in diameter).[63]

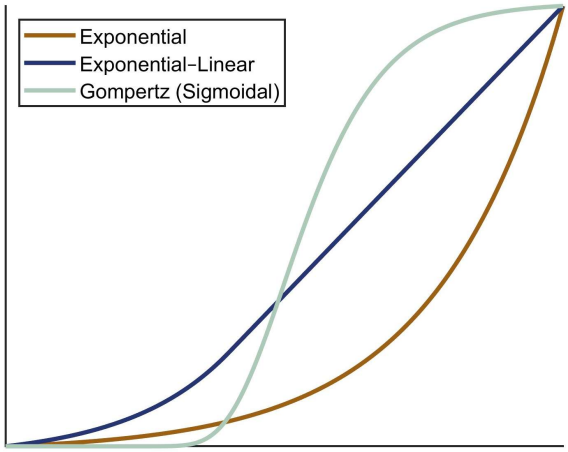

Figure 3. Common tumor growth models
Illustration of three widely used mathematical models of tumor growth: exponential growth (continuous acceleration), exponential-linear growth (initial acceleration followed by a constant rate), and Gompertz growth (sigmoidal growth with deceleration and plateau). The curves are normalized to enable direct comparison of their characteristic growth behaviors.

As the tumor grows, these accompanying biological changes also alter the surrounding tissue, often making tumors denser and stiffer compared to the surrounding normal tissues.[64] These are features that influence how tumors appear on mammographic images, as discussed in the following chapter of *Breast imaging*.

Treatment and epidemiology

Today, breast cancer management in Sweden typically involves surgery for local control, often followed by radiotherapy and adjuvant systemic therapy to reduce the risk of recurrence.[65] Systemic treatment is guided by molecular profile and may include chemotherapy, endocrine therapy, and targeted therapy toward specific markers.[65]

Because prognosis varies widely between subtypes, early and accurate diagnosis is critical. Breast imaging supports detection, characterization, and staging, enabling early and tailored treatment. In most countries, 5 and 10-year survival has had an steady increase due to earlier detection and more specialized therapies, although disparities between high- and low-income countries remain.[2,66] Reports indicate that regions in Sweden have experienced nearly a 50% reduction in 5-year mortality from the 1990s to the 2010s, with comparable declines observed in e.g. the UK.[67,68] At the same time, an important current challenge is treatment de-escalation, aiming to avoid unnecessary treatment of low-risk lesions such as some cases of DCIS or slow-growing invasive tumors.[61,69]

Breast imaging

Prior to Wilhelm Röntgen's discovery of X-rays in 1895, the detection of breast cancer relied mainly on palpation or, occasionally, post-mortem examination. Today, we know that tumors detected by palpation are at least two times larger than those found through mammography and are associated with a poorer prognosis due to more advanced disease progression.[70,71] X-ray imaging techniques have enabled us to diagnose breast cancer at earlier stages, before it presents clinically, and quickly became a cornerstone of medical imaging. It was not until the mid- to late 20th century that additional imaging modalities emerged, beginning with ultrasound and followed by advanced tomographic techniques such as computed tomography (CT) and MRI, and eventually tomosynthesis.[72] Despite these innovations, diagnostic breast imaging still relies heavily on mammography, which, more than a century later, remains the gold standard for early breast cancer detection.

Digital mammography

System components

At its core, a mammography unit relies on two key components: hardware and software. The hardware of a mammography unit (Figure 4) includes the X-ray tube which generates the X-ray spectra, detectors that capture transmitted photons, and a breast compression system that compress the breast to reduce scatter, improve image resolution, and minimize dose. Tube voltage, tube current, and exposure time are factors affecting the image quality and radiation dose.[73]

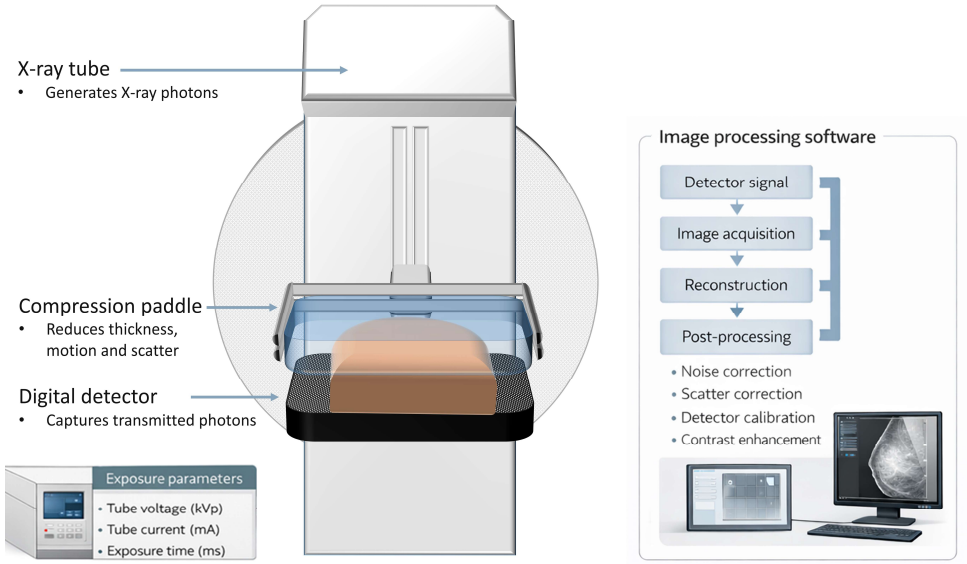

Figure 4. Schematic overview of a digital mammography unit
Illustration of the main hardware components involved in breast imaging and the associated software workflow that converts detected X-ray signals into clinically interpretable images. The reconstruction step is applied only in digital breast tomosynthesis. Illustrations adapted from originals by Magnus Dustler.

Software is required for the image acquisition and post-processing, converting raw detector signals into high-contrast, high-resolution images suitable for clinical interpretation. Additional algorithms correct for noise, scatter, and detector imperfections.

Challenges of digital mammography

Although digital mammography offers high spatial resolution and can detect microcalcifications down to ~0.2 mm in size, its fundamental limitation is its two-dimensional, projective imaging.[74-76] Because the breast is a three-dimensional structure, all anatomical components along the X-ray path are superimposed into a single 2D image. Tissue overlap can mask underlying lesions, reducing sensitivity, or create pseudo-lesions, reducing specificity.[77,78] This issue is particularly pronounced in dense breasts, where fibroglandular tissue increases X-ray attenuation and reduces contrast between lesions and surrounding tissue. To overcome these limitations, digital breast tomosynthesis was developed as a pseudo-3D technique aimed at minimizing the effect of tissue overlap.

Digital breast tomosynthesis

System components

Digital breast tomosynthesis (DBT) builds upon the physical principles of mammography (both in terms of hardware and software) but adds limited tomographic capability to reduce tissue overlap. Instead of a single projection, DBT captures multiple low-dose X-ray projection images over a limited angular range as the X-ray tube moves in an arc around the compressed breast (Figure 5). These projection images are then reconstructed into a stack of thin slices, creating pseudo-3D images, where each slice represents a different depth within the breast volume.[73]

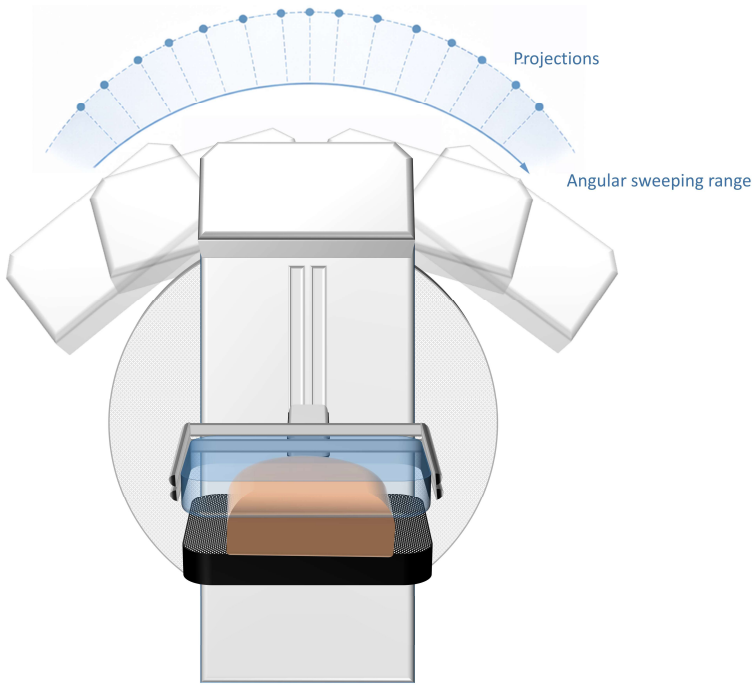

Figure 5. Schematic overview of a breast tomosynthesis unit
During breast tomosynthesis imaging, the X-ray tube moves in an arc around the breast, capturing multiple projection images along its path. The total angular range and the number of projections acquired can differ depending on the system manufacturer. Illustrations adapted from originals by Magnus Dustler.

Challenges of digital breast tomosynthesis

Clinically, DBT has demonstrated improved cancer detection rates compared to DM, particularly in women with dense breasts.[9,79,80] However, the modality introduces larger data volumes and longer interpretation times in cases when DBT is used together with DM.[81,82] In addition, DBT has shown varying effects on recall

rates, with increases reported in European screening settings, while decreases have been observed in settings with higher baseline recall rates, such as in the United States.[83] These factors highlight the importance of robust, standardized evaluation methods to ensure consistent image quality and diagnostic performance across systems and clinical settings.

Other imaging modalities

Other imaging techniques serve complementary roles. Ultrasound is commonly used for further characterization of targeted areas and as guidance for interventions such as biopsies.[73] MRI offers high sensitivity and may be particularly useful for screening high-risk populations, including women with dense breasts and those with an increased genetic risk of breast cancer.[11] Contrast enhanced mammography (CEM) provides functional information similar to MRI through contrast uptake, but is more accessible, as it can be performed on standard mammography systems with only minor modifications to filters and software.[73,84] Dedicated breast computed tomography (breast CT) is another potential breast imaging modality that provides fully 3D volumetric reconstruction, in contrast to DBT.[73] These modalities are not routinely used for population based screening and are beyond the primary scope of this thesis. However, they are being explored for more personalized screening strategies, for example MRI for women at high risk of breast cancer or MRI/ultrasound for women with extremely dense breasts.[85,86]

Radiographic characteristics of breast lesions

On radiographic images, such as DM and DBT, lesions typically present in one of three forms: as a mass, as calcifications, or as architectural distortion.

Masses

Breast masses typically appear as brighter (hyperdense) areas on radiographic images and can be either benign or malignant. They are commonly assessed using the BI-RADS malignancy classification, which visually describes lesion appearance (Figure 6-7).[52] Masses are characterized by size, shape, and margins: malignant tumors often appear irregular, spiculated, or infiltrative (Figure 8), whereas benign lesions are usually round or oval with smooth edges (Figure 9).[52] Both IDC and ILC mainly appear in mammographic images as masses with irregular shapes and non-circumscribed margins, often spiculated.[87] Either subtype can also present themselves as architectural distortions, as detailed below.[87] However, ILC is known to be slightly more difficult to assess as they generate less fibrotic tissue and tend to have less hyperdense appereances.[88]

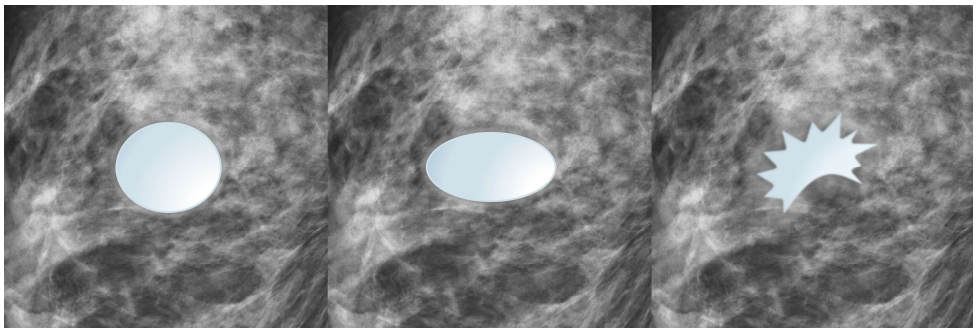

Figure 6. BI-RADS (5th Edition) categories of breast mass shapes
Schematic illustrations of mass shapes, from left to right: round, oval, and irregular.

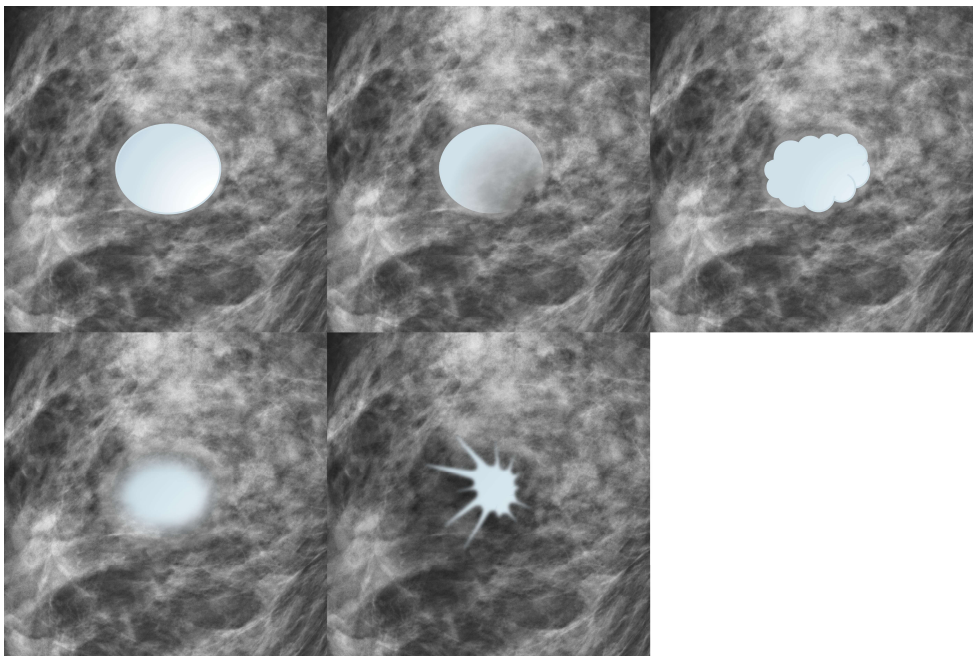

Figure 7. BI-RADS (5th Edition) categories of breast mass margins
Schematic illustrations of different margin types, shown from left to right (top row first, then bottom row): circumscribed, obscured, microlobulated, indistinct, and spiculated.

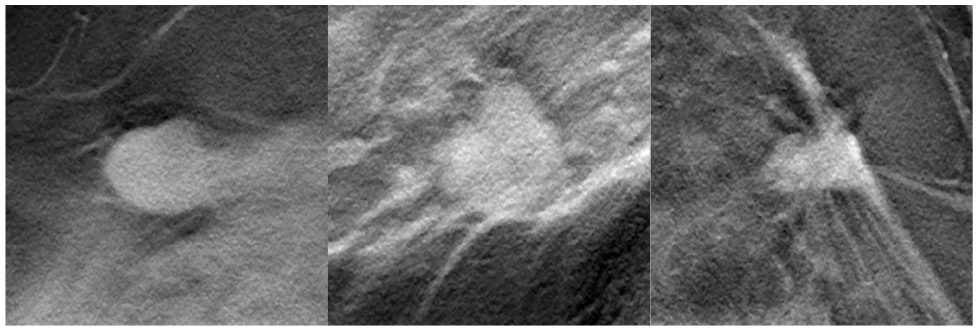

Figure 8. Malignant breast masses with different margin characteristics
Representative case examples of three biopsy-proven malignant breast masses, shown on DBT images. The leftmost lesion has partly indistinct margins, while the middle lesion has a microlobulated margin, where the edges form several small rounded bumps rather than a completely round outline. The third mass is spiculated, meaning that thin lines radiate outward from the lesion into the surrounding tissue, creating a star-like appearance.

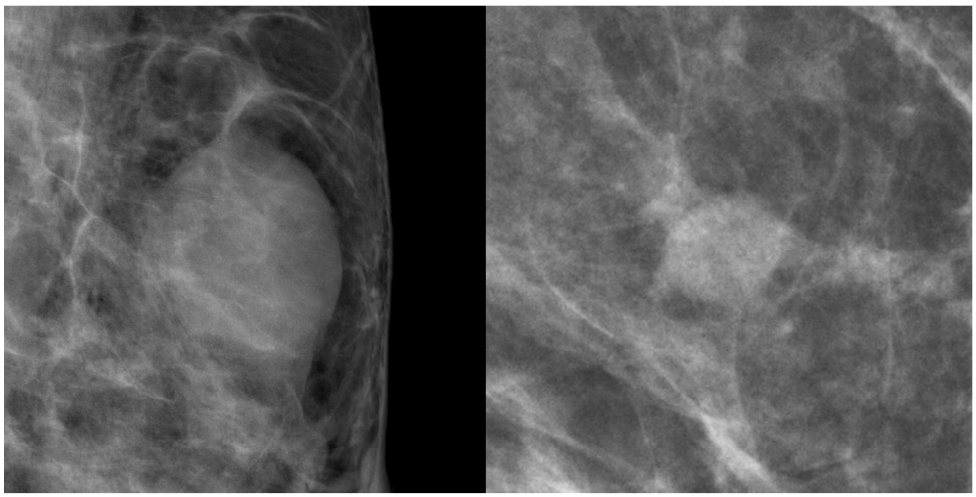

Figure 9. Benign breast masses
Representative DM images showing round, well-circumscribed cysts with smooth margins and relatively uniform internal density. The cysts demonstrate similar radiographic density to surrounding fibroglandular tissue.

Recent advances in image analysis enable quantitative analysis of lesions through radiomics. Radiomics is the extraction and analysis of large amounts of quantitative features from medical images, capturing tissue characteristics such as intensity, shape, and texture that are not always visible to the human eye.[89] These metrics provide additional information beyond visual inspection and may aid in distinguishing benign from malignant masses.[53]

Microcalcifications

Calcifications are a common benign finding associated with the normal aging process, particularly within the ducts. However, certain morphologic patterns of calcifications may indicate early stages of carcinoma, specifically DCIS.[59] Malignant calcifications are typically fine, clustered, and localized (Figure 10). Benign calcifications are usually larger and more diffusely scattered within the breast tissue.[52]

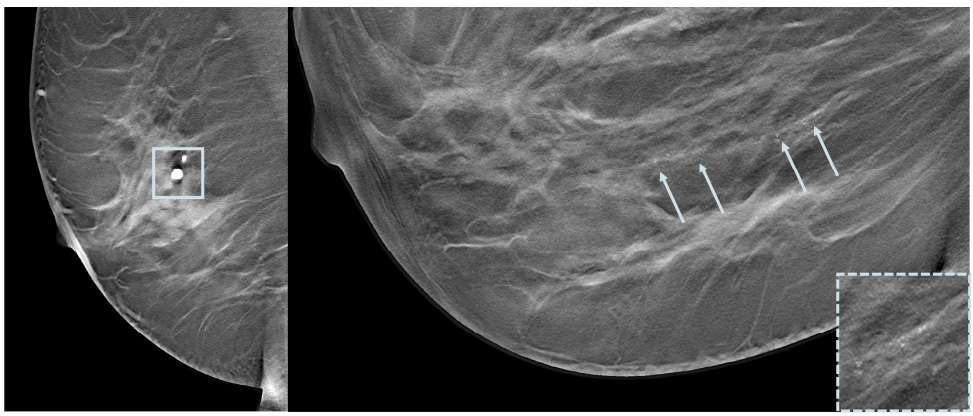

Figure 10. Microcalcifications
DBT images of benign calcifications (left) and malignant calcifications (right). The benign calcifications are larger, coarser, and more conspicuous/high-attenuation. In contrast, the malignant calcifications are fine and tightly clustered, with a linear/segmental distribution suggestive of ductal involvement.

Architectural distortion

Architectural distortion refers to a disruption of the normal breast tissue pattern, where normal tissue lines appear pulled or distorted without a distinct mass.[52] It may result from benign causes, such as fibrosis or postsurgical scarring, or from malignant processes, including IDC or ILC (Figure 11).[87]

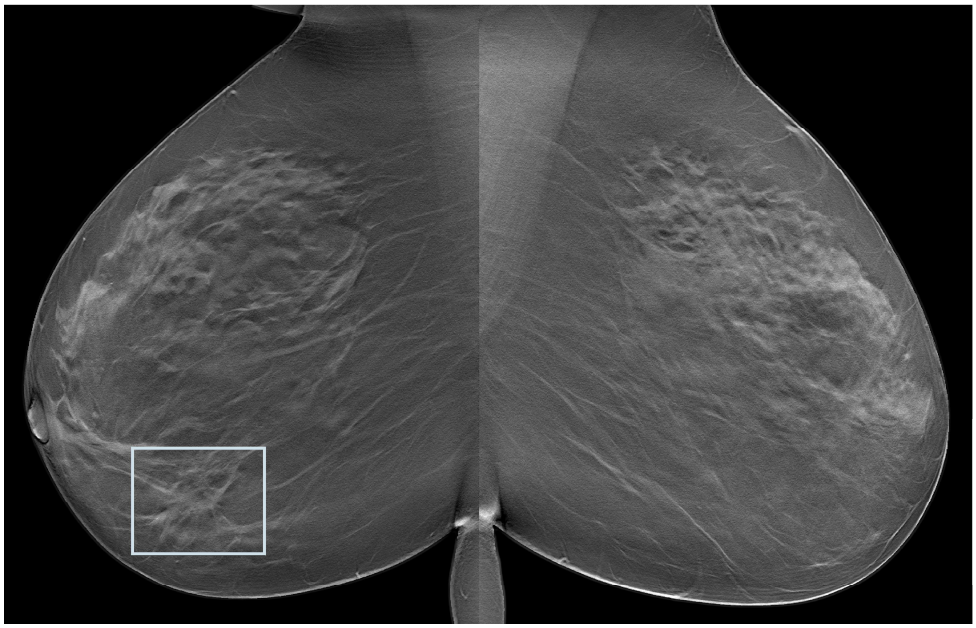

Figure 11. Architectural distortion
DBT slices of the right and left breasts are shown. The area of architectural distortion is highlighted within the black box, demonstrating a clear structural asymmetry between the two breasts. This finding is associated with a biopsy-confirmed breast malignancy.

Breast cancer screening

A historical perspective

Beginning in the mid- to late 20th century, screening programs were developed and studied as a way to detect cancers at early stages, before they became symptomatic. The first randomized controlled trial designed to evaluate the impact of breast cancer screening on mortality began in 1963 (the HIP trial)[90], and was followed by several additional trials during the 1970s and 1980s.[91] Sweden was one of the pioneering countries to investigate breast cancer screening using mammography through studies in the 1970s, although the Swedish national screening program was not clearly established until the 1990s.[8,92-95] Early evidence demonstrated that screening reduced breast cancer specific mortality by enabling detection of tumors at earlier, more treatable stages.[3] Sweden has since been part of transitioning screening from film-based mammography to digital systems in the early 2000s, and today advancing into the era of tomosynthesis, synthetic images, artificial intelligence and machine learning.[96-101]

Overview of current practices

Screening programs differ slightly between countries when it comes to the targeted age and screening frequency. Currently, The Swedish National Board of Health and Welfare recommend inviting Swedish women aged 40–74 to participate in routine mammographic screening every 18–24 months, depending on age.[65] Two digital mammograms of each breast are acquired in craniocaudal (CC) and mediolateral oblique (MLO) views (Figure 12), and each examination is independently interpreted by two radiologists (double reading) as advised by the European guidelines.[102] Double reading is standard practice in Swedish mammography screening, however, AI-assisted reading has more recently been evaluated as an alternative to the second reader.[98] As a result of growing evidence, several Swedish regions began implementing AI-supported mammography screening in routine practice as of 2025.[103]

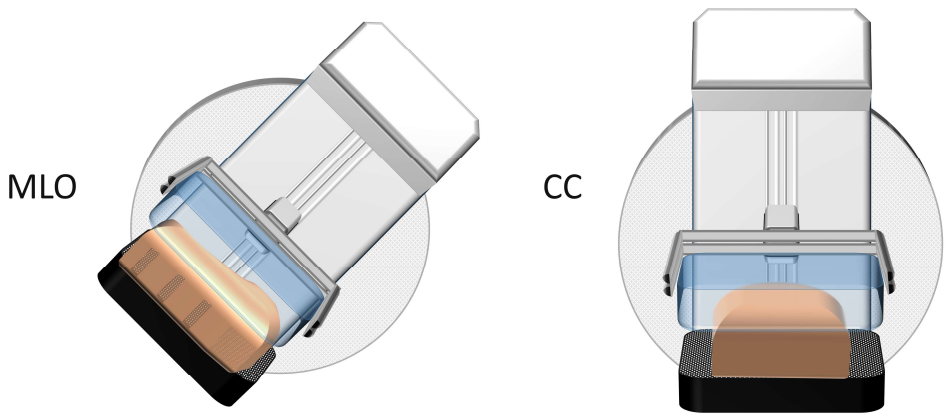

Figure 12. Schematics of MLO and CC views
In the MLO view the unit is tilted and the breast is positioned against the detector and the armpit high on its upper corner. In the CC view the unit is horizontal and the breast is placed on top of the detector. Illustrations adapted from originals by Magnus Dustler.

Most countries invite women aged 50–70 for screening, whilst other may follow slightly different invitation schemes.[104] In the United States, DBT has already been incorporated into population-based breast cancer screening programs.[105,106] In contrast, Sweden currently continues to utilize DM as the standard modality for national screening, a decision that remains somewhat debated given the growing evidence supporting the potential benefits of DBT in screening contexts.[107]

Challenges of breast cancer screening

Screening with mammography has been shown to reduce breast cancer-specific mortality, however, several challenges remain. From a technical perspective, these challenges primarily relate to minimizing interval cancers, missed cancers, recall rates, and overdiagnosis.[69,107,108] Interval cancers are cancers that arise in between two screening rounds, and are often aggressive and fast growing.[109] They differ from missed cancers, in that they were not present at the time of the previous screening. Missed cancers are lesions that were present but not detected at the previous screening, often because they were obscured by dense breast tissue or limited by suboptimal image quality or resolution.[107] Dense breast tissue not only masks cancers but also reduces image contrast between normal and malignant structures, thereby complicating lesion detection and interpretation.[37] High recall rates are largely driven by false-positive findings, frequently caused by overlapping normal tissue structures that mimic suspicious lesions.[107] Overdiagnosis leading to overtreatment represents another complex issue, referring to the detection of cancers or precancerous lesions that would not have become clinically significant within the patient's lifetime.[69,110] Distinguishing such cases from clinically relevant cancers remains a major challenge in screening programs.

Future perspectives

Many of these challenges could potentially be addressed through individualized screening strategies that stratify women according to their risk profiles. For example, by incorporating breast density assessments into screening protocols, thereby allowing women at higher risk or with dense breasts to be referred to imaging modalities with higher sensitivity, such as MRI.[10,11] Artificial intelligence and radiomics also hold promise for enhancing lesion detection and characterization beyond the capabilities of the human eye.[12,111] To ensure that these emerging technologies and tailored screening approaches truly improve diagnostic performance and clinical outcomes, it is essential to establish robust evaluation frameworks that can rigorously assess their effectiveness under controlled and reproducible conditions.

Virtual imaging trials

Introduction

Motivation for virtual imaging trials

Detecting abnormalities in the breast relies on the imaging modalities to provide sufficient image quality, and on the effectiveness of the screening program in identifying lesions at an early stage. As mentioned earlier, the current program is still a one-size-fits-all solution.

Evaluation of breast imaging technologies and screening efficacy, in terms of sensitivity and specificity, has traditionally relied on a mix of clinical studies and technical experiments. Clinical trials and reader studies offer real-world insights but are often limited by cost, ethics, and repeatability. Technical studies, using physical phantoms provide controlled, reproducible measurements of image quality. However, they fail at capturing the full complexity and variability of real breasts.

These challenges, including imperfect ground truth and inter-reader differences, highlight the trade-off between realism and control. Virtual imaging trials (VITs) have emerged as a tool that enable fully controlled, reproducible simulations of anatomy (computational phantoms), imaging physics, and observer behavior, providing a complement to clinical and phantom-based studies.

A brief history

The terms "virtual imaging trials", "virtual clinical trials" or "in silico trials" were first introduced in the early 2000's when the movement of computational breast phantoms truly gained momentum through the development of simulation frameworks such as OpenVCT, DukeSim and VICTRE.[112-114] These newer phantoms offered more realistic anatomical detail compared to earlier models[115], incorporating structures such as ligaments, glandular tissue, skin, and a variety of lesion types. An important milestone for the adoption of VITs was the VICTRE initiative, through which the US Food and Drug Administration (FDA) demonstrated how in silico clinical trials can provide credible evidence to support regulatory decision-making for imaging systems.[116] The FDA has since recognized that in silico evidence can be used to support regulatory submissions, provided its credibility is demonstrated for the specific context of use.[117] Today there is a large number of software and frameworks available for simulating imaging trials.[18] A list of some of the existing software developments is provided in Table 1, including STELLA-R framework (Paper III).

Table 1. Overview of existing simulation frameworks
A selection of virtual imaging trial frameworks. The list is limited to frameworks included in the VITM survey, additional tools and frameworks may be available beyond those included.[18] The majority of the breast imaging frameworks focus on digital mammography and digital breast tomosynthesis, although XRAYImagingSimulator also includes phase-contrast breast imaging. The STELLA-R framework was formally deployed under its name as part of this thesis (Paper III), but earlier demonstration versions existed.

Framework	Origin (institution type)	Main modality focus
BreastSimulator[118]	Academic (University of Varna)	Breast imaging
XRAYImagingSimulator[119]	Academic (University of Varna)	Breast imaging
CatSim/XCIST[120]	Industry (GE Healthcare)	X-ray/CT
XCAT/DRASIM[121]	Industry (Siemens)	CT
DukeSim[113]	Academic (Duke University)	CT
Hybrid Tool[122]	Academic (KU Leuven)	Breast imaging
CBCT Tool[123]	Academic (KU Leuven)	CBCT
OpenVCT[112]	Academic (University of Pennsylvania)	Breast imaging
VICTRE[116]	Regulatory (U.S. Food and Drug Administration)	Breast imaging
STELLA-R[124]	Academic (Lund University)	Breast imaging

The field has continued to expand, supported by dedicated conferences, organizational task groups, and workshops that foster ongoing research and collaboration, highlighting the growing recognition of VITs as a valuable tool for both scientific investigation and regulatory assessment of medical imaging technologies.[20,125,126]

Basic principles

A virtual imaging trial consists of four essential simulation components (or modules), each representing a critical aspect of the simulation process. Figure 13 provides an overview of each module, sequentially ordered from left to right, and the following subsections describe each module in detail.

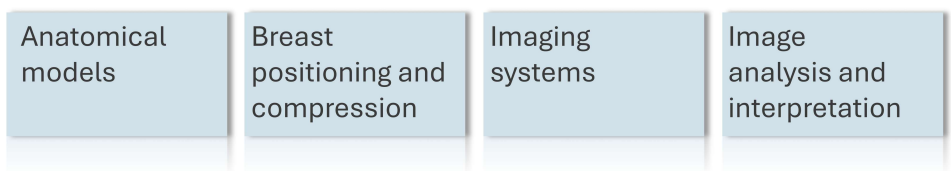

Figure 13. Principles of virtual imaging trials in breast imaging
Virtual imaging trials are built by modeling the full imaging chain, shown here in sequential order: the breast phantom, breast positioning and compression, the imaging system, and image analysis and interpretation. Together, these modules simulate how images are formed and evaluated in a clinical setting.

Anatomical models

Models of the breast

Over the years, several approaches have been developed to model breast parenchyma. Both OpenVCT and VICTRE base their breast phantoms on compartmental models, to simulate regions of adipose and fibroglandular tissue, though they differ in how these compartments are generated. OpenVCT utilizes region-growing algorithms to create anatomically plausible tissue regions[127], whereas VICTRE grows cell-like structures from preallocated seed points using a Voronoi-based approach (Figure 14).[128]

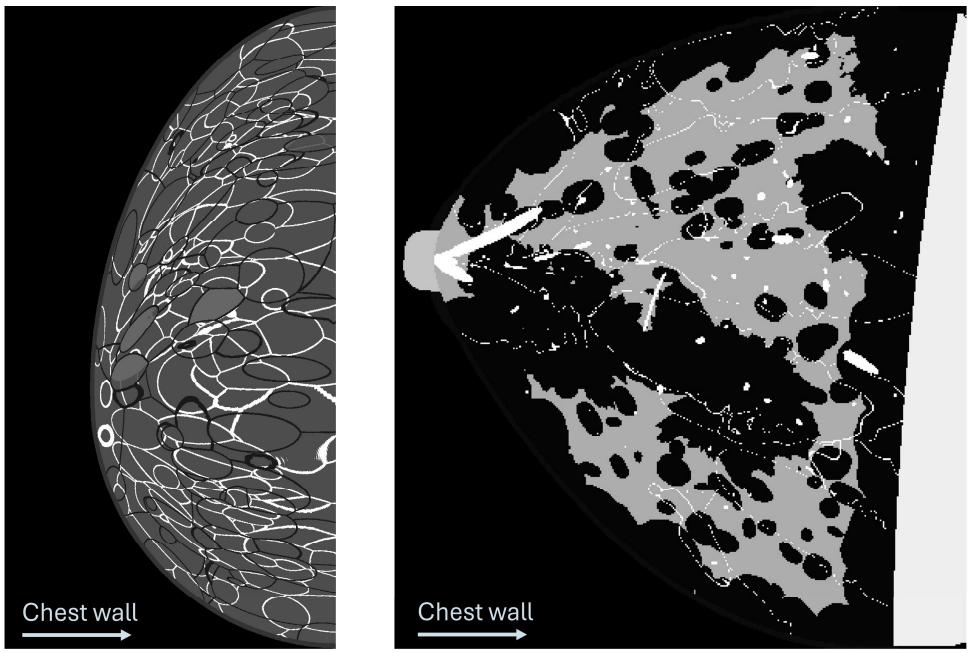

Figure 14. Computer simulated breast models
A cross-sectional slice from three-dimensional computational breast phantoms generated using OpenVCT (left) and the VICTRE phantom generation framework (right). Both images show a transverse slice through the phantom. Arrows indicate the chest wall direction.

Noise based approaches, such as power-law noise, have also been applied to simulate breast tissue.[129] Power-law noise is particularly suited for this purpose because it reproduces the anatomical noise observed in mammographic images.[130-133] However, although it reflects the statistical properties of tissue, it lacks precise spatial control, limiting its ability to generate e.g. specific tissue features.

More recently, procedural methods such as Perlin noise, have been introduced as a controllable and reproducible means of generating complex, natural looking tissue patterns.[134,135] Through its algorithmic construction, Perlin noise enables realistic simulation of fibrous strands, glandular clusters, and overall parenchymal texture, forming the basis of the computational phantoms presented in this thesis.[136] A more detailed explanation of Perlin noise is presented in the subsequent section.

Models of breast abnormalities

Several strategies have been explored for modeling soft tissue breast lesions (masses), which can be broadly divided into mathematical models and models based on real masses.[19] Mathematical models are generated using algorithms to create lesion shapes. Many approaches use simple 3D geometric shapes, such as spheres or ellipsoids, which could be combined or overlapped to produce more irregular masses. [137-139]

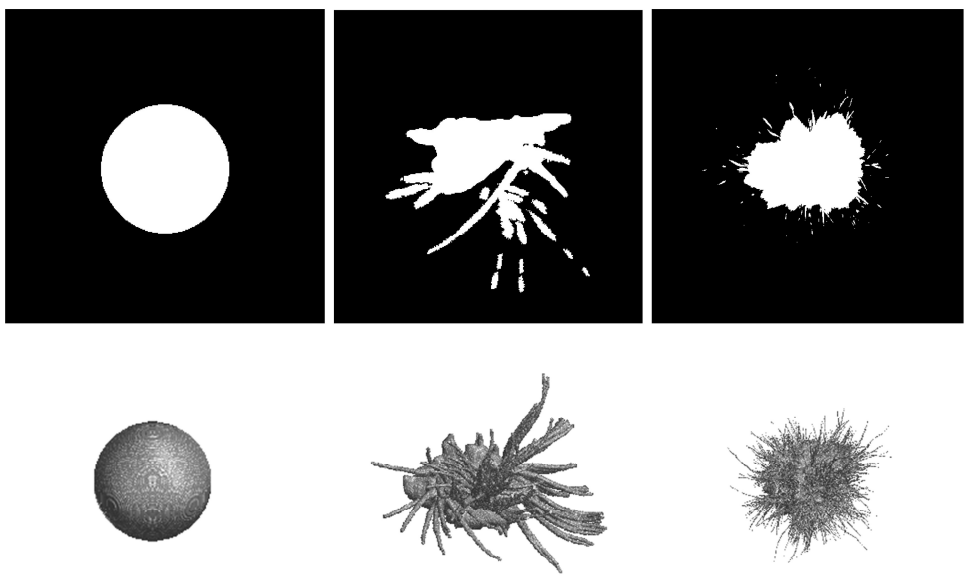

Figure 15. Computer simulated breast lesions
Top row: Cross-sectional slices of breast lesions generated using OpenVCT (left and middle) and VICTRE (right). Bottom row: Corresponding three-dimensional visualizations of the same lesions.

Some models represent tumors as concentric layers, with a central core surrounded by shell-like layers.[137] More advanced mathematical methods use simple shapes as a base but include stochastic growth algorithms, such as iterative branching, random walks, or diffusion-limited aggregation, which produce irregular or spiculated surfaces.[140-142]

Models based on real tumors use patient images as a starting point. These methods typically involve segmenting actual lesions from CT or MRI scans to capture 3D structure, or extracting key features, which can then guide the generation of simulated lesions.[142-144] Figure 15 presents three examples of different lesion models.

Perlin noise

Most of the phantoms developed and used in this thesis are derived based on the Perlin noise algorithm.[145-147] Perlin noise is a procedural, gradient-based noise used to generate smooth and natural looking structures. Unlike uncorrelated stochastic noise, such as Gaussian noise which changes randomly from voxel to voxel, Perlin noise produces spatially continuous patterns. It is constructed by assigning pseudorandom gradient vectors to a grid and interpolating between them across space (Figure 16).

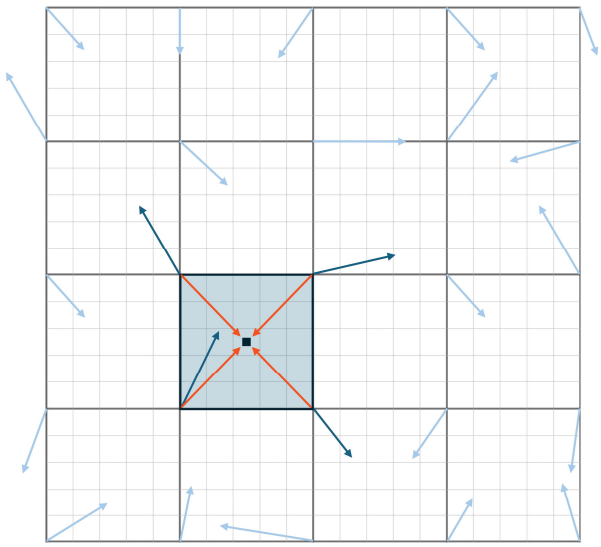

Figure 16. Two-dimensional Perlin grid
Illustration of a two-dimensional grid, where each corner contains a random vector (noise gradient). To compute the value at the selected pixel, a vector is formed from each grid corner to the pixel (orange arrow), and the dot product with the corresponding gradient vector is calculated. As a final step, the four dot products are interpolated to obtain the final pixel value. The same procedure can be generalized to arbitrary dimensions.

The result is a repeatable and visually smooth function whose frequency and amplitude can be adjusted, or combined across multiple octaves, to control the level of detail (Figure 17). The level of control makes Perlin noise well suited for creating realistic textures and natural structures.

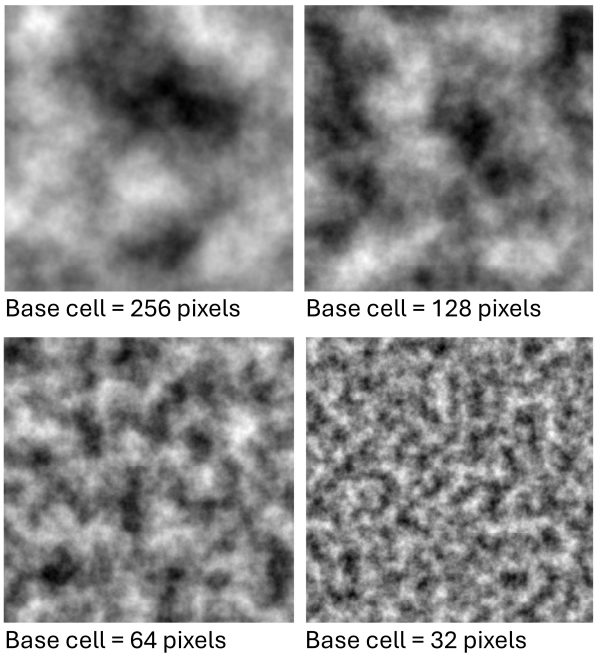

Figure 17. Perlin noise at different grid scales
Examples of Perlin noise generated using different grid cell sizes, ranging from 256 pixels to 32 pixels. Each image shows the sum of six superimposed octaves, where the base cell size defines the largest-scale structures in the noise pattern.

The concept of Perlin noise was first introduced by Ken Perlin in 1985, who described it as a novel algorithm for computer-generated imagery (CGI).[146] The technique was designed to create natural looking textures and structured surfaces on computer generated 3D objects. Since its introduction, Perlin noise has become a cornerstone of CGI, with widespread use in the gaming, film, and animation industries to simulate realistic natural phenomena such as terrains, clouds, and materials.

In the 2010s, Perlin noise began to attract attention in the field of computational breast modeling. A pioneering study by Dustler et al. demonstrated how its principles could be used to simulate tissue textures resembling those observed in mammographic images.[134] In observer studies involving radiologists, approximately 43% of Perlin noise-based image patches were mistaken for real mammographic images, underscoring its potential for realistic tissue simulation.[136]

Since then, Perlin noise has been adopted by other research groups, including integration with the VICTRE simulation pipeline.[145,148] It has also inspired the development of alternative or refined noise-based functions to further improve realism of simulated mammographic images.[149]

Modeling of breast positioning and compression

Breast positioning and compression is typically modeled using finite element methods, in which the structural components of the phantom are represented as a mesh of discrete elements.[150-154] Mechanical properties such as stress, strain, and material elasticity are applied to these elements to simulate realistic deformation of the phantom under compression forces (Figure 18).

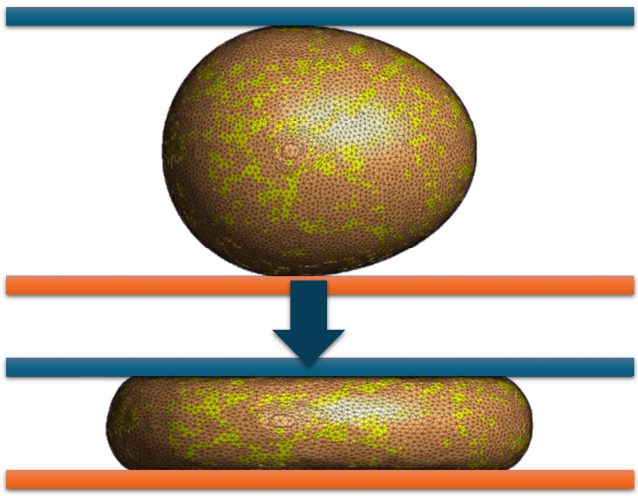

Figure 18. Finite element compression of a Perlin noise phantom
Illustrative example of a finite element simulation in which external forces are applied to compress a deformable virtual phantom generated using Perlin noise, simulating the breast compression experienced during mammographic screening. Image courtesy of John-Henry Markbo.

Modeling of imaging systems

Simulating an imaging system requires the use of a ray-tracing algorithm, such as the Monte Carlo (used by VICTRE) or Siddon algorithm (applied in OpenVCT and the OPTIMAM platform)[155-157], to model the propagation of individual photons through the material. Each photon's path is tracked as it interacts with the medium primarily through absorption and scattering processes. Every voxel within the simulated volume is assigned a material with a corresponding attenuation coefficient, which determines the probability that a photon will be absorbed or scattered. Based on these interactions, the cumulative photon trajectories are used to generate a projection image, based on specific geometric configuration and acquisition parameters of the imaging system. This resulting dataset represents the raw projection prior to any image reconstruction or post-processing steps.

Additional noise and scatter models can be applied to give a more realistic image appearance.[158]

Image analysis and interpretation

For a fully virtual study, interpretation and evaluation of imaging systems is ideally performed through model observers, ensuring reproducibility and scalability. A typical example is the Channelized Hotelling Observer (CHO) model, which is commonly used.[17,156] The CHO mimics how the human visual system processes images by filtering them into different spatial frequency bands (or "channels") and then measuring how well a signal, such as a lesion, can be distinguished from background noise.

More recently, AI-based observers, particularly those using deep learning (e.g., convolutional neural networks), have been developed as an alternative.[17,159-161] These models learn directly from image data to identify subtle patterns or features that distinguish signal-present from signal-absent cases.

Challenges of virtual imaging trials

VITs provide a powerful framework to systematically control imaging and anatomical parameters, enabling the simulation of diverse real-world clinical scenarios under reproducible conditions. This level of control allows researchers to isolate specific factors influencing image quality, lesion detectability, and diagnostic performance. These are capabilities that are often difficult or impossible to achieve in traditional clinical studies.

However, current models have limitations in achieving full realism. Many lesion models rely on simple geometric shapes that do not capture the complex morphology of real tumors, so features such as lesion shape, margin irregularity, and internal texture may be poorly represented. Algorithms can reproduce jagged spicules, but often fail to model internal heterogeneity or integrate tumors naturally within surrounding tissue.[17,19] Models based on real tumors are limited by the dataset, require labor-intensive segmentation, and allow little opportunity to introduce new variation, making it difficult to generate diverse, controllable lesions.[17,19]

Moreover, the generation of virtual populations is typically not sampled from real-world demographic or physiological distributions. Although parameters such as breast density, size, and glandular composition are informed by clinically reported values, they are generally implemented as representative settings rather than drawn from real-world population data. Notably, existing review studies of virtual imaging trials do not report any work in which virtual populations are generated by direct sampling from real patient cohorts, indicating a lack of population-level representativeness.[17,156]

Finally, at the time this thesis was initiated, existing models were typically static, representing a single time point rather than capturing temporal changes in the tumor or breast parenchyma over time. This remains largely true today, however, at least one recent study has begun to incorporate temporal components (e.g., explicit tumor growth) into breast dedicated VIT pipelines.[162] At present, this approach is not connected to real-world, patient-specific growth rates which limits their ability to support clinically grounded, time-dependent investigations. Incorporating patient-specific longitudinal or dynamic modeling would be essential to simulate disease progression, treatment response, and other temporal phenomena, thereby enhancing the biological and clinical realism of virtual imaging trials.

Aims

This thesis aims to advance virtual imaging trials for breast imaging by improving the realism of computational phantoms and virtual populations, and by enabling longitudinal modeling based on real-world data. To achieve this, the thesis aims to:

- Enhance the realism of tumor models to more accurately reflect biological (tumor growth) and radiological characteristics (tumor appearance).
- Improve the realism of virtual populations to accurately reflect real-world populations, in terms of anatomical and physiological characteristics.
- Develop a virtual imaging trial framework capable of performing longitudinal simulations of breast and tumor changes over time.
- Demonstrate that the developed tumor models can be used in a virtual imaging trial to evaluate cancer detection performance across women's subgroups.

Methods

Simulating human anatomy and its temporal changes is inherently complex, and describing the methods behind such an extensive body of work is equally challenging. To provide as much clarity as possible, the Methods section is organized around the central methodological themes of this thesis: anatomical modeling, population modeling, and longitudinal modeling. In addition, imaging simulation pipelines, image analysis and observer studies, computational and programming tools, and statistical methods are presented as supporting techniques used for validation.

Anatomical modeling

Central to Papers II and III is the development and optimization of virtual breast phantoms, including computational models of both parenchymal tissue (Paper III) and breast lesions (Papers II and III). Perlin noise has been widely used for generating three-dimensional computational breast models and serves as a foundation for much of this work, while other modeling approaches were applied in Papers I and IV. This section therefore describes the methods used to construct the anatomical models that are used throughout the papers included in this thesis.

Perlin noise

An in-house Perlin noise algorithm was used as the foundation for generating the soft tissue breast lesion and parenchymal models described in Papers II–IV.[134,135] The algorithm, implemented in MATLAB (MathWorks Inc., Natick, MA, USA), generates 3D blocks of Perlin noise, with each block representing a single octave at a desired frequency. The appearance of Perlin noise can be controlled by two parameters, persistence and lacunarity. Persistence controls the amplitude of each octave, determining the contribution of finer details to the overall texture, while lacunarity determines the frequency scaling between octaves (Figure 19). Individual octave blocks are then superimposed to produce a combined volume (Figure 19). Additional mathematical functions are applied to enhance or suppress specific structures. Several volumes are created, binarized through thresholding (Figure 20) and combined into the final 3D visualization of breast tissue (Figure 21).

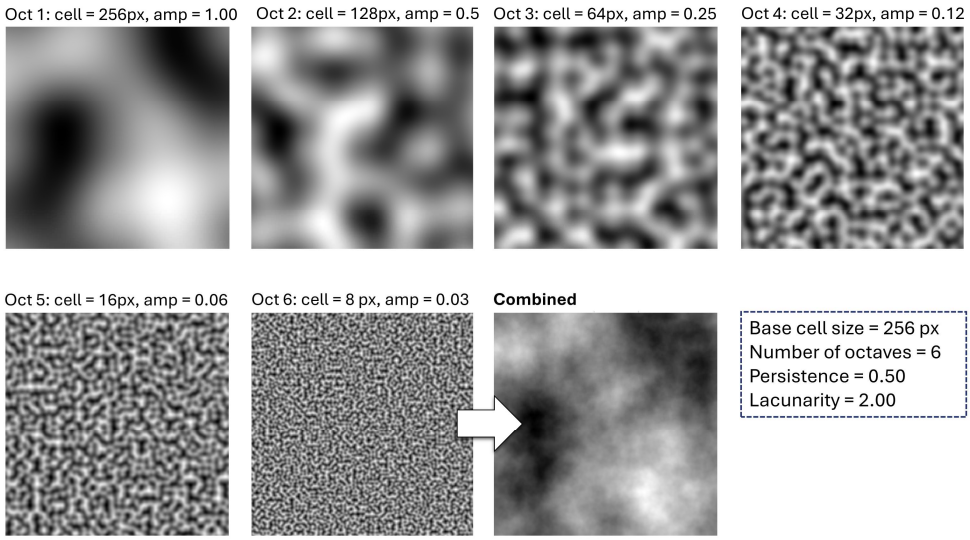

Figure 19. Perlin noise octaves
Examples of individual Perlin noise octaves (oct) are shown. The persistence is set to 0.5, meaning that the amplitude (amp) is reduced by half for each successive octave. A lacunarity of 2 indicates that the spatial frequency doubles at each octave, corresponding to a halving of the grid cell size in terms of number of pixels (px). Finally, the six octave volumes are superimposed to produce the resulting combined noise volume.

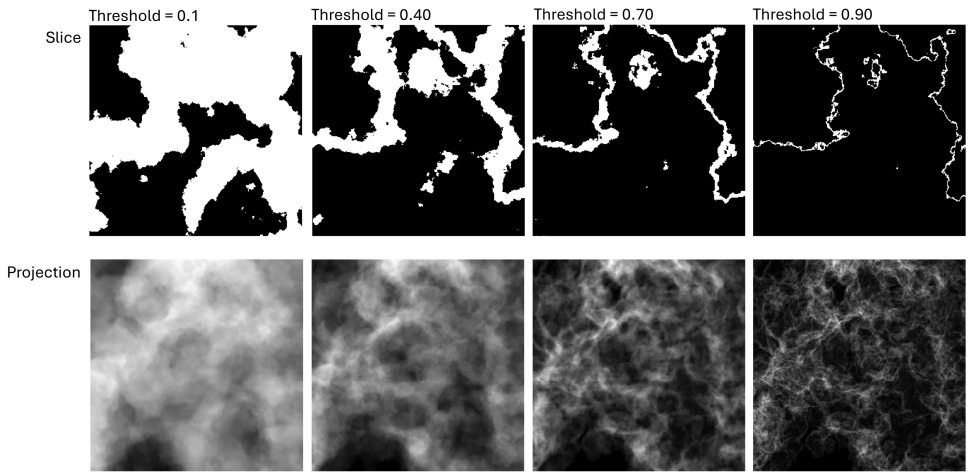

Figure 20. Perlin noise thresholding
Applying different threshold levels to the combined Perlin noise volume produces varying structural patterns and shapes. The columns show different threshold values, with the top row displaying a slice through the phantom and the bottom row showing the corresponding projection formed by summing the voxel values through the volume.

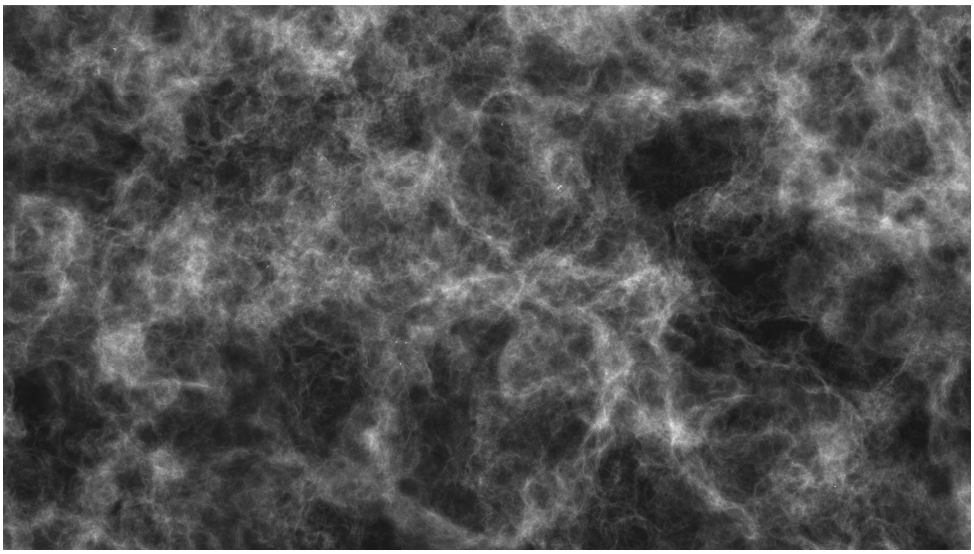

Figure 21. Final Perlin noise volume
The final breast tissue representation based on Perlin noise, generated by combining several thresholded volumes, such as those illustrated in Figure 20. Image courtesy of Magnus Dustler.

Breast parenchyma modeling

In Paper I, we worked within the OpenVCT framework and used its built-in virtual breast phantoms.[112] These phantoms provided a ready foundation for simulating breast anatomy, allowing us to focus on modeling tumor growth.

In Paper II, our work shifted toward the in-house Perlin noise algorithm, which we used to generate the breast parenchyma and in Paper III, we optimized this technique further. Specifically, we introduced masking techniques to highlight dense tissue regions and systematically applied thresholding to the Perlin noise to control how much structure appeared in the simulated breasts. This made it possible to create a wide range of breast appearances with different amount of breast density. For both Papers II and III, these simulated tissues were placed within realistic breast outlines generated from the breast shape models proposed by Rodríguez et al.[163,164]

In Paper IV, we combined real and simulated data in a hybrid approach. Instead of creating the entire breast phantom computationally, we used real DBT breast images and inserted simulated lesions into them. This allowed us to study lesion detectability under controlled conditions while maintaining the realism of real-world clinical images.

Lesion modeling

In Paper I, we used the lesion models already available in the OpenVCT pipeline. These consisted of simple spherical masses with a basic shell-like internal structure.[127] They served as a practical starting point for simulating tumor growth.

In Paper II, the goal was to generate more complex and more realistic lesion shapes using the Perlin noise algorithm. We began by defining a geometric base shape and modifying its spatial domain with Perlin noise patterns. By tuning parameters such as persistence and lacunarity, we were able to control both the overall shape and the margin characteristics. This allowed us to produce a wide range of lesion morphologies resembling those encountered in clinical imaging, as defined by BI-RADS malignancy scoring system.[52] The attenuation properties of the simulated lesions were selected using values similar to those in OpenVCT and were further optimized with input from radiologists.

In Paper III, we extended the lesion model from Paper II. To ensure that lesions blended more naturally with the surrounding parenchyma, we retained and enhanced the background tissue structures within the lesion region. We also incorporated additional Perlin noise components to represent features such as abnormal vascularity and fibrosis. These additions provided the lesions with richer internal texture compared to the lesions presented in Paper II.

In Paper IV, we introduced a hybrid lesion model. Here, the spiculated outlines generated by the VICTRE pipeline[114,148] were combined with the Perlin noise-based lesion interiors developed in Papers II and III. This hybrid approach enabled the simulation of spiculated masses with detailed internal structure, making them suitable for controlled insertion into real DBT images.

Population modeling

The initial concept for this thesis originated from the motivation to model a virtual continuation of the Malmö Breast Tomosynthesis Trial (MBTST)[96], as detailed in the following section. It soon became evident that such an extension would require modeling the underlying characteristics of the study population, as well as capturing how these characteristics evolve over time. This led to the central idea of developing methods to construct virtual populations. Since then, population modeling has been an essential component of nearly all papers in this thesis. Here, the term “population modeling” refers to fitting statistical or probabilistic distributions that describe the behavior and variability of real-world population data. Once estimated, these distributions were used to generate virtual populations by sampling from them.

In Paper I and III, such models were used to reproduce real-world characteristics and, in Paper III in particular, to investigate how variables co-vary and evolve over time in time-dynamic simulations. Paper II focused on optimization of the lesion model and therefore did not rely on a population model, while Paper IV used an actual real-world study cohort rather than a virtual one. The four primary study populations mentioned throughout the thesis papers and their roles across the papers are described in the following subsections.

Table 2 provides an overview of the study populations, simulation frameworks and software components used throughout the papers (I–IV).

Table 2. Overview of simulation frameworks and software used in the thesis studies
Frameworks and software used across Papers I–IV, presented in the order they are applied within the VIT simulation pipeline.

Study	Study Population	Phantom Generation	Lesion Generation	Imaging Modality	Image Generation	Image Processing	Image Reconstruction	Image Analysis and Interpretation
I	Malmö tumor cohort[165] + MBTST[96]	OpenVCT[112]	OpenVCT[137]	DM Hologic	OpenVCT[112]	Briona	-	Human interpretation + statistics
II	-	In-house Perlin noise algorithm + Radboud breast outlines[163,164]	In-house Perlin noise algorithm	DM Siemens	OpenVCT[112]	Local Siemens unit	-	Human interpretation + statistics
III	Malmö DM Screening Population[166,167] + MBTST[96]	In-house Perlin noise algorithm + Radboud breast outlines[163,164]	In-house Perlin noise algorithm	DBT Siemens	OpenVCT[112]	USP noise[168]	Vimieiro et al.[169]	Statistics
IV	Pennsylvania cohort	Real breast images	VICTRE[114] + In-house Perlin noise algorithm	DBT Hologic	-	Hologic Modulation Transfer Function	Vimieiro et al.[169] + Briona	Barco Medical Virtual Imaging Chain (MeVIC)[170] + radiomics + statistics

Study populations

Malmö Breast Tomosynthesis Screening Trial

MBTST[96] was a prospective screening study conducted in Malmö, Sweden between 2010 and 2015. MBTST aimed to compare DBT with DM in a screening setting and showed that DBT detected 34% more cancers than DM, with 40% lower odds of interval cancers.[96,166] The trial enrolled a randomly selected sample of women, aged 40–74, from the routine national screening programme during the same period. Participants underwent the standard two-view (MLO and CC) DM protocol as well as an additional one-view (MLO) DBT examination.

Of the 21 691 women invited, 14 851 agreed to participate. Pregnant women and individuals who did not speak Swedish or English were excluded, and three participants subsequently withdrew consent. In total, the MBTST population contained 139 screen-detected cancers, of which 110 were masses. Additional methodological details and population characteristics are provided in the full MBTST publication.[96]

The MBTST dataset served two specific purposes in this thesis. First, age distributions used for generating the virtual population in Paper I were sampled from MBTST. Second, pathological tumor sizes from this population were used to create realistic tumor size distributions for the VIT pipeline developed in Paper III.

At the time Paper I was prepared, the MBTST cohort already existed as a fully processed, ethics-approved dataset, which made it immediately suitable for early methodological development. In addition, MBTST was the only available population-based dataset with measured tumor sizes, needed to model realistic tumor sizes in Paper III. For these reasons, MBTST data were used in Papers I and III instead of the full Malmö DM screening population.

Malmö DM screening population

The Malmö DM screening population consists of the remaining women that attended the routine screening programme at Skåne University Hospital in Malmö between 2010 and 2015 (i.e., women not included in MBTST), and includes all routine two-view DM examinations.[166,167] All examinations were acquired on Siemens mammography systems, and the full dataset forms part of the M-BIG image database[171], which has since been expanded. The Malmö DM screening population therefore represents the complete real-world screening population during this period.

For the analyses in Paper III, a refined subset of the Malmö DM screening population was required. Paper III focused on modeling volumetric breast density and breast volume, including longitudinal changes, using data processed and described by Olinder et al.[167] To ensure consistent follow-up intervals and valid density measurements, women were excluded if the interval between consecutive

screening examinations exceeded 30 months (to exclude irregular follow-up beyond the expected age-dependent screening interval of 1.5–2 years), if they had breast implants, or if density data were missing.

After applying these study-specific criteria, the final cohort used in Paper III comprised 25 188 women.

Malmö TVDT cohort

Another specific cohort used in this thesis is the TVDT cohort, a cohort from Malmö designed for studying tumor volume doubling times (TVDT) across two consecutive screening rounds.[165] This cohort included all 111 invasive breast cancers diagnosed at Skåne University Hospital during the latter part of 2014.

For the purpose of tumor growth estimation, several exclusions were necessary. Non-invasive tumors were excluded, tumors that measured < 5 mm at diagnosis (to exclude lesions that would not have been visible on the prior screening mammogram), cases without a prior mammogram, and tumors that could not be reliably measured on the screening images. In total, 31 cases met the inclusion criteria.

This population was used for the tumor growth models developed in Papers I, and later applied in Paper III, where growth rates and tumor progression dynamics are key components of the simulation framework.

Penn population

Lastly, Paper IV used a population-based DBT screening cohort from the University of Pennsylvania. The dataset comprised 19 184 women imaged between 2015 and 2022. Images were acquired using the Selenia Dimensions DBT system (Hologic Inc.), with two-view DBT (CC and MLO). Eligible examination included those with available raw imaging data and women with no prior history of breast cancer. Two women were excluded due to missing demographic information. From this dataset, a case-control sample was assembled: cases consisted of 451 women who later developed breast cancer and had a true-positive screening finding, while controls consisted of 451 women who did not develop breast cancer during approximately six years of follow-up. For all cases, only the screening examinations acquired prior to the cancer diagnosis were included in the analysis.

To support the primary aim of Paper IV, assessing lesion detectability, the case examinations were subsequently modified by inserting simulated lesions (8–15 mm in diameter) at predefined regions of interest.

Probabilistic modeling

As described earlier, population modeling refers to fitting statistical distributions to real-world population data. Each distribution is mathematically defined by its probability density function, but can also be described in terms of summary characteristics such as mean, variance, skewness, and tail behavior. These fitted distributions then serve as the basis for generating new samples. In this thesis, virtual populations were modelled using both univariate and multivariate distributions.

Univariate statistical distributions

In Paper I, tumor growth was modelled by fitting a univariate probability density function to the TVDT data from the Malmö TVDT cohort. To identify the most appropriate distribution for our data, several candidates were evaluated using the goodness-of-fit procedure described in the section *Statistics*. The gamma distribution produced the best fit and was therefore selected to model tumor growth and to sample TVDT values for the virtual population. The gamma distribution was well suited for this purpose, as it is defined only for non-negative values, consistent with growing tumors. It also naturally accommodates right-skewed behavior, which was present in the clinical data.[172]

Multivariate statistical distributions

For Paper III, we modelled breast density, breast volume, age, and their corresponding annual changes using data from the Malmö DM Screening population. To capture the correlations between these variables, we used a multivariate approach that models both the marginal distributions of each variable and the dependence structure among them, such as the correlations (Figure 22).

The marginal distributions were modeled using kernel density estimation. This approach estimates the probability density function from the data itself, avoiding the need to assume a particular distributional form. Several dependence structures were evaluated, but because many variable pairs exhibited tail dependence, we selected the t-copula as a more robust alternative.[173] The t-copula is defined by a correlation matrix, which specifies the dependence between variables. It also includes an additional parameter, the degrees of freedom ν, which controls the strength of tail dependence. As ν increases, the t-copula converges towards a Gaussian copula. This flexibility allows the t-copula to represent a wide range of dependence patterns, making it a more robust choice.

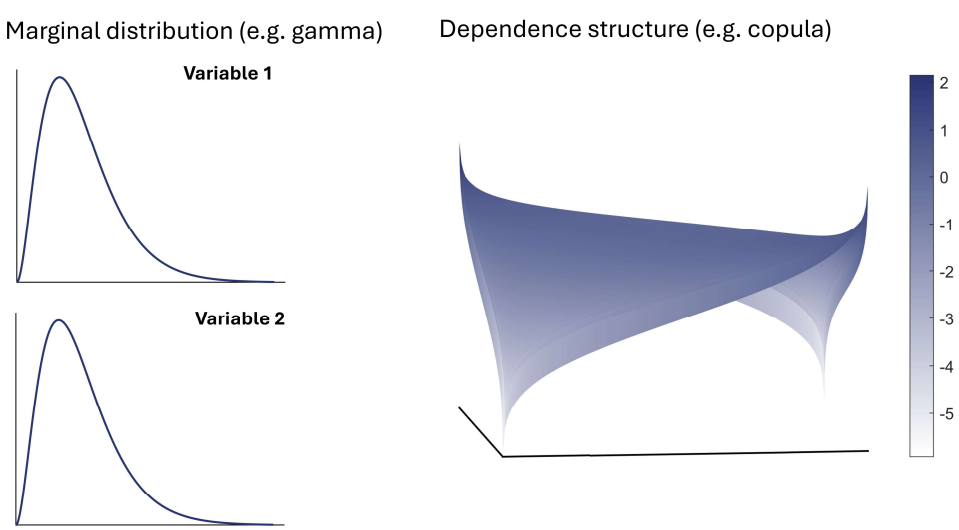

Figure 22. Components of a multivariate distribution with two variables
A multivariate distribution consists of two components: the marginal distributions of the individual variables (left) and the dependence structure between them (right). In this figure, a gamma distribution is shown for illustrative purposes. In practice, however, the kernel density estimation approach estimates the marginal distributions directly from the data rather than assuming a specific parametric form. In this figure, the dependence structure is represented by a copula model, which describes the correlation between the two variables.

Sampling procedures

To generate a virtual population, the probability distributions were sampled. In the case of multivariate distributions, it is possible to ensure that the correlations between variables are preserved. In the case of univariate distributions this is not achievable. For the examples mentioned, all samples were drawn using MATLAB's *random()* function which in turn applies a suitable sampling method depending on the distribution.

Longitudinal modeling

As previously discussed, the original aim of this work was to simulate longitudinal virtual imaging trials. Achieving this required the ability to model temporal changes in both breast tissue and lesions in order to follow a virtual population over time. An early effort toward this goal, initiated during my master's thesis project in 2020, focused on modeling tumor growth (Paper I). This work was later expanded to include temporal changes in breast density and breast volume (Paper III), enabled by the increasingly comprehensive datasets made available by colleagues from our

research group. This section describes both tumor growth modeling and modeling of the breast evolution.

Tumor growth modeling

For Paper I, we initially modeled tumor growth using an exponential function, motivated by its use in the original study describing the Malmö TVDT cohort. The tumor volume $V(t)$ at time t, with initial tumor volume $V(0) = V_0$, is described by:

$$V(t) = V_0 * e^{(r*t)} \quad (1)$$

where r denotes the tumor growth rate. Our model used TVDT values sampled from the Malmö TVDT cohort.[165] By definition, the tumor volume doubles after one tumor volume doubling time (t_{TVDT}):

$$V(t_{TVDT}) = 2 * V_0 \quad (2)$$

Substituting into the exponential growth equation gives:

$$2 * V_0 = V_0 * e^{(r*t_{TVDT})} \quad (3)$$

$$r = ln(2)/t_{TVDT} \quad (4)$$

Thus, the tumor volume can be expressed as:

$$V(t) = V_0 * e^{((ln(2)/t_{TVDT})*t)} = V_0 * 2^{(t/t_{TVDT})} \quad (5)$$

This formula formed the basis for the tumor growth model used in Paper I.

Subsequent analyses revealed that exponential growth has limitations, particularly when modeling larger or later-stage tumors (>7 mm in diameter).[57,63] Exponential growth tends to overestimate volume increases beyond the early stages of cancer. To address this, in Paper III we adopted a linear growth model, which also approximates the sigmoidal growth behavior observed in clinical screening studies. The linear model assumes a constant absolute growth rate, reflecting a biologically plausible slowdown and providing a more realistic representation of macroscopic tumor growth:

$$V(t) = V_0 + k * t \quad (6)$$

After one doubling time, t_{TVDT}, the tumor volume is:

$$2 * V_0 = V_0 + k * t_{TVDT} \quad (7)$$

$$k = V_0/t_{TVDT} \quad (8)$$

Hence, the linear growth model can be written as:

$$V(t) = V_0 + (V_0/t_{TVDT}) * t = V_0 * (1 + t/t_{TVDT}) \quad (9)$$

This approximation was used for the tumor growth model in Paper III.

The initial tumor diameter and TVDT were sampled from the real-world data described in the section *Study Populations*. These parameters were then used to calculate tumor size at each subsequent time point, generating a series of simulated lesions that reflect the expected tumor dimensions over time.

Breast evolution

In Paper III, we modeled changes in both breast density and breast volume over time. Breast density was assumed to decrease exponentially as defined by the literature[48,49], whereas breast volume was modeled with a linear increase. The annual changes in volumetric breast density (VBD) and breast volume observed in the DM Screening Population provided two data points for each variable, from which the respective functions were fitted. These functions were then used to compute the expected VBD and breast volume at each simulated time point.

When generating a virtual woman, the initial breast volume and VBD were jointly sampled using the copula model described earlier, ensuring that the correlation between the two measures was preserved.

To achieve the target VBD in the simulated phantom, we adjusted the Perlin noise parameters that control the amount of fibroglandular tissue. VBD was calculated voxel-wise by counting dense tissue, and the Perlin parameters were iteratively tuned until the simulated breast matched the target VBD from the exponential decay function. The spatial distribution of fibroglandular tissue was preserved across time, with density reductions achieved through thresholding within the Perlin noise field. This approach produced physiologically plausible decreases in fibroglandular volume while maintaining structural consistency across simulated time points.

Breast repositioning

To further account for realistic longitudinal modeling, we also incorporated breast re-positioning across different imaging occasions. This allowed the simulation to capture the natural variation and deformation that occurs when the breast is repositioned between acquisitions (Paper III). Breast repositioning was achieved by rotating the phantom around all three axes (x, y, and z), creating the appearance of different views relative to the X-ray tube.

Imaging simulation pipelines

For image generation, OpenVCT[112] was adopted in most studies by producing DM projections (Papers I and II) and DBT projections (Paper III). The raw DM projections were processed using either commercial software as for Paper I (Briona Standard, Real Time Tomography, LLC, Villanova, Pennsylvania, United States) or local clinical systems (Siemens Mammomat Inspiration, Siemens Healthineers, Forchheim, Germany) as for Paper II. DBT projections were reconstructed using open-source tools developed by Vimieiro et al.[169] (Paper III and IV) as well as commercial products (Briona, Paper IV). Additional open-source tools related to quantum and electronical noise simulation, developed by Borges et al., were also incorporated in Paper III.[168]

Image analysis and observers

Human observers were used for phantom and lesion optimization in Papers I and II, whereas a virtual observer, the Barco Medical Virtual Imaging Chain (MeVIC) framework, was applied for model observer studies in Paper IV.[170] Descriptive statistics were used throughout all studies, and Paper IV additionally included radiomics analysis for breast parenchymal characterization.

Computational and programming tools

Throughout this work, a variety of computational tools and programming environments were used to generate and analyze the simulated data. MATLAB formed the backbone of the workflow, handling everything from the Perlin noise-based generation of breast and lesion anatomies to mathematical population modeling and statistical analyses. R (R Foundation for Statistical Computing, Vienna, Austria) complemented the statistical analyses, particularly in Paper II. Python (Python Software Foundation) was used to run and manage the VICTRE and OpenVCT simulation pipelines. The open-source Python package PyRadiomics was used for radiomic feature extraction in Paper IV.[174] For visualizing and analyzing the images, ImageJ (National Institutes of Health, Bethesda, Maryland, United States) or MATLAB was used as the main tool through the research projects, while ViewDEX[175-177] supported the observer study in Paper II.

The simulations themselves were performed on high-performance workstations, the most recent of which featured NVIDIA GeForce RTX 4090 Ti GPUs (NVIDIA Corporation, Santa Clara, California, United States). AI-based software, Transpara (version 2.0.0, ScreenPoint Medical, Nijmegen, Netherlands)[32,33], provided estimates of breast volume and volumetric breast density used in Paper III.

Statistical methods

Because the papers in this thesis involve statistical modeling, simulations, and validation of virtual imaging methods, statistical analysis have a central role throughout the work. A range of statistical methods were used to evaluate the simulations and models, compare them with real-world observations, and assess observer performance within virtual imaging trials. The following section summarizes the key statistical approaches that recur throughout the thesis and provides an overview of how they were applied in the individual papers.

Descriptive statistics

A common foundation throughout all papers is the use of descriptive statistics, which serve as the first step in understanding the characteristics of the data at hand. Measures such as the mean, standard deviation, and distribution summaries have consistently been used to describe different variables of interest, e.g. simulated tumor volume doubling times (Paper I), lesion geometry (Paper II), simulated breast density and volume (Paper III) or population demographics (Paper IV).

Goodness-of-fit tests

Goodness-of-fit tests were used to evaluate whether a dataset is appropriately described by a particular probability distribution. They can be either based on hypothesis testing or visual assessment. In Paper I, the Shapiro-Wilks test was used to determine if data follows a normal distribution.[178] Assessing whether data are normally distributed is important for choosing appropriate hypothesis tests that assume normality. The Anderson-Darling goodness-of-fit test[179] was also used to identify an appropriate probability distribution for the TVDT data, ultimately supporting the use of a gamma distribution. In Paper III, goodness-of-fit was assessed primarily through visual inspection and by comparing descriptive statistics, for example to evaluate the suitability of the t-copula model for simulating breast density, breast volume, and age.

Comparison of data sets

In Paper I, we applied non-parametric hypothesis tests, as several of the datasets did not meet the normality assumptions required for parametric testing. To evaluate the consistency of the repeated tumor size measurements, we used the Friedman test[180], which is well suited for non-parametric repeated-measures data. The comparison between clinical and simulated TVDT values was carried out using the two-sample Kolmogorov–Smirnov test[181] and the Wilcoxon signed-rank test[182], allowing us to

assess both their distributions and paired differences (median). In Paper II, the non-parametric Mann-Whitney U-test[183] was used to compare observer realism scores across different lesion shape and margin categories. In later papers, such as Paper III, visual evaluation of the datasets became more prominent for comparing real and simulated data, through e.g. histograms and scatter plots. These visual approaches were used alongside descriptive statistics to provide a more intuitive understanding of the data. In Paper IV, we applied logistic regression and ROC analysis (detailed below), methods commonly used for evaluating diagnostic performance, to assess how lesion detection performance varied across subgroups of women with different breast parenchyma characteristics.

Sensitivity, specificity, and ROC

For a lesion detection tasks (as in Paper IV), sensitivity and specificity are key statistical metrics. Sensitivity describes how effectively true lesions are identified, while specificity reflects how accurately non-lesion cases are recognized as normal (Figure 23).

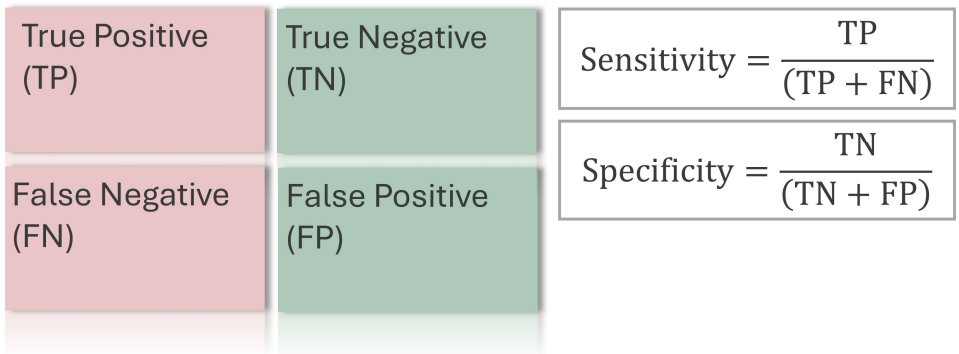

Figure 23. Sensitivity and specificity
The figure shows the four possible outcomes of a diagnostic test: true positives (TP), false negatives (FN), true negatives (TN), and false positives (FP). Sensitivity is defined as the proportion of correctly identified diseased individuals. Specificity is defined as the proportion of correctly identified healthy individuals. Together, these measures describe the test's ability to distinguish between the presence and absence of disease. In the figure, color represents the ground truth: pink indicates cases with a lesion, while green indicates cases without a lesion, independent of the test result.

A frequently used statistical tool for comparing sensitivity and specificity is Receiver Operating Characteristic (ROC) analysis.[184,185] ROC analysis evaluates detection performance using the numbers of true positives, false positives, true negatives, and false negatives, based on a known ground truth. From these values, the sensitivity (true-positive rate) and false-positive rate (1 − specificity) are calculated and plotted against each other. By varying the operating threshold, i.e.

the cutoff that determines whether a mammogram is classified as having a lesion or not, the ROC curve illustrates the detection performance across all possible threshold settings. A diagonal (linear) ROC curve indicates performance no better than chance, while a curve that bends toward the upper left corner reflects better ability to distinguish between e.g. lesion-present and lesion-absent (Figure 24). The area under the ROC curve (AUC) is a common metric, where a larger AUC represents better overall diagnostic performance.

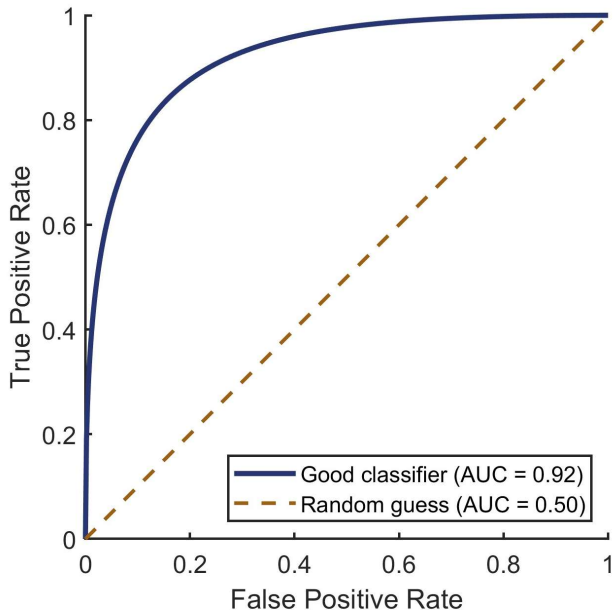

Figure 24. Receiver Operating Characteristic (ROC) curve
Illustrative example of a ROC curve. The solid curve represents a model with good discriminative ability between e.g. signal present (lesion) and signal absent cases (no lesion), while the diagonal dashed line indicates random guessing (no discrimination). The area under the curve (AUC) summarizes overall classification performance.

Additional statistical concepts

In Paper IV, logistic regression[186] was used to identify which variables were associated with the probability of a lesion being present. For example, we compared variables such as breast parenchymal characteristics, density measures, or CHO detection scores. Odds ratios quantified how strongly each variable related to a lesion-present outcome. We also used mediation analysis[187-189], a method that examines whether the effect of one variable on an outcome is partly explained through another variable, to evaluate whether differences in breast parenchyma patterns helped explain variations in detection performance across subgroups of women.

A note on hypothesis testing

It should be noted that current recommendations in statistical practice have shifted from a strict reliance on hypothesis tests and p-values toward a greater emphasis on confidence intervals and visual assessment of data.[190-192] This shift is reflected in the differences between Paper I and Paper III, where the statistical approaches differ noticeably. Paper I follows a more traditional approach with a stronger reliance on statistical tests, whereas later work places more weight on descriptive summaries and graphical evaluation. This is particularly relevant in studies involving large datasets, where statistical tests can easily become significant due to high statistical power through large sample size.[193] For this reason, p-values should be used cautiously with such large data sets. Complementary measures, as graphical visualizations of data, can provide a more balanced assessment.

Summary of papers

The work presented in this thesis is built around a series of interconnected studies, each addressing various aspects of breast modeling and VITs. The section that follows brings these studies together by summarizing the papers included in the thesis, outlining their main methodological approaches, key findings, and overarching conclusions. These summaries are concise, and a more detailed and complete understanding of the work can be found in the original publications, as well as in the *Method* and the *Discussion* of this thesis.

Paper I

In Paper I, we aimed at developing a method for simulating breast tumor growth as a component of a broader VIT framework. We modeled clinical tumor volume doubling times using a gamma distribution and sampled from it to assign realistic growth rates to simulated tumors. The simulated tumors were inserted into virtual breast phantoms. Mammograms were generated at two virtual screening time points, and a radiologist measured tumor size in order to estimate TVDTs from the simulated images (Figure 25).

Mean TVDT were similar across datasets (Figure 26), with values of 297 ± 169 days in the real-world data (clinical fit), 322 ± 217 days in the simulated cohort, and 340 ± 287 days for the estimated TVDT. The median difference between simulated and estimated TVDT was small (12 days, corresponding to 4% of the mean clinical TVDT). No significant differences were found between datasets ($p > 0.5$).

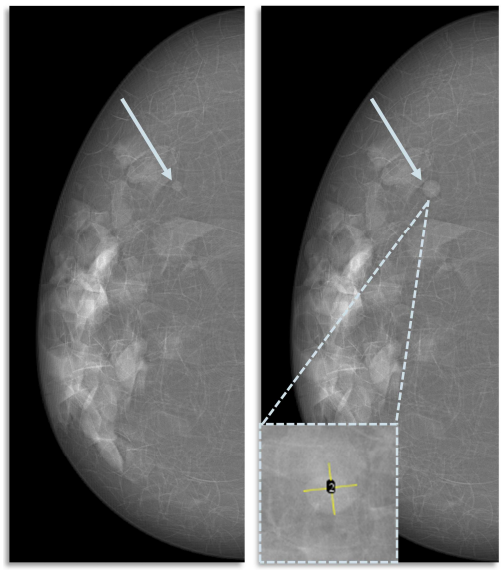

Figure 25. Simulated mammograms
Simulated mammograms of the same virtual breast at two screening time points, illustrating tumor growth over a 24-month interval. The tumor is indicated by the light blue arrows. The box shows how the radiologist performed tumor size measurements using two orthogonal lines (yellow).

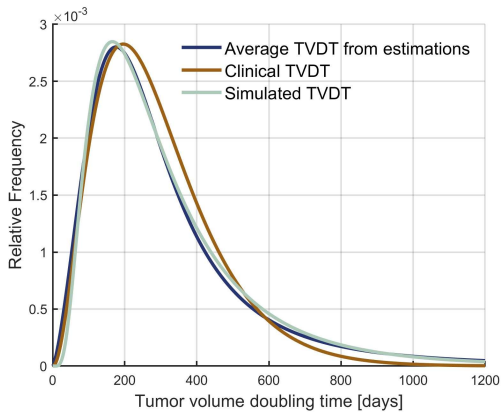

Figure 26. Tumor volume doubling time across datasets
Probability density functions of TVDT derived from clinical data (real-world data), simulated tumors (ground truth), and radiologist-based estimations. The curves illustrate the similarity in TVDT distributions among the three datasets.

Through this work, we demonstrated the potential for longitudinal virtual screening studies and future applications in personalized screening and tumor progression modeling.

Paper II

In Paper II, we developed and evaluated a method for generating soft tissue breast lesions for virtual imaging trials, extending the simpler lesion models used in Paper I by introducing more complex morphologies through Perlin noise. The lesions were generated by adjusting Perlin noise parameters, including lacunarity and persistence, to achieve variability in lesion shape. The lesions were inserted into virtual breast phantoms to create simulated mammograms (Figure 27). Three radiologists then assessed lesion shape, margin, and density using BI-RADS descriptors for malignancy scoring, as well as overall lesion realism (Figure 28 and 29).

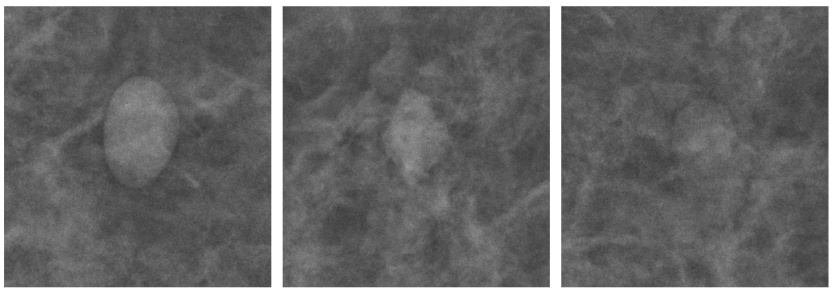

Figure 27. Morphological variation in simulated soft tissue breast lesions
Simulated digital mammography images of three virtual tumors demonstrating varying shape and margin features, evaluated by radiologists according to BI-RADS malignancy scoring system.

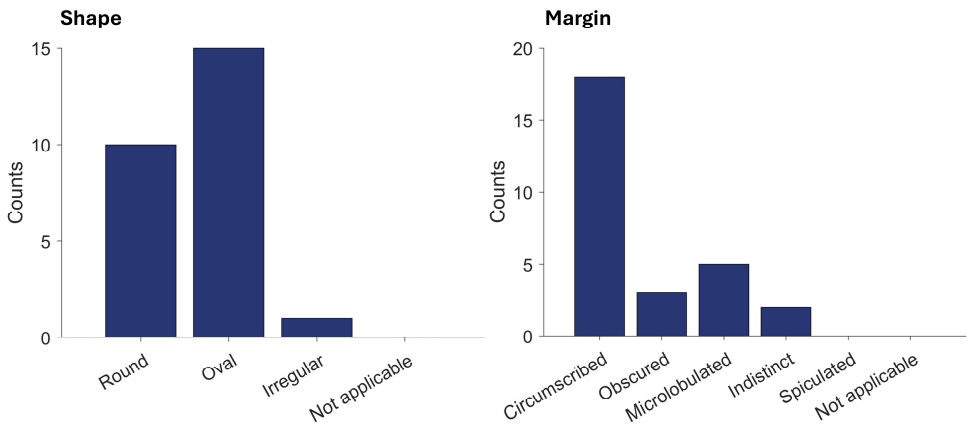

Figure 28. Shape and margin classification of simulated soft tissue breast lesions
Simulated lesions were classified by radiologists according to BI-RADS malignancy scoring system. All shape and margin features were represented except for spiculated margins, which were not simulated.

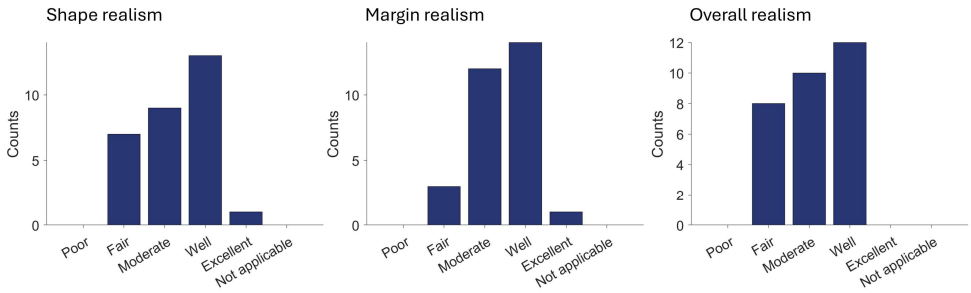

Figure 29. Realism assessment of simulated soft tissue breast lesions
Radiologists evaluated the shape, margin, and overall realism of the simulated soft tissue breast lesions. The majority of lesions were classified as *moderate* or *well* in terms of realism, with *well* being the most frequent category.

The radiologists' ratings indicated that the proposed method can reproduce clinically relevant lesion shapes and margin characteristics beyond simple geometric models. As a preliminary study, the results demonstrate the feasibility and flexibility of using Perlin noise for soft tissue lesion modeling in virtual imaging trials.

Paper III

In this paper, we developed a novel simulation framework, STELLA-R (Simulation of Temporal Evolution and LongitudinaL studies of breast Anatomy in Radiology). The goal was to develop a modular framework for modeling breast anatomy, breast density, and breast lesions, with the ability to generate virtual populations that reflect real-world characteristics (Figure 30).

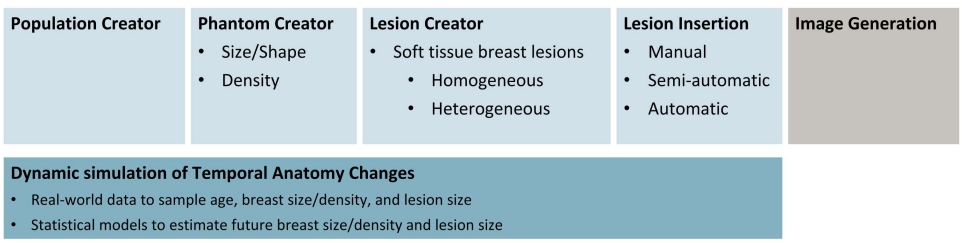

Figure 30. The STELLA-R framework
An overview of the five modules that comprise the STELLA-R framework. The Image Generation module is implemented externally, as it relies on open source software. The key innovation of the framework is the Dynamic Simulation module, which integrates all modules (from virtual population creation to phantom and lesion generation) enabling simulations in which the virtual population evolve over time.

In this work, we modeled the Malmö DM screening population and captured the dependencies between age, breast volume, and breast density using t-copulas. We showed that the resulting model accurately reproduced the observed correlation structure among these key variables, as shown in Figure 31 and Table 3.

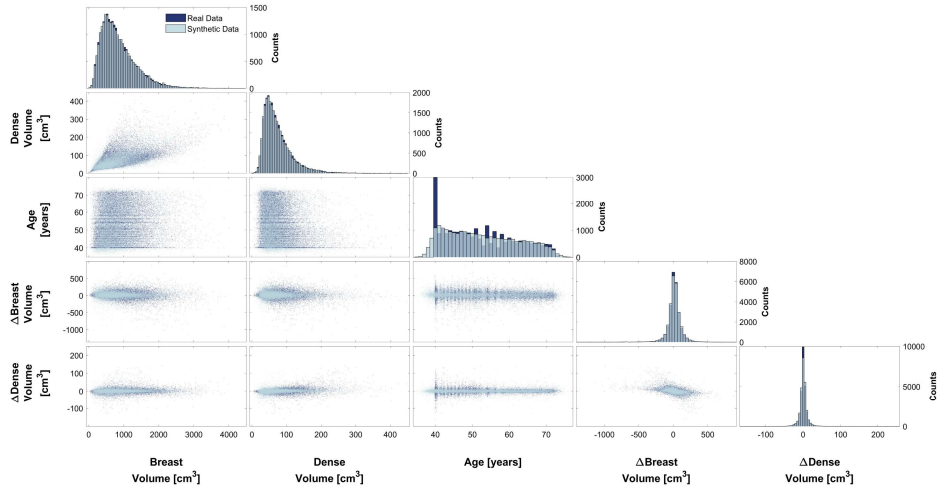

Figure 31. Real-world vs. simulated data
Comparison of real-world (dark blue) and simulated (light blue) data. The overlap between the two data sets (real-world vs. simulated) indicates that both the marginal behavior of each variable (diagonal histograms) and the pairwise dependencies between variables (off-diagonal scatter plots) are accurately reproduced.

Table 3. Quantitative comparison between real-world vs. simulated correlations
For each variable pair, we present Kendall's tau correlation τ from the real-world data (τ_r) and the bootstrap-averaged τ from 100 simulated samples (τ_s), together with the 95% confidence intervals (CI, lower and upper) for τ_s. Also reported is $\Delta\tau$, the difference between real-world and simulated correlations.

Variable pair	Real-world τ_r	Mean Simulated τ_s	95% CI of simulated τ_s	Mean difference $\Delta\tau$
Breast volume;densevolume	0.444	0.446	0.438 – 0.452	0.001
Breast volume;age	0.112	0.116	0.109 – 0.123	0.004
Breast volume;Δbreast volume	-0.024	-0.032	(-0.040) – (-0.025)	-0.009
Breast volume;Δbreast density	0.044	0.047	0.038 – 0.055	0.003
Dense volume;age	-0.103	-0.101	(-0.108) – (-0.092)	0.002
Dense volume;Δbreast volume	-0.012	-0.022	(-0.030) – (-0.014)	-0.010
Dense volume;Δbreast density	0.126	0.126	0.118 – 0.134	0.000
Age;Δbreast volume	-0.048	-0.046	(-0.055) – (-0.038)	0.001
Age;Δbreast density	0.009	0.012	(0.002) – (0.021)	0.003
ΔBreast volume; Δbreast volume	-0.350	-0.348	(-0.356) – (-0.340)	0.002

Temporal changes in breast density and volume were simulated using data from two consecutive screening rounds. Density involution was modeled by gradually adjusting Perlin noise-based tissue thresholds, allowing progressive reductions in fibroglandular tissue over time. Lesion behavior was modeled independently using a linear tumor volume growth model, with growth rates sampled from the Malmö TVDT cohort. The resulting simulations reproduced expected longitudinal trends. Example cases demonstrated density reductions of 14%, 9%, and 6%, while overall density accuracy remained within 2% of the target values (Figures 32 and 33).

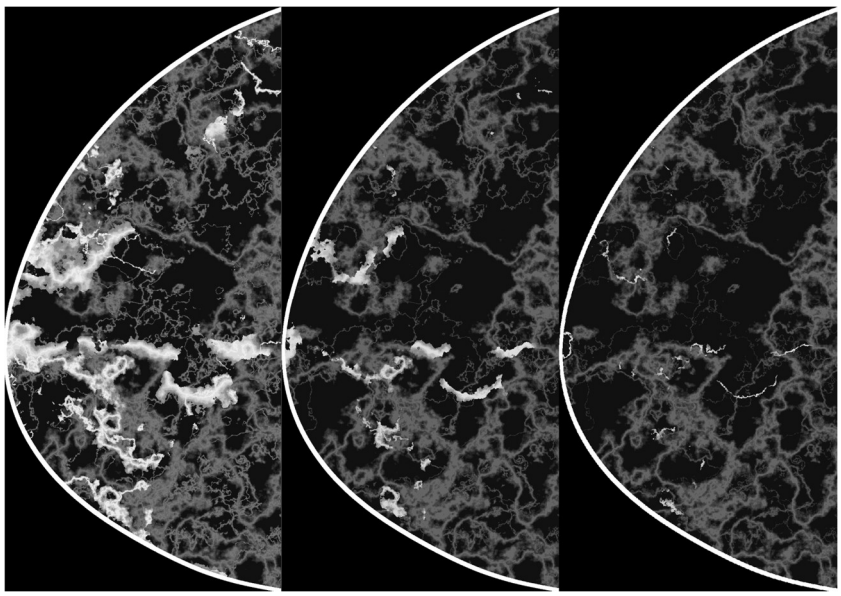

Figure 32. Time-evolving phantom
Example of a time-evolving breast phantom illustrating age-related reduction in fibroglandular tissue. Cross-sectional views are shown for a virtual patient at ages 40, 57, and 74 years, with corresponding volumetric breast densities of 14%, 9%, and 6%, respectively.

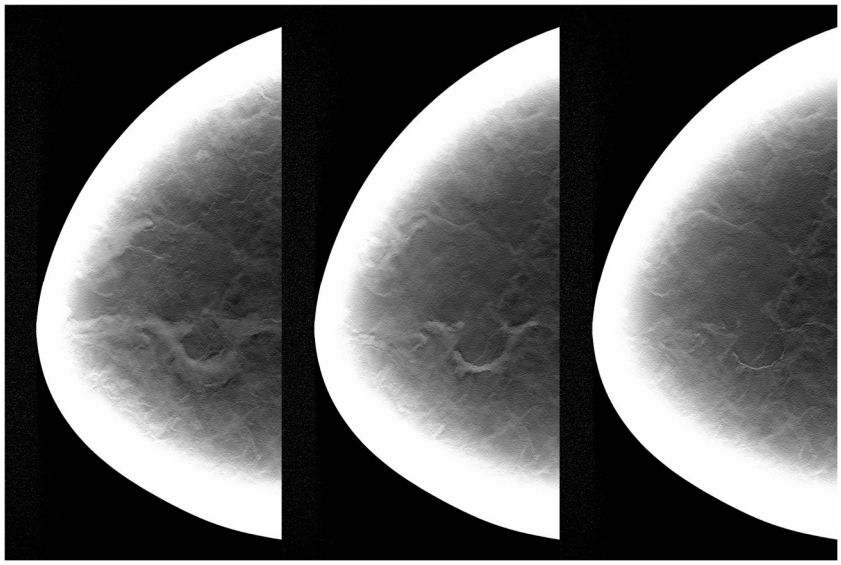

Figure 33. Time-evolving phantom: DBT reconstruction
DBT reconstructions of the same time-evolving breast phantom shown in Figure 32, illustrating age-related reduction in fibroglandular tissue. Reconstructions are shown for a virtual patient at ages 40, 57, and 74 years, with corresponding volumetric breast densities of 14%, 9%, and 6%, respectively.

We demonstrated that the proposed framework accurately captures population characteristics and longitudinal trends, and enables their transformation into corresponding virtual breasts.

Paper IV

In this paper we investigated how breast density and parenchymal structure influence lesion visibility in DBT. The central aim was to support efforts to reduce inequalities in breast imaging outcomes by assessing whether differences observed between participants from different ethnic backgrounds reflect underlying individual tissue characteristics, rather than being related to ethnicity itself. Ethnicity was self-reported and used as a sociodemographic variable reflecting lived experience and social context. Women were stratified into non-Hispanic White (NHW), non-Hispanic Black (NHB), or Asian American and Pacific Islander (AAPI).

This retrospective case-control study included DBT examinations from 902 women (451 cases and 451 matched controls), as illustrated in Figure 34. Cases and controls were matched on BI-RADS density category (A–D), self-reported ethnicity and the closest age at screening.

For each case, a simulated spiculated mass (generated by combining lesion models from the STELLA-R and VICTRE pipelines) were inserted into prior DBT projections in which the real (non-simulated) lesion was not yet visible (Figure 35). DBT images were then reconstructed (Figure 35).

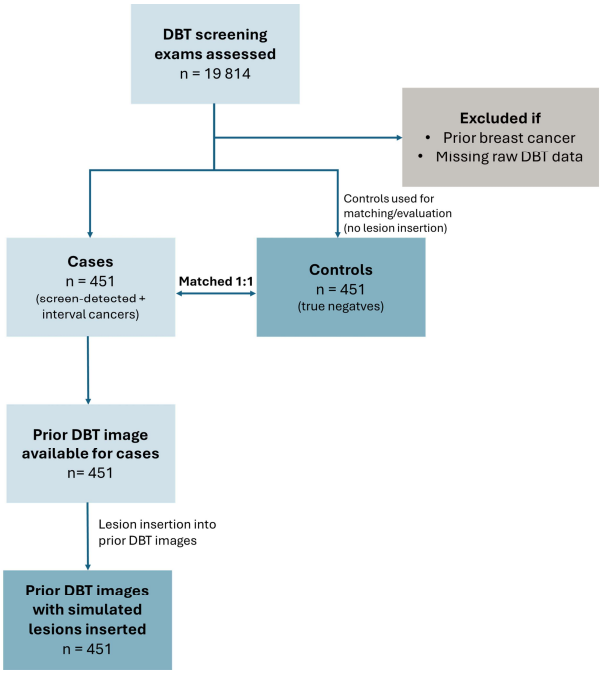

Figure 34. Study cohort for Paper IV
From the eligible exams, 451 screen-detected and interval cancer cases (follow-up: ~6 years) and 451 controls (true negatives) were selected and matched 1:1 based on BI-RADS density category (A–D), self-reported ethnicity and age at screening. For all cases, a prior DBT acquistion was available (n = 451) and used to generate a corresponding set of DBT images with a simulated lesion inserted (n = 451). Dark blue boxes indicate the final refined datasets used in the study, the grey box indicates exclusion criteria.

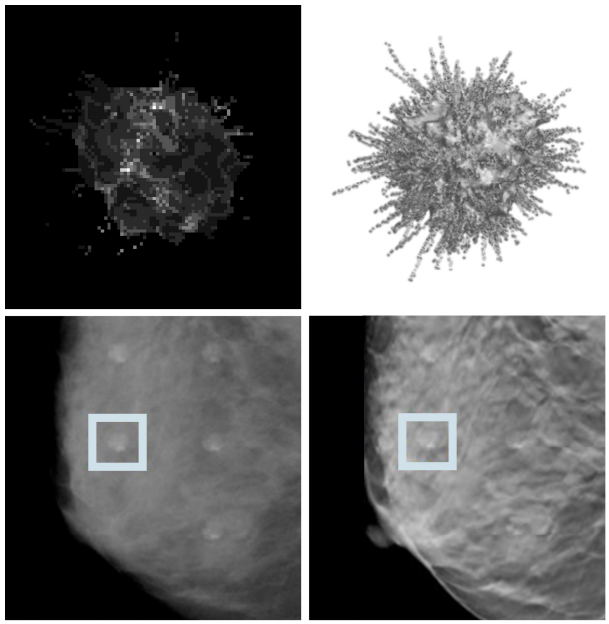

Figure 35. Hybrid approach: simulated lesion inserted into real DBT image
Illustration of cases generated using a hybrid approach that combines simulated lesions with real DBT images. The top row shows a cross-sectional slice of the lesion, with internal texture generated using Perlin noise (left), and a 3D rendering of the spiculated lesion shape produced with the VICTRE pipeline (right).The bottom row shows the lesion inserted into a projection image (left) and in the reconstructed DBT slice (right). The insertion site is indicated by the blue square.

Lesion detectability was quantified using the MeVIC CHO model observer and tissue complexity was characterized using radiomics features. Outcomes were analyzed using ROC curves and regression models. Mediation analysis was applied to assess the hypothesized causal relationship between breast density, parenchymal structure, and ethnicity in relation to lesion detectability.

The analysis showed a consistent decline in detectability as density increased (Figure 36). NHB women had slightly higher odds of lesion detectability (3%). Mediation analysis indicated that between 38% and 55% of the apparent ethnicity-related variation in detectability was explained by density alone. These findings emphasize that parenchymal complexity, and not ethnicity, is the factor influencing lesion detectability.

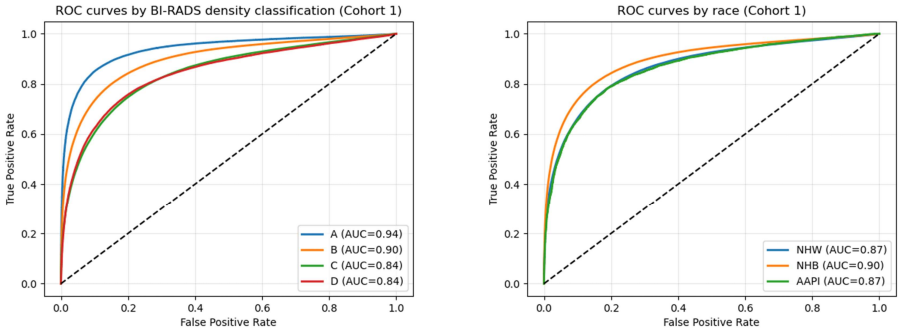

Figure 36. ROC analysis
ROC curves stratified by BI-RADS breast density categories (A–D) are shown in the left panel, and in the right panel by ethnicity: non-Hispanic White (NHW), non-Hispanic Black (NHB), and Asian American and Pacific Islander (AAPI).

These results underscore the importance of accounting for individual tissue characteristics and suggest that parenchymal patterns may help guide more personalized screening strategies, supporting more equitable lesion detection across patients.

Discussion

With all four papers presented, this section first provides an overview of the thesis contributions to the field. It then discusses each paper in relation to the overarching aims of the thesis. The discussion then expands to consider the thesis as a whole, addressing methodological limitations and placing the thesis in a broader context. This includes reflection on wider questions related to virtual imaging trials, such as ethical consideration, trust, and other aspects related to the acceptance of VITs in clinical practice.

Contributions to the field

Prior to this thesis, virtual imaging trials in breast imaging offered strong experimental control but were often limited by a few recurring gaps that reduced their ability to address clinically relevant screening questions over time. These gaps included:

- Restricted lesion realism, where lesion models were frequently geometrically simplified and typically lacked internal heterogeneity.
- Insufficient population representativeness, as virtual cohorts were commonly based on representative parameter settings rather than being sampled directly from real-world cohort distributions.
- Predominantly static anatomy, with limited ability to simulate temporal changes in the breast parenchyma.
- Limited incorporation of longitudinal clinical data within unified simulation frameworks.

This thesis was specifically designed to address these limitations through a stepwise methodological progression. Across Papers I–IV, the thesis introduces probabilistic tumor growth modeling (Paper I), advances lesion morphology and parenchymal simulation using Perlin noise-based approaches, including the incorporation of internal tumor heterogeneity (Papers II–III). Moreover, it establishes comprehensive longitudinal population modeling using multivariate real-world

distributions, while explicitly modeling temporal breast changes such as tissue involution (Paper III). The thesis also demonstrates how the developments can be used for controlled hypothesis testing using a hybrid virtual imaging trial design (Paper IV). Together, these developments directly target the gaps by increasing anatomical realism and variability, improving population-level representativeness, and enabling dynamic simulations that capture temporal anatomical change.

These advances culminated in the STELLA-R framework, which integrates the developments into a unified longitudinal pipeline, thereby moving beyond traditional static phantoms toward dynamic, data driven breast VITs.

The thesis also demonstrates the power of modular, collaborative development. Spiculated lesion models, projection physics, reconstruction algorithms, shape outlines, and noise models from multiple contributors came together in a unified system. The result is a pipeline designed not only for theoretical investigation but for translational use, bridging imaging physics, radiology, tumor biology, and statistical modeling.

Paper I

In this first study, we introduced an initial approach for simulating tumor growth within a virtual breast imaging framework, applicable for both DM and DBT imaging. Paper I served as a necessary starting point, a way to map the current possibilities and limitations for simulating tumor growth within virtual imaging trials. It also acted as a springboard for follow-up papers and projects, both in terms of improving lesion realism and in refining the simulation of temporal changes.

The methodology related to Paper I was well received within the VIT community, particularly the integration of probabilistic tumor growth distributions into virtual breast imaging pipelines, which to our knowledge had not been done before. The design principles introduced here, such as selecting appropriate statistical distributions and sampling from them to generate realistic virtual populations, remain highly relevant for this type of work. The paper provides a methodological foundation for how such modeling can be carried out, underscoring the translational nature of the project: it brings together imaging physics, tumor biology, and the substantial mathematical and statistical framework required to model growth in a realistic and reproducible way.

A fundamental challenge in tumor growth modeling is that, for ethical reasons, tumor progression cannot be monitored in vivo with frequent imaging. To create a growth model, at least two imaging time points are needed where the tumor is measurable (for example, two screening rounds), or an additional assumption that provides a baseline when the tumor is not visible on the earlier exam. In such cases,

growth estimation can be enabled by assuming a reasonable starting size (e.g., 5 mm), as was done in the original study that provided our real-world TVDT data.[165] However, the sparsity of measurements and the need for assumptions limit research on long-term biological progression at the individual level, making it necessary to rely on mathematical growth models. For Paper I we selected an exponential growth model, which is commonly used and supported in the literature. However, exponential growth may overestimate tumor progression at larger sizes, as real tumors often exhibit slowed growth due to biological constraints such as limited nutrient supply.[57,194]

In Paper I, lesions were modeled as spheres, resulting in limited morphological variability compared with clinical tumors. This simplification ensured highly reproducible size measurements and enabled clean, controlled comparisons between clinical and simulated TVDTs. This highlighted the value of introducing more clinically representative morphological variation, directly motivating Paper II, where we expanded the lesion model to include more complex and realistic shapes using Perlin noise. Although mammographic detectability tends to increase with tumor size[71], Paper I showed no clear differences in measurement difficulty between small and large tumors. This could suggest that morphology and parenchymal masking may be more important drivers than size alone, and that increased morphological complexity is an important next step for capturing a wider range of measurement challenges.

Paper I also made clear that incorporating breast density and temporal breast changes would be important for moving toward more realistic scenarios. Breast density influences lesion visibility and measurement uncertainty, but the tumor and breast models available at the time were not yet sufficiently advanced to support meaningful density-stratified analyses. In addition, temporal changes in the breast parenchyma were not modeled, even though such changes may affect tumor size estimation across screening rounds. These insights naturally shaped the direction of the thesis and became key motivations for Paper II and III, where more advanced lesion models and temporal breast changes were explicitly simulated within the virtual cohort.

Paper II

In this study, we introduced Perlin noise as a novel method for simulating breast lesions, an approach that, to our knowledge, had not previously been applied to breast tumor modeling. Our primary aim was to explore whether Perlin noise could generate plausible variation in lesion appearance, particularly in terms of shape and margin characteristics as defined by the BI-RADS 5th Ed. classification system for likelihood of malignancy.[52] By systematically tuning the amplitude and frequency

components of the noise function, we demonstrated that this method could reproduce a broad spectrum of lesion morphologies in a controlled and reproducible manner. This flexibility represented a significant advantage over earlier geometrically constrained models.[137-139]

The behavior of Perlin noise also helped define where complementary modeling approaches are needed. In particular, Perlin noise is inherently smooth, which makes it well suited for rounded or irregular mass shapes but less capable of producing the sharp structures that characterize spiculated lesions. For this reason, spiculation could not be modeled in Paper II. In addition, at the time of Paper II, we had not yet implemented a strategy for introducing internal structural heterogeneity within the lesion. This limitation later became a clear development target and was addressed in Paper III, where internal heterogeneity was incorporated into the modeling framework.

A part of the work was dedicated to assessing the realism of the simulated lesions. Realism in a simulation context is inherently difficult to quantify. In our observer study, most lesions received realism ratings of "moderate" or "well". However, in hindsight, the concept of "realism" could have been examined more critically, which was partly addressed by asking more detailed questions about visual appearance. Importantly, the generated lesions fell into clinically meaningful categories: round, oval, irregular shapes and circumscribed, microlobulated, obscured, or indistinct margins. This indicated that it is possible to produce the types of visual patterns radiologists rely on in practice with Perlin noise. This study also helped identify which parameter settings and lesion types were suitable for this modeling approach. It provided an early mapping between Perlin noise parameters and the resulting shape–margin, and served as a first optimization step.

This paper also marked an early step in demonstrating the broader potential of noise-based modeling for breast imaging, moving beyond early studies that utilized e.g. power-law noise.[129] Perlin noise, and its expansion toward simplex noise, have been adopted in other virtual frameworks, as OpenVCT and VICTRE.[148,149] These developments underscore the value and scalability of noise-based anatomical modeling. It is therefore encouraging that this study was able to show early that breast tumor morphology can be modelled effectively using Perlin noise, providing a foundation for more advanced simulation frameworks.

Altogether, this study served as a proof of concept demonstrating that Perlin noise can be used to model breast lesion morphology with clinically recognizable features. The work established a methodological foundation that has since influenced both our own subsequent research and developments in the broader simulation community. It showed that noise-based modeling is not only feasible but also highly promising for generating lesion variability in virtual imaging trials, an encouraging step toward richer and more realistic simulation environments.

Paper III

Paper III emerged as the pinnacle of our joint work on longitudinal virtual imaging trials. Over the years, several smaller projects, many of which resulted in conference papers, were gradually brought together under a single framework when we decided to establish a dedicated pipeline for longitudinal VITs: the STELLA-R pipeline. Drawing on feedback and insights accumulated throughout these earlier studies, we aimed to address the remaining gaps. This meant incorporating lesion location probabilities, modeling temporal parenchymal changes such as tissue involution, introducing internal lesion heterogeneity, and constructing more advanced virtual populations using larger datasets and multivariate distributions that preserve real-world correlations between variables such as breast density and breast volume.

It is important to acknowledge that this work was truly a collaborative achievement. The last module in the framework "Image Generation" (Figure 30), relied heavily on contributions from other researchers in the field, for example, spiculated lesion modeling from the VICTRE framework[114], noise modeling[168], breast shape outlines[163,164], projection and reconstruction algorithms[169], and image analysis tools[170]. The pipeline exemplifies what can be achieved when a community adopts an open and generous mindset.

Building on the longitudinal capabilities already implemented in the STELLA-R framework, further progress will depend on access to larger and richer longitudinal clinical datasets. Such data are essential if we want to validate simulated trajectories at an individual level. Current simulations rely on population-level patterns, which are difficult to translate to personal growth trajectories. As the MBIG dataset continues to expand, we aim to integrate more longitudinal data points per individual, enabling us to model changes in breast density and volume over much longer time spans.[171] Tumor growth will remain challenging to validate in this way due to ethical constraints, but more extensive datasets would nonetheless allow us to move toward stronger prediction models for density and parenchymal change, benefiting not only the VIT community but also risk-prediction modeling more broadly. These developments highlight the role of large datasets in advancing the field.

In the current implementation, the pipeline does not include a dedicated breast compression module. Existing modules, such as those provided by OpenVCT or VICTRE, can instead be incorporated with suitable plugin adaptations.[112,195] We did however note the ongoing development of such a module specific for the Perlin noise phantoms by Markbo et al.[154] Likewise, we reference the possibility of incorporating scattered radiation simulation, as demonstrated by Díaz et al.[158] Another important future direction is to make the pipeline more practically accessible and adjustable. A compact and user-friendly interface would allow users

outside physics and engineering, clinicians, statisticians, and imaging researchers, to explore and apply the simulation tools more easily.

At the time of writing this thesis, Paper III has only recently been published, and the future use and development of the proposed pipeline are yet to be established. Its practical use in virtual imaging trials may be either as a complete framework or through modular adoption of its individual components, such as for Paper IV.

Paper IV

Complete experimental control over subject characteristics, such as tumor size, shape, and spatial location within the breast, would be highly advantageous in clinical studies, yet is fundamentally unattainable in vivo. VITs offer a partial solution to this limitation by enabling controlled and repeatable experimental conditions. Paper IV therefore represents an important step toward demonstrating the value of in silico trials in breast imaging research. In this respect, it is conceptually aligned with the VICTRE and OpenVCT trials[16,116], which compared lesion detection performance between DBT and DM. This illustrates how virtual trials can be used to test clinically motivated hypotheses within a controlled environment.

Trials, like this one, provide support for assessing whether clinical observations remain valid when confounding factors, such as differences in lesion morphology, lesion location, or reader variability, are minimized. In Paper IV, we demonstrated that lesion detectability decreases with increased BI-RADS density category (A–D). The controlled framework further allows systematic lesion insertion across multiple breast regions, revealing that BI-RADS C breasts can be as challenging for lesion detection as BI-RADS D breasts, as seen in Figure 36. This has implications for ongoing discussions on personalized breast cancer screening.

As personalized screening strategies gain increasing attention, careful consideration is required when stratifying women for supplemental imaging, such as suggesting MRI for women with dense breasts. Restricting such strategies solely to women classified as BI-RADS D may be overly simplistic, as BI-RADS C breasts can contain highly complex and heterogeneous fibroglandular patterns that mask lesions. This further strengthens the motivation to define BI-RADS categories based on parenchymal complexity and masking risk, rather than relying solely on percentage breast density.[196] This is reflected in the evolution from the percentage-based definitions of the BI-RADS 4th Edition to the parenchymal pattern-focused descriptors introduced in the BI-RADS 5th Edition.[197] Software-based methods have already been shown to be more predictive than volumetric breast density alone for assessing masking risk.[198,199]

By controlling lesion insertion and enabling multiple lesions with known ground truth within a single breast volume, combined with the use of virtual observers that are not affected by fatigue, bias, or inter-reader variability, this study enables a rigorous and controlled investigation of lesion detectability across density categories and across cohorts stratified by ethnicity. Importantly, the work also demonstrates the feasibility and value of the proposed hybrid framework and, to the best of our knowledge, represents the first application of Perlin noise within such a hybrid breast imaging simulation framework.

However, because this hybrid trial is conducted under highly controlled conditions, the findings primarily reflect lesion detectability driven by image characteristics. As such, the study does not fully capture the complexity of performance in a real clinical screening setting. For example, detection performance observed in clinical practice may also be influenced by differences in adherence to screening programs. Regular screening attendance allows radiologists to compare current images with earlier examinations (prior images), making it easier to identify subtle changes over time, distinguish true abnormalities from normal anatomical variation, and thereby reduce false positive findings.[4] Socioeconomic factors, which affect screening participation, may therefore act as important confounders that are not captured within a virtual trial framework. And as mentioned earlier, human readers are inherently prone to both intra-reader and inter-reader variability, which can influence diagnostic consistency. Nevertheless, the present study highlights parenchymal complexity as an important factor influencing cancer detection.

Future investigations should extend this work by incorporating more comprehensive models of the screening process, with possibility of modeling more advanced tumor and patient characteristics. One such effort is the STELLA-R framework (Paper III), which aims to incorporate a broader range of population characteristics, particularly changes over time. It is important to continue examining differences in cancer detection between BI-RADS C and BI-RADS D breasts in a clinical setting. This issue is partially addressed in the BI-RADS 5th Edition, which incorporates aspects of parenchymal complexity rather than relying solely on percentage dense volume.[197] In the future, radiomics-based analyses of parenchymal patterns for mammographic risk assessment[198,199], together with models integrating imaging and population-based risk factors[200-202], may support a transition from BI-RADS-based assessment to fully quantitative risk assessment.

General limitations

Population specificity and generalizability

Although this thesis advances several methodological components of virtual imaging trials, it is important to acknowledge its overarching limitations. First, the simulations (Paper I–III) were developed and validated primarily using data from a single geographical and clinical population, the Malmö-based Swedish screening cohort. While the modeling framework is designed to be generalizable, there is no guarantee that parameterizations derived from one population will transfer seamlessly to others. Differences in breast density distributions, age structure, screening intervals, imaging practices, and tumor phenotypes may influence model behavior. In practice, extending this framework to a new population would require its own appropriate model fitting. We strongly anticipate that the methodology would apply broadly, assuming the availability of epidemiological and imaging data to support model fitting and validation.

Use of population-level averages

Several aspects of the modeling rely on population-level averages rather than fully personalized data. Tumor growth distributions, density involution patterns, and multivariate correlations were estimated from available datasets that contain only a limited number of longitudinal time points per individual. The longitudinal digital twins produced in this thesis should therefore be interpreted as plausible population-based trajectories rather than personalized predictions.

Anatomical modeling constraints

The anatomical models in this work still rely on simplifications that come with using noise-based methods. Perlin noise is flexible and reproducible, but in its current implementation it can only approximate the actual biological structures of the breast. Features such as Cooper's ligaments, vascular structures, and fine parenchymal patterns are therefore represented in a simplified manner rather than mapped explicitly to real anatomy. In principle, these structures could be modeled more accurately, but doing so would require a dedicated project based on specialized anatomical datasets, which was beyond the scope of this thesis. For many imaging tasks, such as studying noise behavior or reconstruction parameters, the current level of anatomical approximation is sufficient.

Moreover, the pseudo-random nature of Perlin noise limits the ability to control the spatial directionality of generated structures. In real breast tissue, anatomical structures tend to converge toward the nipple, a directional organization that is difficult to explicitly encode within the current algorithm.

Imaging-system modeling constraints

STELLA-R is a modular simulation pipeline that can be adapted to different imaging configurations, including vendor-specific setups. In this thesis, the projection and reconstruction methods for DM and DBT were evaluated under a limited range of acquisition conditions. As a result, the findings may not fully reflect differences in detector technology, post-processing, imaging parameters, or compression geometry across clinical systems. Moreover, the Perlin noise phantoms and their use in other imaging environments, such as ultrasound, CT, and MRI, has not yet been demonstrated.

Validation constraints

Finally, although this thesis brings together multiple components into a cohesive longitudinal VIT pipeline, validation is still constrained by the availability of longitudinal clinical data. Current datasets limit the extent to which temporal changes can be confirmed on an individual level.

Virtual imaging trials in a broader context

Realism and purpose driven virtual imaging trials

A central theme across this thesis is the role of realism in virtual imaging trials. Within the VIT community, we often talk about the need for realism and validation, yet realism is often treated as a universal goal. The term "realism" is borrowed from art and literature, referring to a style that attempts to depict things exactly as they appear in real life. This analogy is imperfect in a scientific context. Simulating the human body is not comparable to painting on a canvas, because we are not only trying to reproduce visual appearance, we are also modeling anatomy at multiple scales, physiology, and sometimes mechanistic or biological behavior. This raises an important conceptual question: What does realism actually mean in virtual imaging trials? If realism were defined as perfectly modeling everything that occurs in the human body, it would be an impossible standard, because we do not fully understand all biological processes ourselves.

Through the development of Perlin noise-based breast models and virtual population modeling, this thesis illustrates that realism is not an absolute objective in virtual imaging trials. Instead, the level and type of realism required are inherently task dependent, as also noted by Abadi et al.[125] Different research questions demand different levels of anatomical, physiological, or biological level of detail, and one model cannot serve all purposes equally well.

In this context, it is helpful to consider the types of tasks that virtual imaging trials are designed to support and how these tasks determine the realism required. VITs can address physics driven system studies, lesion detection tasks, observer performance studies, population level screening analyses, and longitudinal modeling. Each category demands a different degree of anatomical and physiological accuracy. For example, system performance or reconstruction studies primarily require accurate physics and signal modeling, and therefore limited anatomical detail can still be sufficient. Observer performance tasks depend on realistic lesion shapes, margins, and parenchymal backgrounds. Population-based studies rely on correct statistical correlations between variables such as age, density, and volume, while longitudinal VITs such as those developed in this thesis, require realistic temporal behavior rather than microstructural accuracy. By explicitly linking realism to the purpose of the study, we can determine when a model is "realistic enough," avoid unnecessary complexity, and design simulations that are fit for purpose.

Therefore, the field must define realism in a more practical and goal-oriented way. FDA recently published guidance on assessing the credibility of VITs, emphasizing that credibility should be evaluated in relation to the question of interest.[117] However, the guidance provides a general framework for assessing credibility, and does not specify which anatomical details are required for a given application. For example, a radiologist's inability to distinguish real from simulated lesions in a visual grading analysis may be a sufficient and meaningful definition of realism for image quality or detection tasks. This does not require the model to simulate every biological detail of a tumor, it requires the simulated lesion to have features that are relevant for the purpose of the study. By clarifying what realism means in specific contexts, VITs can build stronger foundations and gain greater trust, much like physical technical phantoms are trusted for image quality assessment despite completely lacking any resemblance of human anatomy.

Moreover, Abadi et al. highlight the need for virtual patient representations that are not only realistic but also sufficiently diverse and are "*going beyond anthropomorphic reference phantoms with population-average characteristics*".[125] This perspective directly aligns with the virtual population modeling performed in this thesis.

Ethical considerations and the role of VITs in replacing or reducing clinical trials

Virtual imaging trials carry important ethical advantages. Tumor growth, repeated imaging, and radiation exposure cannot be studied freely in vivo, making many research questions ethically inaccessible in clinical populations. Longitudinal VITs, like those developed in this thesis, allow temporal studies that would be impossible or unethical in human subjects, for example, tracking tumor growth across multiple hypothetical screening rounds or isolating the effect of breast involution and density change on lesion detectability.

By using VITs, we avoid exposure of patients to repeated radiation, invasive procedures, or follow-up requirements solely for research purposes. At the same time, ethical responsibility requires transparency: simulated data must not be mistaken for clinical evidence, nor used to replace human trials prematurely. FDA guidance emphasizes that VIT credibility should be evaluated in the context of use, including the consequences of decisions based on model outputs.[117] As a general rule, VITs can inform study design, complement clinical evidence, and help refine research questions, but claims about replacing clinical trials should be made cautiously, in proportion to the potential consequences of decisions based on the results. This thesis reinforces that VITs are ethically valuable tools when used appropriately, especially for exploring scenarios where clinical trials are impractical or unethical.

Trust, validation, and the acceptance of virtual imaging trials

For VITs to gain broad trust among clinicians, regulators, and industry, they must undergo rigorous validation. Despite more than two decades of development, key challenges remain for VITs within breast imaging, such as limited longitudinal datasets or incomplete representation of biological processes. The longitudinal components and incorporation of real-world data in this thesis represent an important step toward addressing these gaps.

Trust requires convincing evidence that simulations can reliably predict clinical behavior. This includes having probabilistic models validated against real-world clinical datasets, comprehensive visual grading analyses for anatomical plausibility, as well as transparent reporting of model assumptions and uncertainties. Similarly, ongoing discussions emphasize the importance of transparency regarding the data used to develop a model, including the populations on which it was trained, the imaging modalities involved, and other relevant characteristics, in order to appropriately inform users of VITs. Recent collaborations within the VIT community have also produced containerized environments that package and bridge simulation components, making workflows more modular and easier to share, promoting transprancy.[203]

Equally important is the need for stronger engagement beyond the research community, as also covered by Samei et al.[204] The field remains small, and progress slows when developers work in isolation. Trust in VITs will grow not only through validated methods, but also through active dialogue with radiologists, technologists, nurses, and other clinical stakeholders. Just as the rise of AI has shown, early transparency and collaboration are essential for gaining acceptance of new computational tools. By sharing datasets, explaining model assumptions, and inviting clinical perspectives early in the development process, VITs can move from a niche research topic toward a technology that clinicians feel confident using in practice. Broader community trust will increase when VITs consistently reproduce clinical patterns, as demonstrated in Paper IV. It will also depend on adherence to existing standards, such as those established by dedicated task groups[125] and the FDA.[117]

Conclusions

This thesis advances virtual imaging trials by improving the realism of computational phantoms and virtual populations, and by enabling longitudinal simulations grounded in real-world data. Through the development of the STELLA-R pipeline, this thesis expands the capabilities of virtual imaging and strengthens the methodological infrastructure of the field.

Specifically, the thesis concludes that:

- Computational phantom realism can be improved by incorporating Perlin noise to reproduce clinically recognizable radiographic characteristics of soft tissue breast lesions, and to simulate heterogeneous breast density patterns that reflect observed anatomical variability and tissue involution.
- Realistic virtual populations can be created by fitting univariate and multivariate models to real-world datasets and sampling from the resulting distributions, thereby capturing population-level variation and correlation between anatomical and physiological characteristics.
- Clinically plausible longitudinal simulations can be achieved by using real-world data to model changes over time, including tumor growth and temporal evolution in breast anatomy such as breast density and breast volume.
- The STELLA-R framework integrates these contributions in a modular and extensible pipeline, allowing individual modules to be used independently or in hybrid studies that e.g. combine simulated and real data.

Taken together, this thesis shows that VITs can be strengthened through data driven methods, enabling more clinically meaningful virtual trials for breast imaging research and evaluation.

Future perspectives

Toward more clinically relevant simulation models

A key direction for future work is to increase clinical relevance by moving from primarily appearance-driven modeling toward models that also reflect histopathological and molecular subtypes. This would require clearer definitions of how tumor biology should translate into radiographic appearance – an area that remains a somewhat open research question.[59,87,88,205] Based on current clinical knowledge, it is possible to formulate plausible assumptions about subtypes, e.g. for the simulated lesions in Papers I and II, related to their differences in growth and appearance. However, a direct one-to-one matching between simulated lesions and histopathology cannot be established in current VITs.

Future tumor growth models could include more advanced cell-cycle dynamics or microenvironmental constraints and represent tumor growth as continuous processes instead of discrete time points. Recent work is trending in this direction by coupling growth to local mechanical resistance, but these models are not calibrated to patient-specific growth rates.[162] This limits their ability to reliably address time-dependent research questions e.g. evaluating screening intervals, time-to-detection, or other relevant predictions that depend on realistic growth kinetics.

As richer longitudinal datasets become available, growth and appearance models could be refined to incorporate clinically meaningful covariates such as age and molecular subtype, supporting more realistic simulations of heterogeneous disease trajectories. Today we know that older women are more likely to present with slower-growing, less aggressive tumors than younger women.[206-208] These factors are likely to influence growth characteristics and should be considered in future, more refined simulation frameworks.

In parallel, strengthening the anatomical correspondence of noise-based breast models would further support clinical interpretability. While simulated tissue generated through Perlin noise can achieve visually realistic mammographic appearance, a more explicit mapping between anatomical structures and model parameters would enable clearer statements about which anatomical structure a specific noise pattern represent. Ongoing work linking parameter tuning to volumetric breast density is a step in this direction and would further strengthen the biological and radiographic relevance of the model.

Data driven modeling and AI integration

Access to large longitudinal datasets will play an increasingly important role in shaping the next generation of virtual imaging trials. These data give simulations a stronger grounding in real-world patterns of anatomy and disease, allowing models to reflect how breasts change over time. As big data resources continue to grow, such as the M-BIG data set[171], they offer an opportunity to enrich our simulations with greater diversity and nuance, ultimately making them more meaningful and trustworthy. This goes along with the emerging idea of digital twins, computational models of individual patients.[204,209] This also offers an exciting future direction, but one that will demand even more stringent validation.

Artificial intelligence has found its way in almost all corners of society and has also become established in advanced simulation workflows.[210] For example, generative adversarial networks (GANs) have been used to produce synthetic lesions and mammograms[211-213], and have shown promise for generating mammograms spanning different breast densities.[214] However, while generative AI can create or modify anatomy, it may introduce artifacts[215] and should not be viewed as a replacement for physics-based simulation. Physics-based models, such as the ones presented in STELLA-R, remain essential because they simulate the full imaging chain, including X-ray interactions, tissue composition, scatter, noise, and detector response.

The choice of simulation model will always depend on the task at hand. For anatomical diversity or population-level variation, AI-generated structures may be sufficient. For tasks requiring accurate image formation or dose realism, physics-based models remain essential. A combined approach, where AI-generated anatomy is constrained by physical imaging principles, is likely the most practical path forward. For example, Perlin noise could be combined with a GAN to generate controllable parenchymal patterns or lesion shapes, while the GAN refines anatomical variations to achieve realistic texture and appearance. The physics model would still determine how the resulting anatomy compresses, attenuates X-rays, and appears in mammography or DBT. In this way, AI contributes with variability, and physics ensures scientific and imaging accuracy.

Standardized benchmarking

As virtual imaging trials advance, standardized benchmarking is becoming crucial for establishing which simulation results can be trusted. Benchmarking involves testing different models under the same conditions using shared datasets and agreed-upon evaluation metrics. Without this, it becomes difficult to compare methods or assess how closely simulations reflect clinical reality. In this context, a relevant next

step for STELLA-R would be to work toward the validation and certification required for potential clinical use.

Successful examples from AI research illustrate the impact of well-designed benchmarks. Initiatives such as the RSNA Screening Mammography Breast Cancer Detection AI Challenge[216] or platforms such as MICCAI (The Medical Image Computing Assisted Intervention Society)[217] that promote challenges have accelerated progress by providing common training datasets and transparent scoring systems. These efforts have shown how shared benchmarks create clarity, enable fair comparisons, and build community confidence. Virtual imaging trials have also begun to adopt challenge-style benchmarks, which is a promising sign for future standardization and more comparable evaluation.[218] Extending this coordinated approach to virtual imaging trials in breast imaging would be a natural next step.

Commercialization

For virtual imaging trials to move toward commercial use, several elements must come together. First, the core simulation framework must be stable, validated, and able to reproduce imaging physics reliably across different scenarios. If the software is intended for use in clinical decision support or device evaluation, regulatory considerations such as documentation, verification, and quality management become necessary as recommended in the FDA guidelines.[117] Commercialization also requires a clear strategy for licensing and intellectual property, as well as computational infrastructure that can scale to large datasets and multi-user environments.

A major barrier to wider uptake is the usability of VIT platforms. For these tools to reach clinicians, engineers, and statisticians who are not programmers, they must include intuitive, user-friendly interfaces with clear workflows and built-in presets. Progress in this direction has begun through containerization and modular simulation platforms, which make deployment and configuration more consistent through various simulation platforms.[203] However, there is still substantial potential to further lower the barrier to use through more polished graphical interfaces. These considerations also apply to STELLA-R, even if the immediate goal is not commercialization, improving accessibility is a key next step for broader adoption. In practice, this motivates translating STELLA-R to Python, packaging it in a containerized workflow, and developing a graphical user interface with guided presets and clearly defined analysis paths.

Ultimately, commercial adoption will depend on demonstrating clear value, for example, by reducing the cost of imaging system development or improving the design of screening studies, while maintaining transparency through open-science principles wherever possible.

Final words

I am hopeful that the growing VIT community will continue to advance benchmarking efforts through coordinated organizational initiatives. Virtual imaging trials hold considerable promise, provided that their scope and evaluation tasks are clearly defined. The ability to generate simulations that are realistic enough to challenge human observers is a powerful demonstration of what these methods can achieve. I also see great potential in hybrid study designs, such as the approach used in Paper IV, where simulations and clinical data inform one another. In this context, I hope to see STELLA-R develop into a more accessible, big-data-driven simulation platform that can support larger longitudinal virtual imaging trials. Continued progress in this field will depend on strong, collaborative efforts across groups, ideally working under a shared framework that promotes comparability, transparency, and collective development.

Acknowledgements

"It takes a village to raise a child" is a phrase I especially want to emphasize as I take this opportunity to thank everyone who has supported me throughout my PhD. Behind this thesis stands a whole village of colleagues, friends, and family, whose generosity, encouragement, and support have carried me through.

First, I want to thank all the women who took part in the studies that form the foundation of my thesis. Your contribution to science is invaluable.

I would also like to express my deepest gratitude to my supervisor **Predrag Bakic**, for your unwavering support throughout this journey. Your positive outlook on life, genuine enthusiasm for science, and curious mind are qualities I greatly admire. Thank you for giving me the chance to learn and grow.

To my dear co-supervisors. **Anders Tingberg**, thank you for giving me this opportunity and for always being a steady source of support. But most importantly, thank you for teaching me that life is all about having fun, I truly think we have perfected that together over the years.

Sophia Zackrisson, thank you for all your support and for helping me grow into my profession. Thank you for leading LUCI with such inspiring and admirable leadership, and for always being the first on the dance floor requesting ABBA.

Magnus Dustler, thank you for all the laughs and jokes along the way. The perfect symbolism of your supervision is when you helped me cross that terrifying suspension bridge in Vancouver – proof that supervision extends far beyond the lab!

I especially want to thank one of my best friends and colleagues, **Anna Bjerkén**. Thank you, first, for introducing me to LUCI. More than that, thank you for doing all of this with me. I can't believe we got to share this PhD journey together!

To the glimmering and sparkling group of LUCI! **John-Henry**, thank you for all the fun, who would have thought that we would become actual phantom (of the opera) experts. **Nadia**, thank you for your friendship beyond work. **Victor D.**, **Akane** and **Kristin**, thank you for always being willing to help with my research. **Anetta, Ann-Sofi, Eva, Li, Lizette, Maria,** and **Mavis** – thank you for being such cool role models! **Jakob** and **Viktor L.**, thank you for making me laugh and for always bringing out the most amazing dance moves. **Pontus** and **Daniel**, thanks for leaving such an awesome legacy from your days as PhD students. **Kajsa** and **Theodora**, thank you for your support and your cheerful energy.

Thank you also to my colleagues at the X-ray department in Malmö/Lund: **Lina, Hannie, Mikael, Marcus, Martin, Marie-Louise, Veronica L.,** and **Sigrid** for contributing to an atmosphere of kindness and support. A special thanks to **Veronica Fransson** – who I have been lucky to have as both a friend and colleague.

To my colleagues in Brazil! Thanks to Professor **Marcelo Vieira** and all of LAVI, for your tremendous hospitality during my visit to your lab in São Carlos. A special thanks to my dear friend **Arthur**, who safely navigated me through the streets of Brazil. Also, thanks to **Renann** and **Marina**, for your generosity and friendship.

I would also like to especially thank **Bruno Barufaldi**, for your encouragement and for steering me in the right direction when I felt stuck in my work.

Moreover, I want to direct a sincere thanks to all colleagues at the departments of Diagnostic Radiology, Medical Radiation Physics, and Unilabs Malmö.

To my friends outside of work. **Lovisa**, I am so outermost thankful for our wonderful friendship, and for you and Jonas becoming like second family. And thanks to **Jonas** for forcing me to eat power bars in a random Himalayan village making sure I survive, literally. To **Augusta, Johan, Victor,** and **Lisa**. Our friendship means the world to me, and may we together sing our ways into old age.

Maria and **Niklas**, for all the memories we share, and for always being my travel buddies. I don't know if anyone will ever understand our humor, but that's ok.

To my high-school friends, thank you for remaining such an important part of my life. A special thanks to **Beatrice, Linn,** and **Ellen** for your sincere friendship.

Skvallerligan, **Johanna, Karro, Laura,** and **Olivia**. Thanks for always spilling the tea and for your friendship.

Thanks to **Belma** and **Emma**, my childhood friends. I feel lucky to have shared so much with you, including our group chat that I am sure breaks every world record.

To my Mastio-family. **Bisse**, I can't have asked for a kinder mother-in-law. To my father-in-law, **Sauro**, thanks for always making me feel so welcome in your big Italian family. To **Cecilia**, for always supporting me and being an important role model. **Alessandra** and **Martina,** my sisters-in-law, for taking me in as a third sister. Thanks to **Enzo**, I hope you grow up to be a cool scientist, because you are the coolest kid! Thanks to **Leo, Simon, Matteo, Mila**, for being part of this family. A special thanks to **Amalia**, **Rosanna,** and **Fausto** for strengthening me with your fantastic meals! And thanks to the rest of the Mastios, for having your arms wide open and welcoming me to your crazy family.

To **Azemina**, thank you for brightening our family with your kindness and warmth.

To my own beloved family. My mom and dad, **Aida** and **Tony**. From the bottom of my heart, thank you! You mean the world to me, and I truly cannot thank you enough for the opportunities you have laid before me. This thesis is mainly dedicated to you, for everything you did so that I could be where I am today. Thank you for teaching me to appreciate nature, to travel through life with an open mind and to be confident in myself. To my little brother, **Daniel**, for always sharing the same quirky sense of humor. You are an amazing person, and I am lucky to have you as my brother. And to my grandmother, baka **Anđa**, thank you for being my number one supporter throughout life, and for always holding me so close in your heart, as I hold you in mine. Thanks to all uncles, aunts, cousins, and family members that have loved me and shaped me. I wish all of you the most amazing things in life. Jag älskar er! Volim vas!

And lastly, to my wonderful fiancé **Roberto Mastio**. Thank you for loving me, caring for me and standing by my side. I could not have done any of this without you. I am so utterly grateful to have found such a kind soul to share this life with and I am so proud of you. Now, as we both close the chapter on our PhDs, I can't wait to see what adventures lie ahead, and I am so glad I get to share them with you. Jag älskar dig!

References

1. Bray F, Laversanne M, Sung H, et al. Global cancer statistics 2022: GLOBOCAN estimates of incidence and mortality worldwide for 36 cancers in 185 countries. *CA Cancer J Clin*. 2024;74(3):229-263. doi:10.3322/caac.21834
2. Kim J, Harper A, McCormack V, et al. Global patterns and trends in breast cancer incidence and mortality across 185 countries. *Nature Medicine*. 2025;31(4):1154-1162. doi:10.1038/s41591-025-03502-3
3. Broeders M, Moss S, Nyström L, et al. The impact of mammographic screening on breast cancer mortality in Europe: a review of observational studies. *J Med Screen*. 2012;19 Suppl 1:14-25. doi:10.1258/jms.2012.012078
4. Akwo JD, Trieu PD, Barron ML, Reynolds T, Lewis SJ. Access to prior screening mammograms affects the specificity but not sensitivity of radiologists' performance. *Clinical Radiology*. 2024;79(12):e1549-e1556. doi:10.1016/j.crad.2024.09.007
5. Webb ML, Cady B, Michaelson JS, et al. A failure analysis of invasive breast cancer: Most deaths from disease occur in women not regularly screened. *Cancer*. 2014;120(18):2839-2846. doi:https://doi.org/10.1002/cncr.28199
6. Schopper D, de Wolf C. How effective are breast cancer screening programmes by mammography? Review of the current evidence. *European Journal of Cancer*. 2009;45(11):1916-1923. doi:10.1016/j.ejca.2009.03.022
7. World Health Organization. Breast cancer. Updated: 2025-08-14. Accessed: 2026-01-19. https://www.who.int/news-room/fact-sheets/detail/breast-cancer
8. Andersson I, Aspegren K, Janzon L, et al. Mammographic Screening And Mortality From Breast Cancer: The Malmö Mammographic Screening Trial. *BMJ: British Medical Journal*. 1988;297(6654):943-948.
9. Houssami N, Zackrisson S, Blazek K, et al. Meta-analysis of prospective studies evaluating breast cancer detection and interval cancer rates for digital breast tomosynthesis versus mammography population screening. *European Journal of Cancer*. 2021;148:14-23. doi:10.1016/j.ejca.2021.01.035
10. Kataoka M. Mammographic Density for Personalized Breast Cancer Risk. *Radiology*. 2023;306(2). doi:10.1148/radiol.222129
11. Ohashi A, Förnvik D, Bengtsson Y, Zackrisson S, Kataoka M. Advances in Risk Management and Screening for Women at Increased Risk of Breast Cancer: The Role of MR Imaging and Personalised Approaches. *Magnetic Resonance in Medical Sciences*. 2025;24(3):403-418. doi:10.2463/mrms.rev.2025-0056
12. Díaz O, Rodríguez-Ruíz A, Sechopoulos I. Artificial Intelligence for breast cancer detection: Technology, challenges, and prospects. *Eur J Radiol*. 2024;175:111457. doi:10.1016/j.ejrad.2024.111457

13. Destounis S, Arieno A, Morgan R, Roberts C, Chan A. Qualitative Versus Quantitative Mammographic Breast Density Assessment: Applications for the US and Abroad. *Diagnostics*. 2017;7(2):30. doi:10.3390/diagnostics7020030
14. Kontos D, Winham SJ, Oustimov A, et al. Radiomic Phenotypes of Mammographic Parenchymal Complexity: Toward Augmenting Breast Density in Breast Cancer Risk Assessment. *Radiology*. 2019;290(1):41-49. doi:10.1148/radiol.2018180179
15. Winham SJ, McCarthy AM, Scott CG, et al. Radiomic Parenchymal Phenotypes of Breast Texture from Mammography and Association with Risk of Breast Cancer. *Radiology*. 2025;315(2):e240281. doi:10.1148/radiol.240281
16. Barufaldi B, Maidment ADA, Dustler M, et al. Virtual Clinical Trials in Medical Imaging System Evaluation and Optimisation. *Radiation Protection Dosimetry*. 2021;195(3-4):363-371. doi:10.1093/rpd/ncab080
17. Abadi E, Segars W, Tsui BM, et al. Virtual clinical trials in medical imaging: a review. *Journal of Medical Imaging*. 2020;7(4):042805. doi:10.1117/1.JMI.7.4.042805
18. Vancoillie L, Abadi E, Ria F, Bosmans H, Samei E. Overview of X-ray Imaging Simulation Tools for Medical Research: Features, Capabilities, and Computational Considerations. In: Bakic PR, Bliznakova K, Bosmans H, et al, eds. *Proceedings of Virtual Imaging Trials in Medicine 2025*. Zenodo; 2025:9-12.
19. Van Camp A, Houbrechts K, Cockmartin L, et al. The creation of breast lesion models for mammographic virtual clinical trials: a topical review. *Progress in Biomedical Engineering*. 2023;5(1):012003. doi:10.1088/2516-1091/acc4fc
20. Samei E, Abadi E, Bakic P, et al. Virtual imaging trials in medicine: A brief takeaway of the lessons from the first international summit. *Medical Physics*. 2025;52(3):1950-1959. doi:10.1002/mp.17587
21. Iavazzo C, Trompoukis C, Siempos I, Falagas M. The breast: from Ancient Greek myths to Hippocrates and Galen. *Reproductive BioMedicine Online*. 2009;19:51-54. doi:10.1016/s1472-6483(10)60277-5
22. Lukong KE. Understanding breast cancer – The long and winding road. *BBA Clinical*. 2017;7:64-77. doi:https://doi.org/10.1016/j.bbacli.2017.01.001
23. Lakhtakia R. A Brief History of Breast Cancer: Part I: Surgical domination reinvented. *Sultan Qaboos Univ Med J*. 2014;14(2):e166-9.
24. Hortobagyi GN. Breast Cancer: 45 Years of Research and Progress. *J Clin Oncol*. 2020;38(21):2454-2462. doi:10.1200/jco.20.00199
25. Bazira PJ. Anatomy and physiology of the breast. *Surgery (Oxford)*. 2024;42(12):859-864. doi:https://doi.org/10.1016/j.mpsur.2024.09.003
26. Yaffe MJ. Mammographic density. Measurement of mammographic density. *Breast Cancer Research*. 2008;10(3):209. doi:10.1186/bcr2102
27. Destounis SF, SM. Grimm, LJ. Poplack, SP. Sung, JS. Mammography. ACR BI-RADS v2025 Manual. *American College of Radiology*. 2025.
28. Newell MS, Destounis SV, Leung JTW, DeMartini WB, Lee CH, Eby PR. ACR BI-RADS® v2025 Manual. *American College of Radiology*. 2025.

29. Haji Maghsoudi O, Gastounioti A, Scott C, et al. Deep-LIBRA: An artificial-intelligence method for robust quantification of breast density with independent validation in breast cancer risk assessment. *Med Image Anal*. 2021;73:102138. doi:10.1016/j.media.2021.102138
30. Highnam R, Brady SM, Yaffe MJ, Karssemeijer N, Harvey J. Robust Breast Composition Measurement - VolparaTM. In: Martí, J., Oliver, A., Freixenet, J., Martí, R. (eds). *Digital Mammography. IWDM 2010. Lecture Notes in Computer Science*. Springer, Berlin, Heidelberg. 2010;6136:342-349. doi:10.1007/978-3-642-13666-5_46
31. Ciatto S, Bernardi D, Calabrese M, et al. A first evaluation of breast radiological density assessment by QUANTRA software as compared to visual classification. *The Breast*. 2012;21(4):503-506. doi:https://doi.org/10.1016/j.breast.2012.01.005
32. Rodriguez-Ruiz A, Lång K, Gubern-Merida A, et al. Stand-Alone Artificial Intelligence for Breast Cancer Detection in Mammography: Comparison With 101 Radiologists. *J Natl Cancer Inst*. 2019;111(9):916-922. doi:10.1093/jnci/djy222
33. Rodríguez-Ruiz A, Krupinski E, Mordang JJ, et al. Detection of Breast Cancer with Mammography: Effect of an Artificial Intelligence Support System. *Radiology*. 2019;290(2):305-314. doi:10.1148/radiol.2018181371
34. Boyd NF, Rommens JM, Vogt K, et al. Mammographic breast density as an intermediate phenotype for breast cancer. *Lancet Oncology*. 2005;6(10):798-808. doi:10.1016/s1470-2045(05)70390-9
35. Yaffe M, Boyd N. Mammographic breast density and cancer risk: The radiological view. *Gynecological Endocrinology*. 2005;21(sup1):6-11. doi:10.1080/09513590400030053
36. Bodewes FTH, Van Asselt AA, Dorrius MD, Greuter MJW, De Bock GH. Mammographic breast density and the risk of breast cancer: A systematic review and meta-analysis. *The Breast*. 2022;66:62-68. doi:10.1016/j.breast.2022.09.007
37. Boyd NF, Guo H, Martin LJ, et al. Mammographic Density and the Risk and Detection of Breast Cancer. *New England Journal of Medicine*. 2007;356(3):227-236. doi:10.1056/nejmoa062790
38. McCormack VA, dos Santos Silva I. Breast Density and Parenchymal Patterns as Markers of Breast Cancer Risk: A Meta-analysis. *Cancer Epidemiology, Biomarkers & Prevention*. 2006;15(6):1159-1169. doi:10.1158/1055-9965.Epi-06-0034
39. Gwak H, Lee D, Kim SH. Association of Breast Density with Breast Cancer Risk and Stage at Diagnosis: A Korean Nationwide Cohort Study. *Cancers*. 2025;17(24):3897.
40. Astley SM, Harkness EF, Sergeant JC, et al. A comparison of five methods of measuring mammographic density: a case-control study. *Breast Cancer Research*. 2018;20(1). doi:10.1186/s13058-018-0932-z
41. BreastScreen Australia Clinical Advisory Group. BreastScreen Australia – Position statement on breast density and screening. *Australian Government – Department of Health, Disability and Ageing*. Published: 2025-05-30. Accessed 2026-01-30. https://www.health.gov.au/resources/publications/breastscreen-australia-position-statement-on-breast-density-and-screening?language=en

42. U.S. Food and Drug Administration. Mammography Quality Standards Act and Regulation Amendments: Small Entity Compliance Guide. FDA. 2024.
43. Hellmann SS, Thygesen LC, Tolstrup JS, Grønbaek M. Modifiable risk factors and survival in women diagnosed with primary breast cancer: results from a prospective cohort study. *Eur J Cancer Prev*. 2010;19(5):366-73. doi:10.1097/CEJ.0b013e32833b4828
44. Kluttig A, Schmidt-Pokrzywniak A. Established and Suspected Risk Factors in Breast Cancer Aetiology. *Breast Care (Basel)*. 2009;4(2):82-87. doi:10.1159/000211368
45. Colditz GA, Hankinson SE. The Nurses' Health Study: lifestyle and health among women. *Nature Reviews Cancer*. 2005;5(5):388-396. doi:10.1038/nrc1608
46. Shiovitz S, Korde LA. Genetics of breast cancer: a topic in evolution. *Annals of Oncology*. 2015;26(7):1291-1299. doi:10.1093/annonc/mdv022
47. Burton A, Maskarinec G, Perez-Gomez B, et al. Mammographic density and ageing: A collaborative pooled analysis of cross-sectional data from 22 countries worldwide. *PLOS Medicine*. 2017;14(6):e1002335. doi:10.1371/journal.pmed.1002335
48. Pike MC, Krailo MD, Henderson BE, Casagrande JT, Hoel DG. 'Hormonal' risk factors, 'breast tissue age' and the age-incidence of breast cancer. *Nature*. 1983;303(5920):767-70. doi:10.1038/303767a0
49. McCormack VA, Perry NM, Vinnicombe SJ, Dos Santos Silva I. Changes and tracking of mammographic density in relation to Pike's model of breast tissue aging: a UK longitudinal study. *International Journal of Cancer*. 2010;127(2):452-461. doi:10.1002/ijc.25053
50. Łukasiewicz S, Czeczelewski M, Forma A, Baj J, Sitarz R, Stanisławek A. Breast Cancer—Epidemiology, Risk Factors, Classification, Prognostic Markers, and Current Treatment Strategies—An Updated Review. *Cancers*. 2021;13(17):4287. doi:10.3390/cancers13174287
51. Bertos NR, Park M. Breast cancer — one term, many entities? *Journal of Clinical Investigation*. 2011;121(10):3789-3796. doi:10.1172/jci57100
52. Sickles EA, D'Orsi CJ, Bassett LW, et al. ACR BI-RADS Mammography. In: ACR BI-RADS Atlas, Breast Imaging Reporting and Data System. *American College of Radiology*. 2013.
53. Qi Y-J, Su G-H, You C, et al. Radiomics in breast cancer: Current advances and future directions. *Cell Reports Medicine*. 2024;5(9):101719. doi:https://doi.org/10.1016/j.xcrm.2024.101719
54. Hanahan D. Hallmarks of Cancer: New Dimensions. *Cancer Discovery*. 2022;12(1):31-46. doi:10.1158/2159-8290.cd-21-1059
55. Quail DF, Joyce JA. Microenvironmental regulation of tumor progression and metastasis. *Nature Medicine*. 2013;19(11):1423-1437. doi:10.1038/nm.3394
56. Binnewies M, Roberts EW, Kersten K, et al. Understanding the tumor immune microenvironment (TIME) for effective therapy. *Nature Medicine*. 2018;24(5):541-550. doi:10.1038/s41591-018-0014-x

57. Talkington A, Durrett R. Estimating Tumor Growth Rates In Vivo. *Bulletin of Mathematical Biology*. 2015;77(10):1934-1954. doi:10.1007/s11538-015-0110-8
58. Spratt JA, Von Fournier D, Spratt JS, Weber EE. Decelerating growth and human breast cancer. *Cancer*. 1993;71(6):2013-2019. doi:10.1002/1097-0142(19930315)71:6<2013::aid-cncr2820710615>3.0.co;2-v
59. Cao J, ed. *Breast Cancer*. Springer, Humana Press. 2016.
60. Weigelt B, Geyer FC, Reis-Filho JS. Histological types of breast cancer: how special are they? *Mol Oncol*. 2010;4(3):192-208. doi:10.1016/j.molonc.2010.04.004
61. Delaloge S, Khan SA, Wesseling J, Whelan T. Ductal carcinoma in situ of the breast: finding the balance between overtreatment and undertreatment. *The Lancet*. 2024;403(10445):2734-2746. doi:10.1016/S0140-6736(24)00425-2
62. Orrantia-Borunda E, Anchondo-Nuñez P, Evelia Acuña-Aguilar L, Octavio Gómez-Valles F, Adriana Ramírez Valdespino C. Subtypes of Breast Cancer. In: Mayrovitz H, ed. *Breast Cancer*. Exon Publications. 2022.
63. Benzekry S, Lamont C, Beheshti A, et al. Classical Mathematical Models for Description and Prediction of Experimental Tumor Growth. *PLoS Computational Biology*. 2014;10(8):e1003800. doi:10.1371/journal.pcbi.1003800
64. Sinkus R, Tanter M, Xydeas T, Catheline S, Bercoff J, Fink M. Viscoelastic shear properties of in vivo breast lesions measured by MR elastography. *Magn Reson Imaging*. 2005;23(2):159-65. doi:10.1016/j.mri.2004.11.060
65. Vårdprogramgruppen för bröstcancer. Nationellt vårdprogram – Bröstcancer. Regionala cancercentrum i samverkan. Updated: 2025-11-11. Accessed: 2025-01-08. https://kunskapsbanken.cancercentrum.se/diagnoser/brostcancer/vardprogram/
66. Tang D-D, Ye Z-J, Liu W-W, et al. Survival feature and trend of female breast cancer: A comprehensive review of survival analysis from cancer registration data. *The Breast*. 2025;79:103862. doi:https://doi.org/10.1016/j.breast.2024.103862
67. Nordenskjöld AE, Fohlin H, Arnesson LG, et al. Breast cancer survival trends in different stages and age groups - a population-based study 1989-2013. *Acta Oncol*. 2019;58(1):45-51. doi:10.1080/0284186x.2018.1532601
68. Cancer Research UK. Breast cancer mortality statistics. 2026-02-06, 2026. Updated: 2025-09-26. Accessed: 2026-02-06. https://www.cancerresearchuk.org/health-professional/cancer-statistics/statistics-by-cancer-type/breast-cancer/mortality
69. Kopans DB, Smith RA, Duffy SW. Mammographic Screening and "Overdiagnosis". *Radiology*. 2011;260(3):616-620. doi:10.1148/radiol.11110716
70. Güth U, Huang DJ, Huber M, et al. Tumor size and detection in breast cancer: Self-examination and clinical breast examination are at their limit. *Cancer Detection and Prevention*. 2008;32(3):224-228. doi:https://doi.org/10.1016/j.cdp.2008.04.002
71. Wang J, Gottschal P, Ding L, et al. Mammographic sensitivity as a function of tumor size: A novel estimation based on population-based screening data. *Breast*. 2021;55:69-74. doi:10.1016/j.breast.2020.12.003
72. Nicosia L, Gnocchi G, Gorini I, et al. History of Mammography: Analysis of Breast Imaging Diagnostic Achievements over the Last Century. *Healthcare*. 2023;11(11):1596. doi:10.3390/healthcare11111596

73. Bick U, Diekmann F. *Digital Mammography*. Medical Radiology. Springer Berlin Heidelberg. 2010.
74. Vancoillie L, Cockmartin L, Marshall N, Bosmans H. The impact on lesion detection via a multi-vendor study: A phantom-based comparison of digital mammography, digital breast tomosynthesis, and synthetic mammography. *Medical Physics*. 2021;48(10):6270-6292. doi:10.1002/mp.15171
75. Monnin P, Damet J, Bosmans H, Marshall NW. Task-based detectability in anatomical background in digital mammography, digital breast tomosynthesis and synthetic mammography. *Physics in Medicine & Biology*. 2024;69(2):025017. doi:10.1088/1361-6560/ad1766
76. Ikejimba LC, Salad J, Graff CG, et al. Assessment of task-based performance from five clinical DBT systems using an anthropomorphic breast phantom. *Medical Physics*. 2021;48(3):1026-1038. doi:10.1002/mp.14568
77. Roth RG, Maidment AD, Weinstein SP, Roth SO, Conant EF. Digital breast tomosynthesis: lessons learned from early clinical implementation. *Radiographics*. 2014;34(4):E89-102. doi:10.1148/rg.344130087
78. Rafferty EA, Park JM, Philpotts LE, et al. Assessing Radiologist Performance Using Combined Digital Mammography and Breast Tomosynthesis Compared with Digital Mammography Alone: Results of a Multicenter, Multireader Trial. *Radiology*. 2013;266(1):104-113. doi:10.1148/radiol.12120674
79. Olinder J, Johnson K, Åkesson A, Förnvik D, Zackrisson S. Impact of breast density on diagnostic accuracy in digital breast tomosynthesis versus digital mammography: results from a European screening trial. *Breast Cancer Research*. 2023;25(1). doi:10.1186/s13058-023-01712-6
80. Weigel S, Heindel W, Hense H-W, Decker T, Gerß J, Kerschke L. Breast Density and Breast Cancer Screening with Digital Breast Tomosynthesis: A TOSYMA Trial Subanalysis. *Radiology*. 2023;306(2). doi:10.1148/radiol.221006
81. Bernardi D, Ciatto S, Pellegrini M, et al. Application of breast tomosynthesis in screening: Incremental effect on mammography acquisition and reading time. Article. *British Journal of Radiology*. 2012;85(1020):e1174-e1178. doi:10.1259/bjr/19385909
82. Dang PA, Freer PE, Humphrey KL, Halpern EF, Rafferty EA. Addition of Tomosynthesis to Conventional Digital Mammography: Effect on Image Interpretation Time of Screening Examinations. *Radiology*. 2014;270(1):49-56. doi:10.1148/radiol.13130765
83. Marinovich ML, Hunter KE, Macaskill P, Houssami N. Breast Cancer Screening Using Tomosynthesis or Mammography: A Meta-analysis of Cancer Detection and Recall. *JNCI: Journal of the National Cancer Institute*. 2018;110(9):942-949. doi:10.1093/jnci/djy121
84. Pediconi F, Moffa G. Contrast-Enhanced Mammography: Bridging the research gaps and defining the future. *European Journal of Radiology*. 2025;192:112351. doi:https://doi.org/10.1016/j.ejrad.2025.112351

85. Isautier JMJ, Houssami N, Hadlow C, et al. Clinical guidelines for the management of mammographic density: a systematic review of breast screening guidelines worldwide. *JNCI Cancer Spectrum*. 2024;8(6). doi:10.1093/jncics/pkae103

86. Monticciolo DL, Newell MS, Moy L, Lee CS, Destounis SV. Breast Cancer Screening for Women at Higher-Than-Average Risk: Updated Recommendations From the ACR. *Journal of the American College of Radiology*. 2023;20(9):902-914. doi:10.1016/j.jacr.2023.04.002

87. Kim SH, Cha ES, Park CS, et al. Imaging features of invasive lobular carcinoma: comparison with invasive ductal carcinoma. *Jpn J Radiol*. 2011;29(7):475-82. doi:10.1007/s11604-011-0584-8

88. Lopez JK, Bassett LW. Invasive lobular carcinoma of the breast: spectrum of mammographic, US, and MR imaging findings. *Radiographics*. 2009;29(1):165-76. doi:10.1148/rg.291085100

89. Gillies RJ, Kinahan PE, Hricak H. Radiomics: Images Are More than Pictures, They Are Data. *Radiology*. 2015;278(2):563-577. doi:10.1148/radiol.2015151169

90. Shapiro S. Periodic Screening for Breast Cancer: The HIP Randomized Controlled Trial. *JNCI Monographs*. 1997;1997(22):27-30. doi:10.1093/jncimono/1997.22.27

91. Jatoi I, Anderson WF, Miller AB, Brawley OW. The history of cancer screening. *Curr Probl Surg*. 2019;56(4):138-163. doi:10.1067/j.cpsurg.2018.12.006

92. Tabár L, Fagerberg CJ, Gad A, et al. Reduction in mortality from breast cancer after mass screening with mammography. Randomised trial from the Breast Cancer Screening Working Group of the Swedish National Board of Health and Welfare. *The Lancet*. 1985;1(8433):829-32. doi:10.1016/s0140-6736(85)92204-4

93. Frisell J, Glas U, Hellström L, Somell A. Randomized mammographic screening for breast cancer in Stockholm. Design, first round results and comparisons. *Breast Cancer Res Treat*. 1986;8(1):45-54. doi:10.1007/bf01805924

94. Bjurstam N, Björneld L, Warwick J, et al. The Gothenburg Breast Screening Trial. *Cancer*. 2003;97(10):2387-96. doi:10.1002/cncr.11361

95. The National Board of Health and Welfare. General guidelines on mammographic screening: health check-up for early discovery of breast cancer. 1986.

96. Zackrisson S, Lång K, Rosso A, et al. One-view breast tomosynthesis versus two-view mammography in the Malmö Breast Tomosynthesis Screening Trial (MBTST): a prospective, population-based, diagnostic accuracy study. *The Lancet Oncology*. 2018;19(11):1493-1503. doi:10.1016/s1470-2045(18)30521-7

97. Lång K, Josefsson V, Larsson A-M, et al. Artificial intelligence-supported screen reading versus standard double reading in the Mammography Screening with Artificial Intelligence trial (MASAI): a clinical safety analysis of a randomised, controlled, non-inferiority, single-blinded, screening accuracy study. *The Lancet Oncology*. 2023;24(8):936-944. doi:10.1016/S1470-2045(23)00298-X

98. Dembrower K, Crippa A, Colon E, Eklund M, Strand F. Artificial intelligence for breast cancer detection in screening mammography in Sweden: a prospective, population-based, paired-reader, non-inferiority study. *The Lancet Digital Health*. 2023;5. doi:10.1016/S2589-7500(23)00153-X

99. Tingberg A, Dahlblom V, Dustler M, et al. Our journey toward implementation of digital breast tomosynthesis in breast cancer screening: the Malmö Breast Tomosynthesis Screening Project. *Journal of Medical Imaging*. 2024;12(S1). doi:10.1117/1.jmi.12.s1.s13006

100. Dahlblom V, Dustler M, Tingberg A, Zackrisson S. Breast cancer screening with digital breast tomosynthesis: comparison of different reading strategies implementing artificial intelligence. *European Radiology*. 2023;33(5):3754-3765. doi:10.1007/s00330-022-09316-y

101. Timberg P, Hellgren G, Dustler M, Tingberg A. Investigating the effect of adding comparisons with prior mammograms to standalone digital breast tomosynthesis screening. *Journal of Medical Imaging*. 2025;12(Suppl 2):S22003. doi:10.1117/1.Jmi.12.S2.S22003

102. Perry N, Broeders M, de Wolf C, Törnberg S, Holland R, von Karsa L. European guidelines for quality assurance in breast cancer screening and diagnosis. Fourth edition--summary document. *Ann Oncol*. 2008;19(4):614-22. doi:10.1093/annonc/mdm481

103. Zackrisson S. Unpublished survery from the Swedish National Board of Health and Welfare on the implementation and use of artificial intelligence in regional breast cancer screening. *Personal communication*. 2025.

104. Altobelli E, Rapacchietta L, Angeletti PM, Barbante L, Profeta FV, Fagnano R. Breast Cancer Screening Programmes across the WHO European Region: Differences among Countries Based on National Income Level. *Int J Environ Res Public Health*. 2017;14(4). doi:10.3390/ijerph14040452

105. Gao Y, Babb JS, Toth HK, Moy L, Heller SL. Digital Breast Tomosynthesis Practice Patterns Following 2011 FDA Approval: A Survey of Breast Imaging Radiologists. *Acad Radiol*. 2017;24(8):947-953. doi:10.1016/j.acra.2016.12.011

106. Richman IB, Hoag JR, Xu X, et al. Adoption of Digital Breast Tomosynthesis in Clinical Practice. *JAMA Intern Med*. 2019;179(9):1292-1295. doi:10.1001/jamainternmed.2019.1058

107. Gilbert FJ, Tucker L, Young KC. Digital breast tomosynthesis (DBT): a review of the evidence for use as a screening tool. *Clinical Radiology*. 2016;71(2):141-150. doi:10.1016/j.crad.2015.11.008

108. Michell MJ. Breast screening review--a radiologist's perspective. *Br J Radiol*. 2012;85(1015):845-7. doi:10.1259/bjr/21332901

109. Zhang Y, Rodriguez J, Mao X, et al. Incidence and Risk Factors of Interval and Screen-Detected Breast Cancer. *JAMA Oncology*. 2025;11(5):519-527. doi:10.1001/jamaoncol.2025.0167

110. Jørgensen KJ, Gøtzsche PC. Overdiagnosis in publicly organised mammography screening programmes: systematic review of incidence trends. *BMJ*. 2009;339:b2587. doi:10.1136/bmj.b2587

111. Tagliafico AS, Piana M, Schenone D, Lai R, Massone AM, Houssami N. Overview of radiomics in breast cancer diagnosis and prognostication. *The Breast*. 2020;49:74-80. doi:10.1016/j.breast.2019.10.018

112. Barufaldi B, Higginbotham D, Bakic P, Maidment AD. OpenVCT: a GPU-accelerated virtual clinical trial pipeline for mammography and digital breast tomosynthesis. *Proceedings of SPIE Medical Imaging, Physics of Medical Imaging*. 2018;10573. doi:10.1117/12.2294935

113. Abadi E, Harrawood B, Sharma S, Kapadia A, Segars WP, Samei E. DukeSim: A Realistic, Rapid, and Scanner-Specific Simulation Framework in Computed Tomography. *IEEE Trans Med Imaging*. 2019;38(6):1457-1465. doi:10.1109/tmi.2018.2886530

114. Badal A, Sharma D, Graff CG, Zeng R, Badano A. Mammography and breast tomosynthesis simulator for virtual clinical trials. *Computer Physics Communications*. 2021;261:107779. doi:10.1016/j.cpc.2020.107779

115. Doi K, Chan HP. Evaluation of absorbed dose in mammography: monte carlo simulation studies. *Radiology*. 1980;135(1):199-208. doi:10.1148/radiology.135.1.7360961

116. Badano A, Graff CG, Badal A, et al. Evaluation of Digital Breast Tomosynthesis as Replacement of Full-Field Digital Mammography Using an In Silico Imaging Trial. *JAMA Netw Open*. 2018;1(7):e185474. doi:10.1001/jamanetworkopen.2018.5474

117. U.S. Food and Drug Administration. Assessing the Credibility of Computational Modeling and Simulation in Medical Device Submissions. Guidance for Industry and FDA Staff. 2023. Accessed 2026-01-13. https://www.fda.gov/regulatory-information/search-fda-guidance-documents/assessing-credibility-computational-modeling-and-simulation-medical-device-submissions

118. Daskalaki A, Bliznakova K, Pallikarakis N. Evaluation of the effect of silicone breast inserts on X-ray mammography and breast tomosynthesis images: A Monte Carlo simulation study. *Physica Medica*. 2016;32(2):353-61. doi:10.1016/j.ejmp.2016.01.478

119. Bliznakova K, Russo P, Mettivier G, et al. A software platform for phase contrast x-ray breast imaging research. *Comput Biol Med*. 2015;61:62-74. doi:10.1016/j.compbiomed.2015.03.017

120. Wu M, FitzGerald P, Zhang J, et al. XCIST-an open access x-ray/CT simulation toolkit. *Phys Med Biol*. 2022;67(19). doi:10.1088/1361-6560/ac9174

121. Fung GSK, Stierstorfer K, Segars WP, Taguchi K, Flohr T, Tsui BMW. XCAT/DRASIM: a realistic CT/human-model simulation package. *Proceedings of SPIE Medical Imaging, Physics of Medical Imaging*. 2011;7961:79613D.

122. Vancoillie L, Marshall N, Cockmartin L, Vignero J, Zhang G, Bosmans H. Verification of the accuracy of a hybrid breast imaging simulation framework for virtual clinical trial applications. *Journal of Medical Imaging*. 2020;7(4):042804. doi:10.1117/1.Jmi.7.4.042804

123. Merken K, Monnens J, Marshall N, et al. Development and validation of a 3D anthropomorphic phantom for dental CBCT imaging research. *Medical Physics*. 2023;50(11):6714-6736. doi:https://doi.org/10.1002/mp.16661

124. Tomic H, Olinder J, Markbo JH, et al. A framework for simulation of temporal evolution and longitudinal studies of breast anatomy in radiology. *Medical Physics*. 2025;52(12):e70207. doi:10.1002/mp.70207

125. Abadi E, Barufaldi B, Lago M, et al. Toward widespread use of virtual trials in medical imaging innovation and regulatory science. *Medical Physics*. 2024;51(12):9394-9404. doi:10.1002/mp.17442
126. Maidment ADA, Vancoillie L. Virtual imaging trials are paving the way for the future of medical imaging. *Medical Physics*. 2025;52(7):e17959. doi:10.1002/mp.17959
127. Pokrajac DD, Maidment AD, Bakic PR. Optimized generation of high resolution breast anthropomorphic software phantoms. *Medical Physics*. 2012;39(4):2290-302. doi:10.1118/1.3697523
128. Ikejimba LC, Graff CG, Rosenthal S, et al. A novel physical anthropomorphic breast phantom for 2D and 3D x-ray imaging. *Medical Physics*. 2017;44(2):407-416. doi:10.1002/mp.12062
129. Bliznakova K, Bliznakov Z, Bravou V, Kolitsi Z, Pallikarakis N. A three-dimensional breast software phantom for mammography simulation. *Physics in Medicine and Biology*. 2003;48(22):3699-3719. doi:10.1088/0031-9155/48/22/006
130. Burgess AE. Mammographic structure: data preparation and spatial statistics analysis. *Proceedings of SPIE Medical Imaging, Physics of Medical Imaging*. 1999;3661. doi:10.1117/12.348620
131. Bochud FO, Valley JF, Verdun FR, Hessler C, Schnyder P. Estimation of the noisy component of anatomical backgrounds. *Medical Physics*. 1999;26(7):1365-70. doi:10.1118/1.598632
132. Burgess AE, Jacobson FL, Judy PF. Human observer detection experiments with mammograms and power-law noise. *Medical Physics*. 2001;28(4):419-437. doi:https://doi.org/10.1118/1.1355308
133. Metheany KG, Abbey CK, Packard N, Boone JM. Characterizing anatomical variability in breast CT images. *Medical Physics*. 2008;35(10):4685-94. doi:10.1118/1.2977772
134. Dustler M, Bakic P, Petersson H, Timberg P, Tingberg A, Zackrisson S. Application of the fractal Perlin noise algorithm for the generation of simulated breast tissue. *Proceedings of SPIE Medical Imaging, Physics of Medical Imaging*. 2015;9412. doi:10.1117/12.2081856
135. Dustler M, Förnvik H, Lång K. Binary implementation of fractal Perlin noise to simulate fibroglandular breast tissue. *Proceedings of SPIE Medical Imaging, Physics of Medical Imaging*. 2018;10573. doi:10.1117/12.2293234
136. Dustler M, Bakic P, Ikeda DM, Lang K, Zwiggelaar R. Realism of mammography tissue patches simulated using Perlin noise: a forced choice reading study. *Proceedings of SPIE Medical Imaging, Physics of Medical Imaging.* 2021;11595: 115954X. doi:10.1117/12.2582094
137. Bakic P, Barufaldi B, Pokrajac D, Weinstein S, Maidment A. Optimized simulation of breast anatomy for virtual clinical trials. *Proceedings of the 14th International Workshop on Breast Imaging*. 2018;10718:78. doi:10.1117/12.2318525
138. Mainprize JG, Alonzo-Proulx O, Jong RA, Yaffe MJ. Quantifying masking in clinical mammograms via local detectability of simulated lesions. *Medical Physics*. 2016;43(3):1249-1258. doi:10.1118/1.4941307

139. Eckstein M, Lago M, Abbey C. Evaluation of search strategies for microcalcifications and masses in 3D images. *Proceedings of SPIE Medical Imaging, Physics of Medical Imaging*. 2018;10577:105770C. doi:10.1117/12.2293871

140. Rashidnasab A, Elangovan P, Yip M, et al. Simulation and assessment of realistic breast lesions using fractal growth models. *Physics in Medicine and Biology*. 2013;58(16):5613-5627. doi:10.1088/0031-9155/58/16/5613

141. De Sisternes L, Brankov JG, Zysk AM, Schmidt RA, Nishikawa RM, Wernick MN. A computational model to generate simulated three-dimensional breast masses. *Medical Physics*. 2015;42(2):1098-1118. doi:10.1118/1.4905232

142. Bliznakova K, Dukov N, Feradov F, et al. Development of breast lesions models database. *Physica Medica*. 2019;64:293-303. doi:10.1016/j.ejmp.2019.07.017

143. Shaheen E, De Keyzer F, Bosmans H, Dance DR, Young KC, Ongeval CV. The simulation of 3D mass models in 2D digital mammography and breast tomosynthesis. *Medical Physics*. 2014;41(8Part1):081913. doi:10.1118/1.4890590

144. Elangovan P, Alrehily F, Pinto RF, et al. Simulation of spiculated breast lesions. *Proceedings of SPIE Medical Imaging, Physics of Medical Imaging*. 2016; 9783:97832E. doi:10.1117/12.2216227

145. Barufaldi B, Abbey CK, Lago MA, et al. Computational Breast Anatomy Simulation Using Multi-Scale Perlin Noise. *IEEE Trans Med Imaging*. 2021;40(12):3436-3445. doi:10.1109/tmi.2021.3087958

146. Perlin K. An image synthesizer. *ACM SIGGRAPH Computer Graphics*. 1985;19(3):287-296. doi:10.1145/325165.325247

147. Perlin K. Improving noise. *ACM Trans Graph*. 2002;21(3):681–682. doi:10.1145/566654.566636

148. VICTRE Breast Phantom documentation. Breast Phantom Documentation. Accessed: 2026-01-13. https://breastphantom.readthedocs.io/en/latest/

149. Barufaldi B, Choi C, Teixeira J, et al. Representation of complex mammary parenchyma texture in tomosynthesis using simplex noise simulations. *Proceedings of SPIE Medical Imaging, Physics of Medical Imaging*. 2024;12925:1292548. doi:10.1117/12.3006839

150. Axelsson R, Tomic H, Zackrisson S, et al. Finite element model of mechanical imaging of the breast. *Journal of Medical Imaging*. 2022;9(3):033502. doi:10.1117/1.JMI.9.3.033502

151. Pacheco G, Michielsen K, García E, Díaz O, Sechopoulos I. Optimization and validation of a mechanical compression model for digital breast phantoms in mammography and tomosynthesis simulations. *Medical Physics*. 2025;52(7):e17980. doi:10.1002/mp.17980

152. Shih TC, Chen JH, Liu D, et al. Computational simulation of breast compression based on segmented breast and fibroglandular tissues on magnetic resonance images. *Phys Med Biol*. 2010;55(14):4153-68. doi:10.1088/0031-9155/55/14/013

153. Mîra A, Payan Y, Carton A-K, et al. Simulation of breast compression using a new biomechanical model. *Proceedings of SPIE Medical Imaging, Physics of Medical Imaging*. 2018;10573:105735A. doi:10.1117/12.2293488

154. Markbo J-H, Bakic P, Isaksson H, Johnson K, Dustler M. Comparison between the results of simulated mechanical imaging on software breast phantom and in vivo measurements. *Radiation Protection Dosimetry (in print)*. 2026.

155. Siddon RL. Fast calculation of the exact radiological path for a three-dimensional CT array. *Medical Physics*. 1985;12(2):252-5. doi:10.1118/1.595715

156. Marshall NW, Bosmans H. Performance evaluation of digital breast tomosynthesis systems: comparison of current virtual clinical trial methods. *Phys Med Biol*. 2022;67(22). doi:10.1088/1361-6560/ac9a34

157. Elangovan P, Mackenzie A, Dance DR, et al. Design and validation of realistic breast models for use in multiple alternative forced choice virtual clinical trials. *Physics in Medicine and Biology*. 2017;62(7):2778-2794. doi:10.1088/1361-6560/aa622c

158. Diaz O, Dance DR, Young KC, Elangovan P, Bakic PR, Wells K. Estimation of scattered radiation in digital breast tomosynthesis. *Physics in Medicine & Biology*. 2014;59(15):4375. doi:10.1088/0031-9155/59/15/4375

159. Tushar FI, Vancoillie L, McCabe C, et al. Virtual Lung Screening Trial (VLST): An In Silico Study Inspired by the National Lung Screening Trial for Lung Cancer Detection. *ArXiv (Preprint)*. 2025.

160. Gong H, Hu Q, Walther A, et al. Deep-learning-based model observer for a lung nodule detection task in computed tomography. *Journal of Medical Imaging*. 2020;7(4):042807. doi:10.1117/1.Jmi.7.4.042807

161. Alnowami M, Mills G, Awis M, et al. A deep learning model observer for use in alterative forced choice virtual clinical trials. *Proceedings of SPIE Medical Imaging, Physics of Medical Imaging*. 2018;10577:105770Q. doi:10.1117/12.2293209

162. Sengupta A, Lago MA, Badano A. In situtumor model for longitudinal in silico imaging trials. *Phys Med Biol*. 2024;69(7). doi:10.1088/1361-6560/ad3322

163. Rodríguez-Ruiz A, Agasthya GA, Sechopoulos I. The compressed breast during mammography and breast tomosynthesis: in vivo shape characterization and modeling. *Physics in Medicine and Biology*. 2017;62(17):6920-6937. doi:10.1088/1361-6560/aa7cd0

164. Rodríguez-Ruiz A, Feng SSJ, van Zelst J, et al. Improvements of an objective model of compressed breasts undergoing mammography: Generation and characterization of breast shapes. *Medical Physics*. 2017;44(6):2161-2172. doi:10.1002/mp.12186

165. Förnvik D, Lång K, Andersson I, Dustler M, Borgquist S, Timberg P. Estimates of breast cancer growth rate from mammograms and its relation to tumour characteristics. *Radiation Protection Dosimetry*. 2016;169(1-4):151-157. doi:10.1093/rpd/ncv417

166. Johnson K, Lång K, Ikeda DM, Åkesson A, Andersson I, Zackrisson S. Interval Breast Cancer Rates and Tumor Characteristics in the Prospective Population-based Malmö Breast Tomosynthesis Screening Trial. *Radiology*. 2021;299(3):559-567. doi:10.1148/radiol.2021204106

167. Olinder J, Förnvik D, Dahlblom V, et al. Assessing mammographic density change within individuals across screening rounds using deep learning–based software. *Journal of Medical Imaging*. 2025;12(S2):S22017. doi:10.1117/1.JMI.12.S2.S22017

168. Borges LR, Barufaldi B, Caron RF, et al. Technical Note: Noise models for virtual clinical trials of digital breast tomosynthesis. *Medical Physics*. 2019;46(6):2683-2689. doi:10.1002/mp.13534

169. Vimieiro RB, Borges LR, Vieira MAC. Open-Source Reconstruction Toolbox for Digital Breast Tomosynthesis. *Proceedings of the XXVI Brazilian Congress on Biomedical Engineering* 2019;70/2:349-354. doi:10.1007/978-981-13-2517-5_53

170. Marchessoux C, Kimpe T, Bert T. A Virtual Image Chain for Perceived and Clinical Image Quality of Medical Display. *Journal of Display Technology*. 2008;4(4):356-368. doi:10.1109/JDT.2008.2001164

171. Dahlblom V, Dustler M, Bolejko A, et al. Malmö Breast ImaginG database: objectives and development. *Journal of Medical Imaging*. 2023;10(6):061402. doi:10.1117/1.Jmi.10.6.061402

172. Bury K. Gamma Distributions. In: Bury K, ed. Statistical Distributions in Engineering. *Cambridge University Press*. 1999:208-237.

173. Bouyé E, Durrleman V, Nikeghbali A, Riboulet G, Roncalli T. Copulas for Finance: A Reading Guide and Some Applications. *SSRN Electronic Journal*. 2000. doi:10.2139/ssrn.1032533

174. van Griethuysen JJM, Fedorov A, Parmar C, et al. Computational Radiomics System to Decode the Radiographic Phenotype. *Cancer Research*. 2017;77(21):e104-e107. doi:10.1158/0008-5472.Can-17-0339

175. Börjesson S, Håkansson M, Båth M, et al. A software tool for increased efficiency in observer performance studies in radiology. *Radiation Protection Dosimetry*. 2005;114(1-3):45-52. doi:10.1093/rpd/nch550

176. Håkansson M, Svensson S, Zachrisson S, Svalkvist A, Båth M, Månsson LG. ViewDEX: an efficient and easy-to-use software for observer performance studies. *Radiation Protection Dosimetry*. 2010;139(1-3):42-51. doi:10.1093/rpd/ncq057

177. Svalkvist A, Svensson S, Hagberg T, Båth M. ViewDEX 3.0— Recent development of a software application facilitating assessment of image quality and observer performance. *Radiation Protection Dosimetry*. 2021;195(3-4):372-377. doi:10.1093/rpd/ncab014

178. Shapiro SS, Wilk MB. An Analysis of Variance Test for Normality (Complete Samples). *Biometrika*. 1965;52(3/4):591-611. doi:10.2307/2333709

179. NIST/SEMATECH. Anderson-Darling Test. e-Handbook of Statistical Methods. National Institute of Standars and Technology. 2012:chap 1.3.5.14. Accessed: 2026-01-14. https://www.itl.nist.gov/div898/handbook/eda/section3/eda35e.htm

180. NIST/SEMATECH. Friedman test. Statistical Engineering Devision Dataplot. *National Institute of Standars and Technology*. 2023. Accessed: 2026-01-14. https://www.itl.nist.gov/div898/software/dataplot/refman1/auxillar/friedman.htm

181. NIST/SEMATECH. Kolmogorov-Smirnov Goodness-of-fit Test. e-Handbook of Statistical Methods. *National Institute of Standars and Technology*. 2012:chap 1.3.5.16. Accessed: 2026-01-14. https://www.itl.nist.gov/div898/handbook/eda/section3/eda35g.htm

182. NIST/SEMATECH. Signed Rank Test. Statistical Engineering Devision Dataplot. *National Institute of Standars and Technology*. 2023. Accessed: 2026-01-14. https://www.itl.nist.gov/div898/software/dataplot/refman1/auxillar/signrank.htm
183. NIST/SEMATECH. Mann Whitney U Statistic. Statistical Engineering Devision Dataplot. *National Institute of Standars and Technology*. 2013. Accessed: 2026-01-14. https://www.itl.nist.gov/div898/software/dataplot/refman2/auxillar/mannwhit.htm
184. Junge MRJ, Dettori JR. ROC Solid: Receiver Operator Characteristic (ROC) Curves as a Foundation for Better Diagnostic Tests. *Global Spine Journal*. 2018;8(4):424-429. doi:10.1177/2192568218778294
185. Nakas CT, Bantis LE, Gatsonis CA. ROC Analysis for Classification and Prediction in Practice. 1 ed. Chapman and Hall/CRC. 2023. doi:10.1201/9780429170140
186. Menard S. Logistic Regression: From Introductory to Advanced Concepts and Applications. *SAGE Publications, Inc*. 2010. Accessed: 2026-01-15. https://methods.sagepub.com/book/mono/logistic-regression-from-introductory-to-advanced-concepts-and-applications/toc
187. Hayes AF. Introduction to Mediation, Moderation, and Conditional Process Analysis. Third Edition. *Guilford Press*. 2022.
188. Tönnies T, Schlesinger S, Lang A, Kuss O. Mediation Analysis in Medical Research. *Dtsch Arztebl Int*. 2023;120(41):681-687. doi:10.3238/arztebl.m2023.0175
189. Iacobucci D. Mediation Analysis. *SAGE Publications, Inc*. 2008. Accessed: 2026-01-15. https://methods.sagepub.com/book/mono/mediation-analysis/toc
190. Wasserstein RL, Lazar NA. The ASA Statement on p-Values: Context, Process, and Purpose. *The American Statistician*. 2016;70(2):129-133. doi:10.1080/00031305.2016.1154108
191. Greenland S, Senn SJ, Rothman KJ, et al. Statistical tests, P values, confidence intervals, and power: a guide to misinterpretations. *European Journal of Epidemiology*. 2016;31(4):337-350. doi:10.1007/s10654-016-0149-3
192. Di Leo G, Sardanelli F. Statistical significance: p value, 0.05 threshold, and applications to radiomics—reasons for a conservative approach. *European Radiology Experimental*. 2020;4(1). doi:10.1186/s41747-020-0145-y
193. Foody GM. Classification accuracy comparison: Hypothesis tests and the use of confidence intervals in evaluations of difference, equivalence and non-inferiority. *Remote Sensing of Environment*. 2009;113(8):1658-1663. doi:10.1016/j.rse.2009.03.014
194. Spratt JA, von Fournier D, Spratt JS, Weber EE. Mammographic assessment of human breast cancer growth and duration. *Cancer*. 1993;71(6):2020-6. doi:10.1002/1097-0142(19930315)71:6<2020::aid-cncr2820710616>3.0.co;2-#
195. Sharma D, Graff CG, Badal A, et al. Technical Note: In silico imaging tools from the VICTRE clinical trial. *Medical Physics*. 2019;46(9):3924-3928. doi:10.1002/mp.13674
196. Von Euler-Chelpin M, Lillholm M, Vejborg I, Nielsen M, Lynge E. Sensitivity of screening mammography by density and texture: a cohort study from a population-based screening program in Denmark. *Breast Cancer Research*. 2019;21(1). doi:10.1186/s13058-019-1203-3

197. Spak DA, Plaxco JS, Santiago L, Dryden MJ, Dogan BE. BI-RADS® fifth edition: A summary of changes. *Diagnostic and Interventional Imaging*. 2017;98(3):179-190. doi:https://doi.org/10.1016/j.diii.2017.01.001

198. Verboom SD, Mainprize JG, Peters J, Broeders M, Yaffe MJ, Sechopoulos I. More than density: validating a mammographic masking prediction model in Dutch breast cancer screening. *European Radiology*. 2025;35(12):8191-8199. doi:10.1007/s00330-025-11687-x

199. Mainprize JG, Alonzo-Proulx O, Alshafeiy TI, Patrie JT, Harvey JA, Yaffe MJ. Prediction of Cancer Masking in Screening Mammography Using Density and Textural Features. *Acad Radiol*. 2019;26(5):608-619. doi:10.1016/j.acra.2018.06.011

200. Darabi H, Czene K, Zhao W, Liu J, Hall P, Humphreys K. Breast cancer risk prediction and individualised screening based on common genetic variation and breast density measurement. *Breast Cancer Res*. 2012;14(1):R25. doi:10.1186/bcr3110

201. Gabrielson M, Eriksson M, Hammarström M, et al. Cohort Profile: The Karolinska Mammography Project for Risk Prediction of Breast Cancer (KARMA). *International Journal of Epidemiology*. 2017;46(6):1740-1741g. doi:10.1093/ije/dyw357

202. Jiang S, Bennett DL, Colditz GA. Deriving a Mammogram-Based Risk Score from Screening Digital Breast Tomosynthesis for 5-Year Breast Cancer Risk Prediction. *Cancer Prevention Research*. 2025;18(6):347-354. doi:10.1158/1940-6207.Capr-24-0427

203. Barufaldi B, Lago MA, Abadi E, Maidment ADA. Container applications for the development and integration of virtual imaging platforms. *Medical Physics*. 2025;52(6):3685-3696. doi:10.1002/mp.17777

204. Samei E. The future of in silico trials and digital twins in medicine. *PNAS Nexus*. 2025;4(5). doi:10.1093/pnasnexus/pgaf123

205. Bae MS, Park SY, Song SE, et al. Heterogeneity of triple-negative breast cancer: mammographic, US, and MR imaging features according to androgen receptor expression. *European Radiology*. 2015;25(2):419-427. doi:10.1007/s00330-014-3419-z

206. Remvikos Y, Magdelenat H, Dutrillaux B. Genetic evolution of breast cancers. III: Age-dependent variations in the correlations between biological indicators of prognosis. *Breast Cancer Res Treat*. 1995;34(1):25-33. doi:10.1007/bf00666488

207. Thomas GA, Leonard RC. How age affects the biology of breast cancer. *Clin Oncol (R Coll Radiol)*. 2009;21(2):81-5. doi:10.1016/j.clon.2008.11.006

208. Clark GM. The biology of breast cancer in older women. *J Gerontol*. 1992;47 Spec No:19-23.

209. Dahal L, Ghojoghnejad M, Vancoillie L, et al. XCAT 3.0: A comprehensive library of personalized digital twins derived from CT scans. *Medical Image Analysis*. 2025;103:103636. doi:https://doi.org/10.1016/j.media.2025.103636

210. Sizikova E, Badal A, Delfino JG, et al. Synthetic data in radiological imaging: current state and future outlook. *BJR|Artificial Intelligence*. 2024;1(1). doi:10.1093/bjrai/ubae007

211. Shen T, Hao K, Gou C, Wang F-Y. Mass Image Synthesis in Mammogram with Contextual Information Based on GANs. *Computer Methods and Programs in Biomedicine*. 2021;202:106019. doi:10.1016/j.cmpb.2021.106019
212. Guan S, Loew M. Breast cancer detection using synthetic mammograms from generative adversarial networks in convolutional neural networks. *Journal of Medical Imaging*. 2019;6(3):031411. doi:10.1117/1.Jmi.6.3.031411
213. Oyelade ON, Ezugwu AE, Almutairi MS, Saha AK, Abualigah L, Chiroma H. A generative adversarial network for synthetization of regions of interest based on digital mammograms. *Scientific Reports*. 2022;12(1):6166. doi:10.1038/s41598-022-09929-9
214. Garrucho L, Kushibar K, Osuala R, et al. High-resolution synthesis of high-density breast mammograms: Application to improved fairness in deep learning based mass detection. Original Research. *Frontiers in Oncology*. 2023;Volume 12 – 2022. doi:10.3389/fonc.2022.1044496
215. Lee J, Mustafaev T, Nishikawa RM. Impact of GAN artifacts for simulating mammograms on identifying mammographically occult cancer. *Journal of Medical Imaging*. 2023;10(5):054503. doi:10.1117/1.Jmi.10.5.054503
216. Radiological Society of North America (RSNA). RSNA Screening Mammography Breast Cancer Detection AI Challenge (2023). *Radiological Society of North America (RSNA)*. Accessed: 2026-02-11. https://www.rsna.org/artificial-intelligence/ai-image-challenge/screening-mammography-breast-cancer-detection-ai-challenge?utm_source=chatgpt.com
217. The Medical Image Computing and Computer Assisted Intervention Society. MICCAI Registered Challenges. Updated: 2026. Accessed: 2026-02-11. https://miccai.org/index.php/special-interest-groups/challenges/miccai-registered-challenges/
218. Abadi E, Segars WP, Felice N, et al. AAPM Truth-based CT (TrueCT) reconstruction grand challenge. *Medical Physics*. 2025;52(4):1978-1990. doi:10.1002/mp.17619

VIRTUAL IMAGING TRIALS (VITs) are a valuable tool for simulating human anatomy, imaging physics, and observer behavior to improve and optimize medical imaging, complementing both clinical and physical phantom studies.

This thesis aims to advance VITs for breast imaging by improving the realism of computational phantoms and virtual populations, while also enabling longitudinal modeling based on real-world data.

HANNA TOMIC is a certified medical physicist at the Department of Translational Medicine at Lund University.

Printed by Media-Tryck, Lund 2026 NORDIC SWAN ECOLABEL 3041 0903

LUND UNIVERSITY

FACULTY OF MEDICINE

Diagnostic Radiology
Department of Translational Medicine

Lund University, Faculty of Medicine
Doctoral Dissertation Series 2026:48
ISBN 978-91-8021-846-7
ISSN 1652-8220